Assessing the Impact of Air Leakage on the Hygrothermal Performance of Wood-Frame Walls Under Historical and Future Climates

Max Junginger

A Thesis

In the Department of

Building, Civil and Environmental Engineering

Presented in Partial Fulfillment of the Requirements

for the Degree of Master of Applied Science (Building Engineering) at

Concordia University

Montreal, Quebec, Canada

August 2023

CONCORDIA UNIVERSITY

SCHOOL OF GRADUATE STUDIES

This is to certify that the thesis prepared

By: Max Junginger

Entitled: Assessing the impact of air leakage on the hygrothermal performance of wood-frame walls under historical and future climates

and submitted in partial fulfillment of the requirements for the degree of

Master of Applied Science (Building Engineering)

complies with the regulations of the University and meets the accepted standards with respect to originality and quality.

Signed by the final examining committee:

      _____Chair
      Dr. Radu Zmeureanu

      _____Examiner
      Dr. Radu Zmeureanu

      _____Examiner
      Dr. Bruno Lee

      _____Thesis Supervisor
      Dr. Hua Ge

Approved by   _____Graduate Program Director
      Dr. Chunjiang An

August 17, 2023   _____Dean of Faculty
      Dr. Mourad Debbabi

Abstract

Assessing The Impact Of Air Leakage On The Hygrothermal Performance Of Wood-Frame Walls Under Historical And Future Climates

Max Junginger

Concordia University, 2023

Air leakage is a crucial factor when assessing the hygrothermal performance of wood-frame walls since it can lead to moisture accumulation during the cold season. The seriousness of this problem may change in a warmer climate in the future and hygrothermal simulations are widely used as a tool to predict this effect. However, since 2D models are required for detailed air leakage assessment and the high number of input variables leads to having to conduct thousands of simulations for a single type of building cladding, downsizing the simulation grid to the lowest number of cells is a crucial task to help ensure reduced computational time. Using a hygrothermal simulation tool, the steps needed to build the smallest 2D grid were explained; as well, convergence and accuracy of the results were evaluated and the functional relations between air leakage rate and air permeability of the insulation were clarified. Hygrothermal simulations were performed for wood-frame walls having brick veneer and stucco cladding for three Canadian cities: Whitehorse, Vancouver, and Ottawa. While the air leakage rate has a significant impact on the inner surface of OSB, wind driven rain is the key factor on the outer surface. The performance of stucco cladding is worse than brick in all cases and the future climate may reduce the risk of mould growth on the inner surface of OSB in all cities. The results also show that the simulation time can be reduced by 90%, with negligible loss of accuracy, when comparing fine to optimized meshes.

Acknowledgement

First, I thank Dr. Hua Ge for being my supervisor and giving me guidance and support throughout this journey. Without all her effort, this task would have been much more difficult or even impossible.

To Dr. Michael Lacasse, my deepest gratitude for offering me the chance to join the National Research Council team at the Construction Research Centre, where I made many friends from several different countries and had access to knowledge and infrastructure. Without that unvaluable opportunity, conducting this research would not have been possible.

To Dr. Maurice Defo, my sincere thanks for all he taught me and for the innumerable hours that he spent on guiding and pushing me, patiently.

I also thank my fellows Travis Moore, Lin Wang, Naman Bansal, Abhishek Gaur and Michal Bartko for the laughs we had together. And special thanks to Chetan Aggarwal, for being a great friend and for all the discussions and support from the beginning to the end of this work.

Although a thesis usually has a single author, this type of work has always a contribution of many different persons who are hidden in the background but are of great value, whether for their suggestions, orientations, discussions, teachings or even for a valuable friendship. Most of the staff from Concordia University and NRC is not visible, but many people from HR, TI, library, and others have their silent contribution to the success of this work, even though I do not know their names. I thank you all.

Table of contents

List of figures

List of tables

Nomenclature

Symbol	Parameter	Unit
MC	Moisture content	%
MI	Moisture Index	-
RH	Relative humidity	%
T	Temperature	$^\circ$C

Abbreviations

ACH	Air Change per Hour
ASHRAE	American Society of Heating, Refrigerating and Air-Conditioning Engineers
ASTM	American Society for Testing and Materials
CSA	Canadian Standards Association
HAM	Heat, Air and Moisture transfer
HDD	Heating Degree Days
HVAC	Heating, Ventilation and Air Conditioning
ISO	International Organization for Standardization
MoI	Mould index
NBC, NBCC	National Building Code of Canada
NRC, NRCC	National Research Council Canada
OSB	Oriented Strand Board
RMSE	Root Mean Square Error
SGT	Surface Grid Thickness
STR	Stretching Factor
WRB	Weather Resistive Barrier

Chapter 1. Introduction

1.1. Background

Since the beginning of the first cavity walls more than 100 years ago, it was thought that vapor diffusion was the main source of moisture inside the cavity, and this could lead to condensation and bio deterioration of sensitive materials. Around 1960, however, it became obvious that air leakage was the most important source of water migration and ways of avoiding it increased in importance (Quirouette, 1989). Over time, researchers found out that the major part of moisture was due to air leakage (exfiltration) instead of vapor diffusion, mostly through the interfaces and joints between components (Kumaran & Haysom, 2000).

Due to this air movement, the most impermeable, most durable vapor barrier may be rendered virtually ineffective by the presence of accidental or intentional openings and will result in excessive condensation within the wall (Handegord, 1960). ASHRAE (2017) also mentions that calculations of water vapor flow, interstitial condensation, and related moisture accumulation using only water vapor resistances are useless when airflow is involved.

At low air leakage rates, the heat flux is also low and there is almost no influence on the temperature of the leakage path; therefore, the only practical effect is the undesirable moisture accumulation, comparatively higher than with high leakage rates. This happens because at higher air leakage rates, heat flux has a greater contribution and the path becomes so warm that the condition for condensation cease to exist (Ojanen & Kumaran, 1992).

Therefore, the maximum acceptable air leakage rate for the air barrier system ultimately depends on the temperature and relative humidity conditions of both warm and cold sides. The NBC proposes some values of maximum air leakage rates for the air barrier system, which are related to the likelihood of condensation on the cold side: the higher the relative humidity inside, the lower should be the air leakage rate. Those values do not consider the impact of future climate, though, but it is anticipated that extreme weather events will intensify in the future due to a warmer climate. Annual average temperature in Canada may rise about twice the global average and this can lead to building long-term performance issues related to temperature increases and rainfall events, which might become more severe and frequent (Bush & Lemmen, 2019). Therefore, a code-compliant wall - which is supposed to perform well - might show unexpected hygrothermal response because of a different climate in the future.

Besides the value for the air leakage rate, other parameters are also needed because the mechanism which explains air leakage may become very complex: it is related to wind pressures, unexpected gaps, stack effect, indoor and outdoor conditions, shape/size/height of the building, HVAC systems, type of assembly etc. (Lstiburek, 2000). Moreover, the properties of the materials vary within certain ranges and make the situation even more complex (Boardman & Glass, 2020; Hurel et al., 2017).

All these possibilities lead to many different exfiltration paths and simulation tools can help to rank different configurations in terms of risk assessment. Then, after deciding the air leakage path and applying some simplifications to the computational model, it is a good strategy to run the same case considering the variability of the inputs, whether related to material properties (Cornick et al., 2003; Salonvaara et al., 2001; Wang, 2018), climate files (Blocken & Carmeliet, 2006; Cornick et

al., 2003; Cornick, Alan Dalgliesh, et al., 2009), and the geometry itself (Bauklimatik, 2022; Paepcke & Nicolai, 2020).

One 3-year simulation takes around 8 hours to complete and, depending on the extent of the simplifications and variability of the inputs, the number of simulations can reach tens of thousands only for a single city, which means computational capacity and time availability may become a real hurdle: therefore, the fewer the number of simulations and the faster they are, the better. So, finding the best relation between accuracy and simulation time is a crucial task.

With faster simulations, it will be possible to evaluate a higher number of scenarios, helping to design safer and more robust assemblies regardless of the uncertainties of the inputs. In this research, Delphin simulation tool was used to model the hygrothermal performance of wood frame walls with stucco and brick claddings in three Canadian cities: Whitehorse, Vancouver, and Ottawa. Key parameters were explored, for instance air leakage path, air permeability of the insulation, wind driven rain, and opening size. After setting up of the model, the hygrothermal performance of five different positions inside the assembly was addressed considering two air leakage rates under historical and future periods.

1.2. Objective

The goal of this thesis is to assess the effect of different air leakage rates on the hygrothermal performance of wood-frame walls. To accomplish that, some questions were answered:

- What is the influence of the air leakage rate and cladding type on the hygrothermal performance on the inner and outer surface of OSB.
- What is the impact of the air leakage on different geographical locations.
- What is the impact of wind driven rain when acting together with air leakage.
- How the future climate might impact the performance of the assembly when compared to the historical climate.

1.3. Outline of the thesis

Chapter 2 reports a literature review, which includes the concepts related to condensation and the main factors involved; also, the history of condensation and air infiltration into the assembly is explained since the beginning of the studies. The importance of air leakage is explored, its major importance when compared to vapor diffusion is made clear, and a comprehensive explanation of how the science of air leakage was incorporated by the National Building Code over the years is given. Lastly, 1D and 2D computational models and the differences between them are explored, and the details about implementing the 2D model is shown with emphasis on the discretization process and air leakage paths.

Chapter 3 exposes the hygrothermal simulations methodology, with the description of the wall assembly, orientation, climate data, locations of interest for performance assessment, and solver configuration.

Chapter 4 details the setup of the 2D model, explaining the whole process of meshing and its influence on the results in terms of time demand, accuracy, and convergence. The basis for grid

creation, thicknesses, stretching factor, and grid sensitivity analysis are provided. In the end, further steps for manual optimization are shown.

Chapter 5 reports the application of the model considering different air leakage and ventilation rates, wind-driven rain, and climate uncertainty from historical and future periods. The results are discussed after applying the model in different cities and claddings.

Chapter 6 shows the conclusions for each chapter of the thesis and discusses future work.

Chapter 2. Literature review

2.1. Background knowledge on condensation

Condensation can happen on any surface whose temperature is below the dew point of the surrounding air. In other words, any surface which could be in contact with humidified air must be kept above the dew point temperature in order to avoid condensation (Hutcheon, 1963a).

When cold air enters a warm environment and is heated, its relative humidity might drop to very low levels. Air at -15°C and 50% RH holds 0.5 g of water per kg of dry air and, when its temperature goes up to 21°C, the RH level drops to about 5% if the humidity ratio is kept constant. However, the cold air from outside mixes with the indoor air where there is also some moisture generation inside the building (Figure 2.1), which stops the RH level from falling fall that low. This situation is further discussed by Hutcheon (1960) and more variables are addressed.
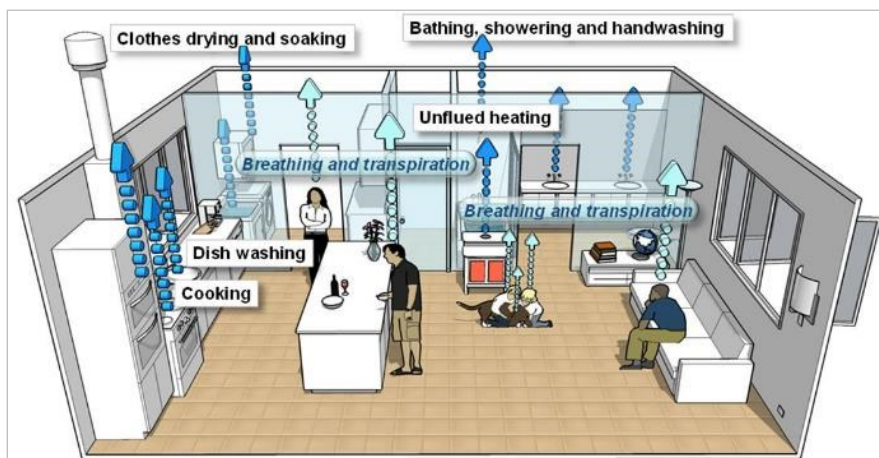
Figure 2.1. Water vapor sources inside a dwelling which can increase relative humidity (ABCB, 2019).

In harsh climates like Canada, indoor conditions may be very different from outdoor conditions; as such, wall assemblies are subjected to gradients of temperature, vapor pressure, relative humidity and these gradients induce vapor and moisture transfer through the layers. Since the most important function of a wall is to keep the indoor conditions within acceptable limits, it must meet many requirements regarding the control of heat, moisture and air flows (Hutcheon, 1963b, 1953).

Tsongas (1995) analyzed the influence of different indoor RH levels and moisture generation rates over the moisture content of the exterior sheathing, where condensation is likely to occur. In houses with low moisture generation and high ventilation rate, vapor barriers may not even be necessary since the RH inside is kept at low levels. On the other side, houses with high moisture generation rate and low ventilation means high indoor RH levels and vapor barriers gain importance. It also might happen that low moisture generation rate with low ventilation is even worse than high moisture generation and high ventilation because ventilation is very important to reduce the indoor RH level.

In a multi-layer assembly, what happens in each layer depends on their properties and the influence of these properties on the overall behavior of the wall was discussed by Babbitt (1939) and Rowley et al (1940) when analyzing different wall configurations. In the case with a non insulated cavity (Figure 2.2a), the heat transfer is high enough to keep the exterior sheathing at such a

temperature that the saturation vapor pressure is higher than the real vapor pressure and condensation does not happen. However, when adding insulation (Figure 2.2b), there is a reduction of heat transfer towards the exterior sheathing and its temperature gets so low that the curves of saturation vapor pressure and real vapor pressure might cross, leading to condensation problems on the inner side of the exterior sheathing.

| a) No insulation | b) With insulation |
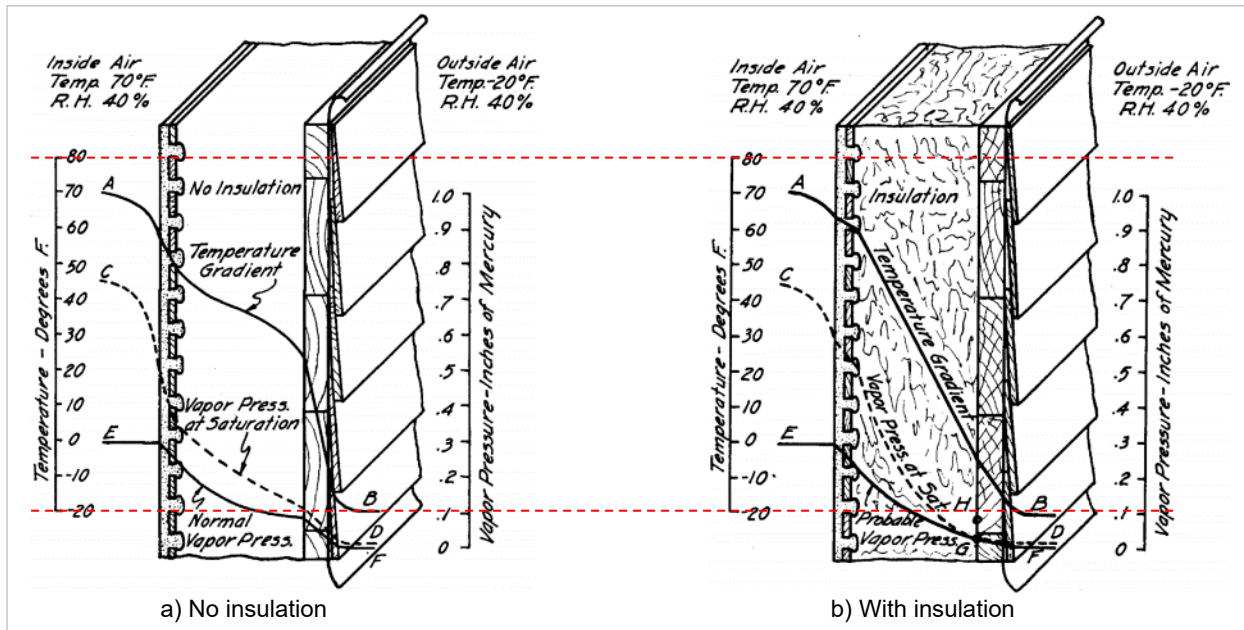
Figure 2.2. Temperature and vapor pressure gradients inside a wall (Rowley et al., 1940).

Figure 2.2 matches with the basic wall described by Hutcheon & Handegord (1980), which was in common use in the 1900s for building simple dwellings: vertical wood studs nailed to the top and bottom plates and wood boards applied mostly horizontally as sheathing; over this, one or more layers of building paper (the latter being tarred) followed by some sort of horizontal wood siding, shingles or rendering. Plaster on wood lath was common on the inside and this wall was accepted for many decades as a good solution against very cold temperatures between -20°C to -40°C; later, other types of walls were developed having this one as a basic standard and great development occurred regarding insulation with a variety of different materials.

Figure 2.2b shows a case where condensation happens in between the sheathing and the insulation, but it can happen in other places also. Rousseau (1984) used the terms "surface condensation" and "concealed condensation" to designate a visible or a hidden condensation problem, respectively. This means the condensing surface does not necessarily need to be visible, it can be hidden by other layers and the user may not even realize the problem is there until it is too late and the damage is already extensive.

When condensation is concealed, four simultaneous factors need to be present (Figure 2.3): a source of moisture, a travel path inside the assembly, a driving force, and a temperature gradient (Figure 2.3). While with those four factors moisture problems might occur, there is still a chance that they do not happen because for a moisture problem to occur it also depends on how

sensitive the materials are, how wet they get and for how long (Rousseau, 2003). In other words, for the moisture problem to happen, there must be a susceptible material (Straube, 1998).
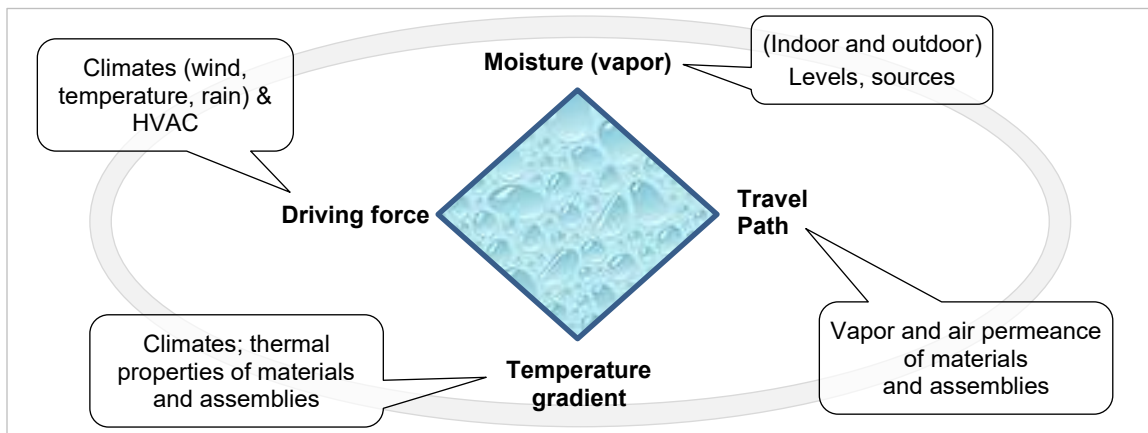
Figure 2.3. Four factors required for moisture to condense in interstitial places (adapted from Rousseau, 2003).

There is something implicit to Figure 2.3, though: the water vapor that reaches the cold surface must be trapped and has nowhere to go or, at least, there is more vapor going towards the cold side than vapor going away from it, which means moisture accumulation. If the cold surface is a sheet of metal, which is vapor impermeable, condensation may occur faster than if the cold surface was plywood, since plywood can absorb part or all the vapor. If the vapor permeance of the cold layer is higher than the amount of vapor going towards it, there might be no moisture accumulation if the surrounding conditions are favorable to take the vapor away.

A comprehensive experimental work was undertaken in the 30s with the objectives of better understanding the relation among insulated walls, indoor/outdoor conditions, vapor barriers and materials properties. Tens of different wall configurations were analyzed as small samples or as parts of the walls of a full bungalow inside a cold room (Figure 2.4). Indoor temperature was kept constant at 21°C and relative humidity was set to different levels: 20, 25, 30 and 40% according to the test being performed; outdoor temperature varied in cycles between approximately -15°C and -25°C as a way of reproducing the real daily variation.

This study took some years to complete and rendered many papers and reports[1]. The conclusions are very well detailed for each wall and it would be impossible to reproduce all of them here; the main findings include (Rowley et al., 1940, 1941, 1947; Rowley & Lund, 1944):

- The lower the outdoor temperature in winter, the lower should be the relative humidity inside to avoid condensation/frost problems.
- There was no frost accumulation on the exterior sheathing when the indoor relative humidity was 20%; all the walls performed adequately, even the ones without vapor barrier. At 25%, the walls without vapor barrier performed well for short periods and the results varied according to the wall configuration. At 30% some of the walls showed frost accumulation on the exterior sheathing, which

---

[1] Those reports can be found at https://conservancy.umn.edu/handle/11299/124212. (Accessed on Aug 10, 2023).

was heavier at 40%. The heaviest accumulation, however, was at the line of joints between the insulation bats.

- When the interior layers have a vapor permeance of 1.16 perms[2] (approximately 66 ng/s.m^2.Pa) or less, the vapor diffusion is reduced and no serious problems with condensation are expected within the wall.

- Some walls performed well without frost accumulation on the exterior sheathing but did present frost accumulation at the joints between the vapor barrier and the top plate, as a possible indication of air leakage.
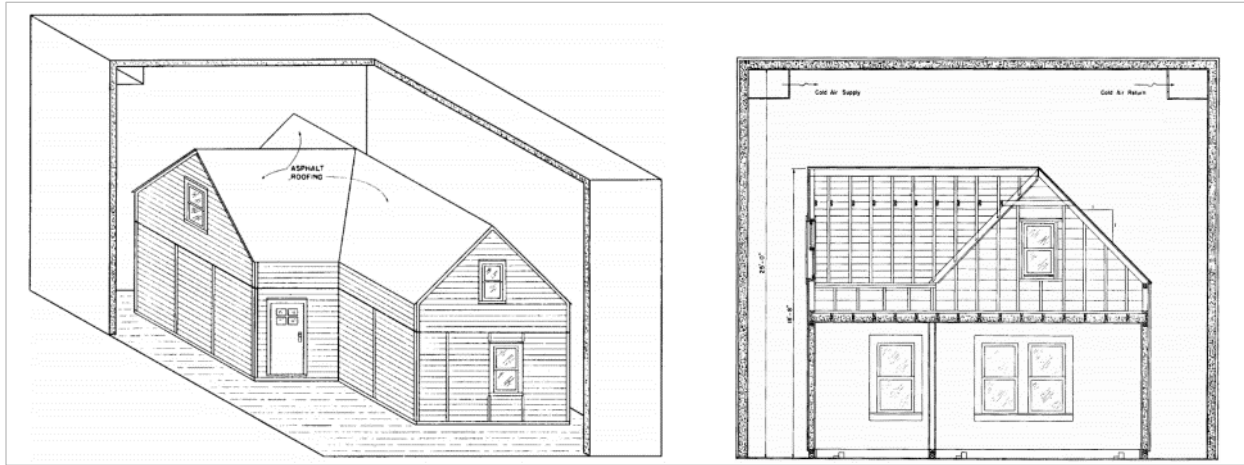
Figure 2.4. 3D view and a cross section of the test bungalow inside the cold room (Rowley et al., 1941).

Once the problem with condensation has been detected, it might be difficult to say precisely where the liquid water came from when inspecting an assembly, since it could be a consequence of any number of sources including rain infiltration. However, since condensation is related to the dew point temperature, one way of being more certain if it is really happening is by instrumenting and measuring the temperature of the innermost and outermost layers and the relative humidity and temperature of the cavity air. Then, if the dew point of this air is higher than the temperature of the outermost layer for a prolonged period, condensation may be one of the sources of water. Although this explanation applies to the cold season, it is also valid for reverse condensation during summertime, when hot air from outside reaches the inner surface at the interior side, cooled down by the HVAC system. Analogous method can be used to detect rain infiltration (Quirouette, 1999, p. 13).

Straube (2001) mentions that reverse condensation is also linked to the vapor permeance of the warm side of the assembly. If the vapor generated outside due to the solar energy can diffuse through the inner part of the wall (where usually the vapor barrier is), there might be moisture accumulation behind the vapor barrier. Although reverse condensation may be more common in mild climates, it can also be problematic in cold ones depending on how the assembly is built, so the dynamics of the system must be analyzed with care. Kan & Piñon (2007) say that adjusting the ACH behind the cladding may be able to reduce or even eliminate sun-driven condensation, since any accumulated moisture is washed away by the circulating air.

---

[2] 1 US perm = 1 grain of water per hour per square foot per inch of Mercury = 57.21 ng/s.m^2.Pa.

Derome et al. (2010) studied 18 different walls assemblies in seven locations across USA and found that large inwards vapor pressure gradients might happen depending on the co-occurrence of rain followed by sun, absorptivity of cladding and the presence of air cavity and ventilation. In case of vapor-tight interior finishes, the vapor transport could be hindered, and moisture would accumulate. The use of hygrothermal simulations, after benchmarking, helps to select the best design for each location.

Maref et al (2007), after analyzing the experimental data from exterior surfaces exposed to solar radiation in summer, found that the heating effect of the exterior surface generates water vapor towards the interior side of the assembly. The consequences are related to an increase of the relative humidity of colder surfaces, which may lead to moisture accumulation and condensation problems.

A practical example of summertime condensation might happen in basements, especially if they are ventilated: when hot and moisture-loaded outdoor air enters the basement and reaches the walls, condensation is likely to happen due to the fact their temperature is probably close to the ground temperature (Rousseau, 1984). For instance, if the outdoor relative humidity is 50% RH at 30°C, this means a dew point of about 18°C; any lower temperature may lead to condensation. Another example might happen due to morning dew. After losing energy to the sky at night, the cladding gets cold and condensation might happen behind it; as the temperature raises during the day, the condensate evaporates and is driven into the cavity (Robinson, 1992).

Most of the time, however, summer condensation is limited to air-conditioned buildings, since the warm outdoor air needs to reach a cold surface whose temperature is below the dew-point of the warm air (Achenbach & Trechsel, 1983). The authors also say:

> *Condensation control in buildings is a systems problem. It is characterized by a continuous, nonuniform release of moisture within a building, which must be re-moved by exfiltration of air, ventilation, air-conditioning, or dehumidification, to maintain an indoor dew point or relative humidity that provides comfort, prevents condensation, and promotes the durability of the building itself.*

This holistic approach was also emphasized by Bomberg & Onysko (2002): when vapor barrier became a requirement in the National Building Code in the 50s, it gave the impression to engineers and architects that moisture control was fully addressed and some jurisdictions stated that no condensation was allowed; however, vapor diffusion was one of the few sources for moisture inside the walls. Moreover, the approach of no condensation at all was not correct in general because moisture storage is possible in many materials without any harm.

In the case of wood materials, moisture-related problems like mould and decay are dependent on the species that have been used to build the frame, since each specie offers different resistance against deterioration and some may need more robust treatment (USDA, 2010, Chapter 14). In Canada, the most common species to make lumber belong to the group SPF (Spruce-Pine-Fir) and they are classified as slightly resistant or nonresistant, according to CMHC (2014).

Although the physics of condensation basically leads to reaching the dew point temperature of the surrounding air, how to avoid that in the field is not a simple task because many interrelated factors

are involved. As a basic guideline, though, ASHRAE (2017, p. 36.10) gives some suggestions (among others):

- Insulate the building envelope so that the temperature of the indoor layer almost never gets below the dew point of the indoor air for typical relative humidities.
- Minimize air leakage (exfiltration and infiltration) by making the envelope as airtight as possible.
- Never design layers with vapor tight materials on both sides because there will be no option for the moisture to escape.
- Avoid air gaps in the envelope, since this can facilitate air/moisture movement inside the assembly.

Crandell (2021, 2017) cites two design approaches to control water vapor: permeance controlled approach and temperature controlled approach (Figure 2.5). The permeance approach relies on the fact that any possible excess of vapor is maintained within tolerable limits by using layers with adequate permeance so that condensation never happens; the envelope assembly is designed to dry to the exterior in cold climates. The temperature approach is fundamentally based on the idea of keeping moisture-sensitive materials warm enough to avoid high relative humidity levels; the envelope is designed to dry to the interior during cold seasons. Both approaches work well but the second one is less prone to the consequences of exfiltration during the winter season and can be balanced to work in all climates.
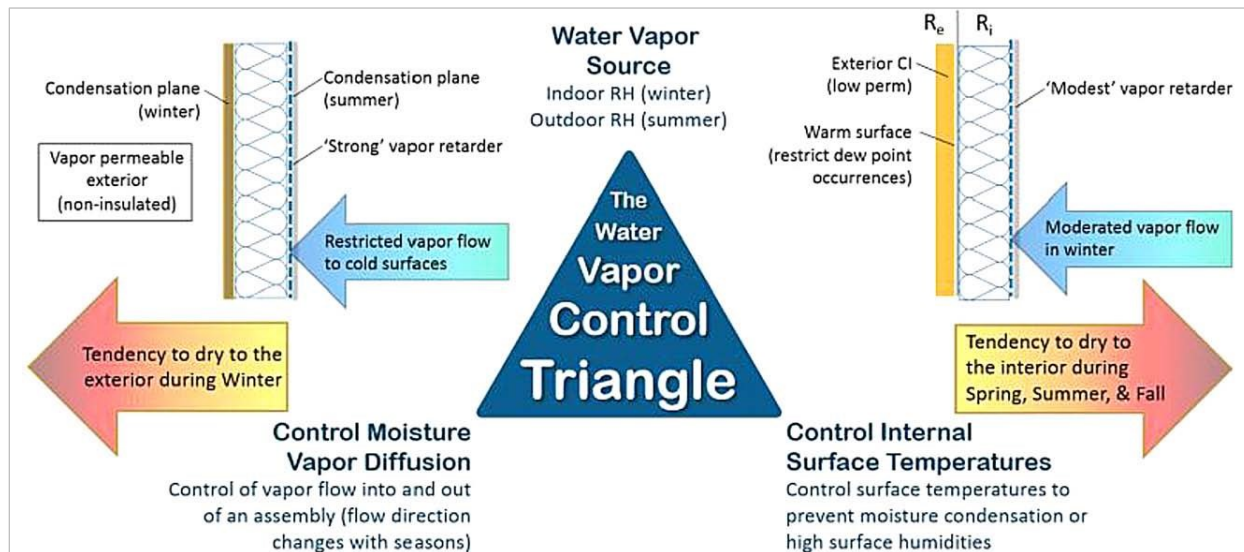
Figure 2.5. Two accepted moisture control design approaches for cold climates (Crandell, 2017).

2.2. Air leakage

The term "air leakage" is used on at least two occasions. First, as a reference to the amount of air that leaks through the entire envelope of the building; this approach is usually related to energy consumption, since heat losses can be high, leading to higher energy consumption during winter. The path for those leakages is mostly represented by the interfaces/connections between exterior walls and ceilings, doors, and windows. Furthermore, the interface between components of the wood-frame system and their connection to the foundation may also increase the air leakage rate and increase the ACH of the building. The discussion about those leakage paths (Figure 2.6) can be found elsewhere (Ananian et al., 2019; Cardoso et al., 2020; CMHC, 2007; Ge & Krpan, 2009;

Gullbrekken et al., 2020; Kalamees et al., 2017; Khemet & Richman, 2021; Straube, 2007; Wolf & Tyler, 2013a, 2013b) and a review of the airtightness of Canadian houses is shown by Parekh et al (2007).
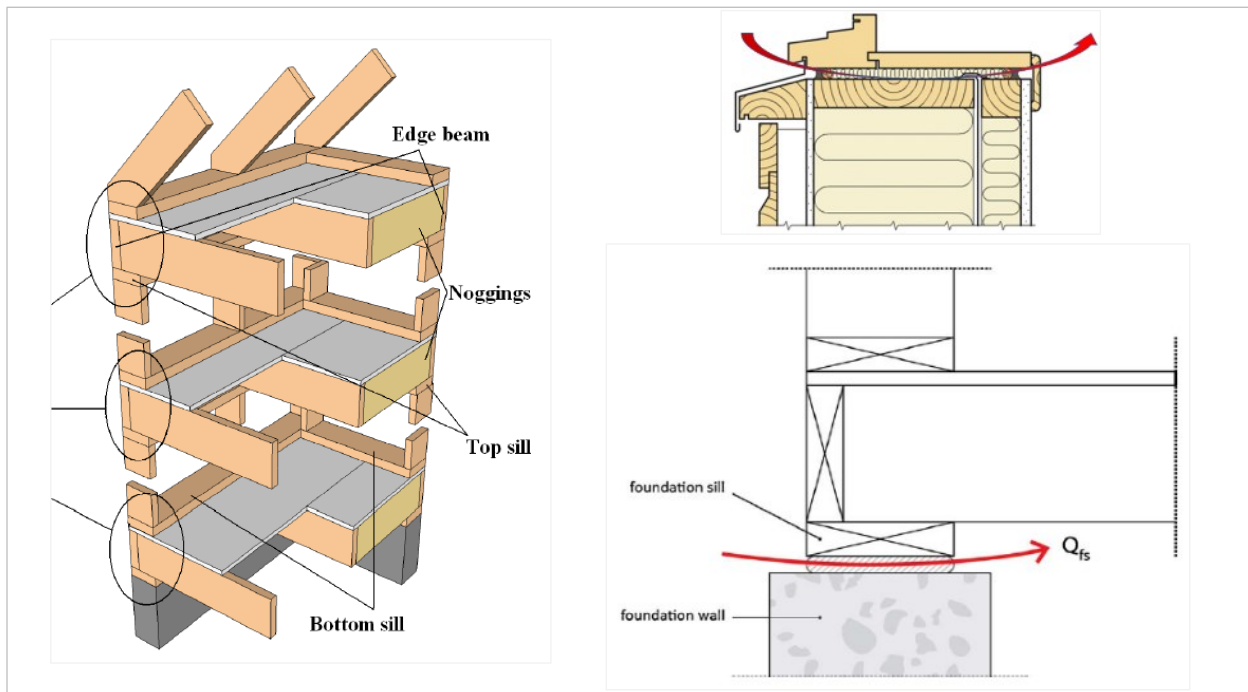
Figure 2.6. Examples of air leakage paths of the whole building (Gullbrekken et al., 2020).

The second occasion when "air leakage" is used is to designate infiltration/exfiltration through the opaque envelope, when the air moves into the insulated cavity through undesirable holes, electrical boxes, defective connections etc. This issue is related to the concern of condensation inside the assembly, since the moisture-laden warm air might reach cold surfaces.

Although "air leakage" may be a self-explanatory pair of words, Garden (1965) translates this subjective idea into a more solid concept:

> *Air leakage is the uncontrolled movement of air through walls and roofs, both into a building (infiltration) and out of it (exfiltration), and the interchange of air from the building with that in spaces in the building envelope. Pressure differences that cause infiltration and exfiltration are produced by wind, chimney effect, and the operation of mechanical ventilation systems.*

The author also explains the consequences air leakage can bring:

> *Air leakage is important because it normally means dirt and odor entry, increased cost of winter heating and summer cooling, cold drafts, and more difficulty in maintaining a controlled relative humidity. Condensation resulting from exfiltration during cold weather can cause rapid deterioration of the building fabric, producing both hazardous situations and the need for costly repairs… Excessive efflorescence, mortar joint spading, discoloration of stonework, masonry unit displacement, corrosion of metals, or icicles hanging from walls are indications of an excess of water in the wall that may be due to air leakage.*

Then, while diffusion happens due to partial vapor pressures gradients, air leakage is the movement of a quite substantial amount of air which carries rates of water vapor according to the balance of the psychrometric chart. Vapor diffusion is related to the concept of "vapor barrier" and exfiltration to the concept of "air barrier", reasons why a clear definition of both is worthwhile (Quirouette, 1985, 1989):

- Vapor barrier: is a material that offers high resistance to the diffusion of water vapor, being used to separate an environment which is at high vapor pressure from an adjacent one which is at low vapor pressure. It is usually located in the warm side of the assembly or in a location near enough the warm side so that its temperature does not reach the dew point during the cold season (also item A-9.25.4.3.(2) of the current NBC). Small cuts or openings on the vapor barrier do not affect its overall performance on reducing vapor diffusion.

- Air barrier: is a system, not a single material, which has the function of preventing both infiltration of the outdoor air into a building and exfiltration of the indoor air to the outside, avoiding problems with moisture deposition, loss of energy and infiltration of rain together with the current of air. Unlike vapor barriers, air barriers must be continuous, since small openings and cuts may compromise the entire system. And, obviously, materials which compose an air barrier must have low air permeability.

Handegord (1960) explained that vapor barriers are, in general, special building papers, membranes, or coatings designed for this specific purpose; some other materials, like insulations and sheathing membranes, may act as vapor barriers because of their properties even though they were not designed to act like that. Whereas a few building materials are impervious to vapor, like glass and metal, a considerable number of materials provide sufficient resistance to be used for vapor control purposes.

Hansen & Brandt (2010), after analyzing intentional damages/holes in the plastic-based vapor barrier behind the interior gypsum board, found that moisture accumulation did not change when comparing with the same assembly with a continuous vapor barrier; this is because the intact indoor cladding already provides enough resistance against vapor diffusion and it is assumed there is no air convection.

Kumaran & Haysom (2000) mention that the use of vapor barriers was introduced in the 1930s to control vapor diffusion into walls and attics; however, when interior humification started in 1950s, moisture accumulation again became a problem in many houses. The same view is given by Hutcheon (1989), who says that commercial and institutional buildings in the 50s which had traditionally been operated at low indoor relative humidities started having problems after being humidified during winter.

Since the beginning of the first cavity walls more than 100 years ago, it was thought that vapor diffusion was the main source of moisture inside the cavity, and this could lead to condensation and bio deterioration of sensitive materials. Around 1960, however, it became obvious that air leakage was the most important source of water migration and ways of avoiding it increased in importance (Quirouette, 1989). Over the time, researchers found out that the most of the moisture was due to air leakage (exfiltration) instead of vapor diffusion, mostly through the interfaces and joints between components (Kumaran & Haysom, 2000).

CMHC (1992), Bomberg & Brown (1993) and Bomberg & Onysko (2002) explain that the understanding of the performance of walls came mainly from the extreme climate in the Prairies of North America, where cold temperatures magnify any fault in the ability of the wall to maintain environmental control. Then, after pioneer research in the University of Minnesota in the 30s, building paper was accepted as a weather barrier, limiting the movement of air and rain while permitting moisture to breathe outdoors. Later, wall cavities were filled with different insulations (wood chips, shredded paper, and mineral fiber batts) for comfort reasons, but this lowered the temperature of the exterior sheathing and condensation appeared. Therefore, vapor barriers were introduced, and homes built as early as the 1940s already included weather resistive barriers outside and vapor barriers inside. Hutcheon & Handegord (1980) say that by the time of the post-war building boom in 1946, insulation and vapor barriers were being widely used in new housing construction.

Lstiburek (1992) reports that insulation was the first major change to the building practice and it was done for comfort reasons as energy was not expensive and "people got tired of sheets freezing to outside walls". This change had two big consequences: a) interior conditions were more pleasant and stable throughout the rooms and b) the outer layers of exterior walls got colder for longer. However, due to high rates of air leakage, problems with condensation were not common: they started later as the airtightness of the buildings increased due to the availability of new building materials, construction techniques at lower costs and new energy requirements. The same view is shared by Robinson (1992).

Hutcheon & Handegord (1980) say that condensation problems have not been widespread and those that have occurred have usually been associated with holes and gaps in the interior cladding and vapor barrier, which may be due to the installation of electrical wiring. By then, a common complaint from the occupants during winter was about cold air leakage into the house through electrical receptacles in exterior walls. Furthermore, wood frame construction has a lot of discontinuities and the effect of drying and shrinkage of the studs and joists may induce cracking between the interior cladding and the framing members, leading to air leakage.

Due to this air movement, "the most impermeable, most durable vapor barrier may be rendered virtually ineffective by the presence of accidental or intentional openings … and will result in excessive condensation within the wall" (Handegord, 1960).

According to Hutcheon (1953):

> *The flows of heat, moisture and air in walls have implications not only by themselves, but for all the other considerations listed. Air merits major consideration mainly because of its influence on heat and moisture flow. The overall transmission of heat, air and moisture through a wall can affect the ease with which the desired environmental conditions may be maintained, and so may have a marked influence on the cost of operation of a building.*

Wilson & Garden (1965) explain a situation with air leakage through a 30 cm thick unplastered brick wall with no inside finish, common practice for walls between suspended ceilings and the floor above. While the moisture accumulation due to vapor diffusion reaches the amount of only 0.22 kg/m^2, air leakage might lead to a much higher amount of 36 kg/m^2 under the same conditions. So, a system of caulking to eliminate those cracks and the use of plastered masonry would increase air tightness and help solving the problem; Hutcheon (1963a) says that this action can

reduce the air leakage by a factor of as much as 100. In another example, with brickwork and cracks, Latta (1976) explains that air leakage has a much greater potential for carrying moisture than vapor diffusion even when neglecting the cracks at the columns. Figure 2.7 illustrates both situations.
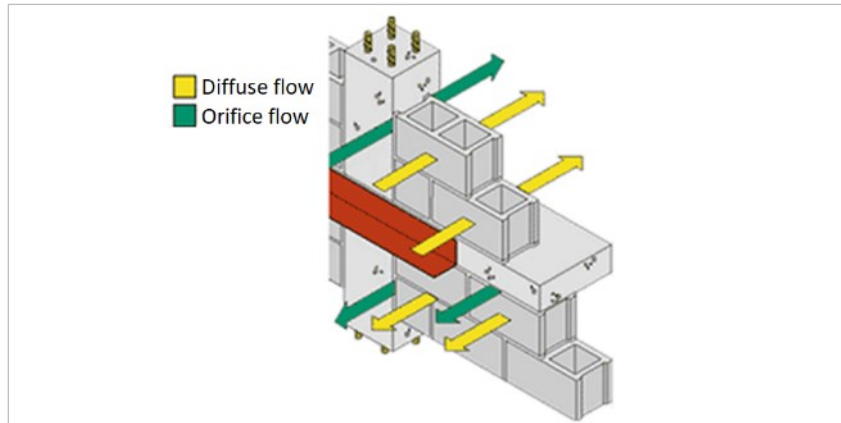
Figure 2.7. Water vapor transport through diffusion and air leakage.
(https://www.wbdg.org/resources/air-barrier-systems-buildings).

Rousseau (1984) also shows the same findings when comparing two situations: a 1 m^2 painted gypsum wall, one continuous and the other with a 4 cm^2 hole under a pressure difference of 10 Pa (Figure 2.8). The air leakage carries about 100 times more moisture than diffusion alone. Some years later, Rousseau & Brown (1995) added:

> *It is now well established that air movement is the dominant means of moisture transport through the building envelope as well as a major component of heat transfer. A high proportion of the problems associated with building envelope deterioration can be attributed to inadequate control of air leakage. The air-barrier system is the assembly installed to provide a continuous barrier to the movement of air. Its performance and durability are of prime importance to the durability of the whole building envelope.*
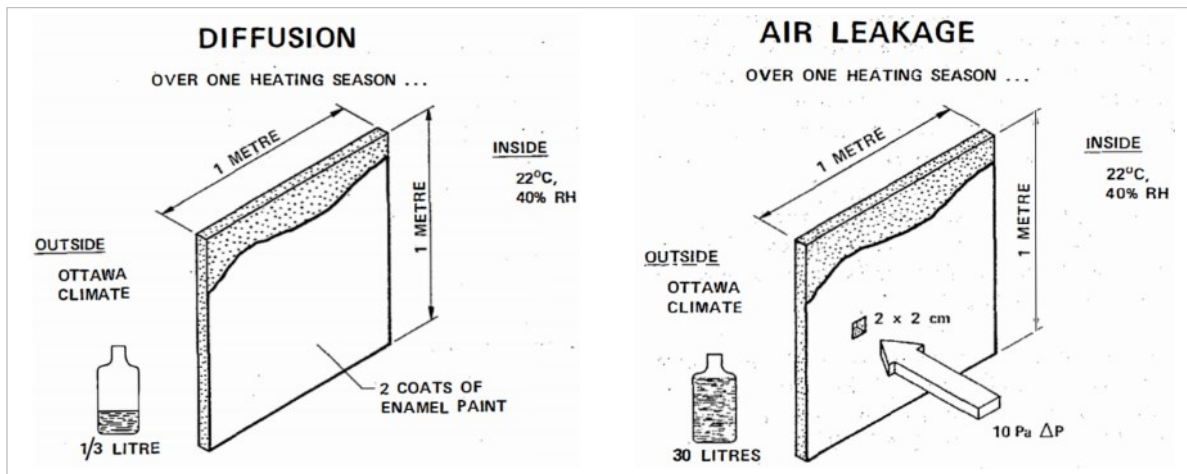
Figure 2.8. Moisture accumulation comparing diffusion and air leakage (Rousseau, 1984).

Handegord (1982) says that a vapor barrier is still effective even with small holes on it; however, if this vapor barrier is also an air barrier, those holes will allow much greater moisture transfer and accumulation under an air pressure difference. Hutcheon (1963a) explains that a few small holes and cracks do not add much to the vapor transfer by diffusion because the area is small even though the permeability may be large. However, without an air barrier these holes are a free way for the air to move even under small pressures, carrying a troublesome amount of moisture towards cold surfaces.

Using a computerized analysis, Tsongas (1995) compared the efficacy of a vapor barrier in a wall subjected to an air leakage rate of 0.15 L/s.m^2. Whether the wall had a vapor barrier or not, the effect of exfiltration is more important and induces a higher level of moisture content in the exterior sheathing: "… exfiltration essentially diminishes the effectiveness of the vapor retarder. When exfiltration is present it is much more important than diffusion as a moisture migration mechanism."

Ojanen & Kumaran (1996), in a simple calculation considering a 2 cm diameter hole, show that the amount of moisture due to air leakage through that single hole can be 100 times greater than the amount due to diffusion only. Similarly, after an extensive laboratory experiment, Kölsh et al (2016) conclude that one single tiny imperfection in the sealing can increase the permeability of the assembly by a factor of 100 if air movement is not eliminated.

A very clear emphasis about air leakage and vapor diffusion is found in ASHRAE (2017, p. 26.6): "calculations of water vapor flow, interstitial condensation, and related moisture accumulation using only water vapor resistances are useless when airflow is involved".

2.2.1. Air leakage and the National Building Code of Canada

According to Brown et al (1998), the National Building Code incorporated the science behind air leakage in the 1995 version, reflecting the industry's knowledge, experience, and practice, acknowledging that air movement is dominant factor in the transport of moisture through building envelope assemblies. Also, due to the high influence of air movement on heat transfer, the importance of an air barrier would be also recognized in the 1997 version of the National Energy Code. This knowledge is present in the current version of the NBC (NRCC, 2020, sec. A-9.25.3.1.(1)), which says:

> *The majority of moisture problems resulting from condensation of water vapor in walls and ceiling/attic spaces are caused by the leakage of moist interior heated air into these spaces rather than by the diffusion of water vapor through the building envelope.*

Protection against air leakage must be provided by a system of air-impermeable materials joined with leak-free joints. However, airtight joints are difficult to obtain in practice and this might compromise the efficacy of the air barrier system; also, the air-barrier and the vapor-barrier system in conventional wood-frame constructions are usually represented by a single membrane that act as a barrier against moisture and against the movement of the interior warm air into the insulated cavity. So, special care should be taken to avoid areas where bulk air movement can occur (like electrical boxes). Lux & Brown (1989) emphasize that "the point to be noted here is that it is not sufficient to include impermeable materials in the air barrier system; a leak-free air barrier system results from having these materials joined with leak-free joints".

Air barrier systems are not redundant and, in terms of risk analysis, if its requirements are not met in practice, condensation problems may happen; so, uncertainties in condensation control are primarily related to uncertainties in air barrier performance. Therefore, it is much more effective to provide means of reducing condensation assuming that the air barrier will be defective at some point in time than trying to duplicate the air barrier itself; sooner or later, both of them will fail to some extent, the air flow will be established and the condensation problem will be there as if there was only one air barrier. (Janssens & Hens, 1998). These same authors, when performing sensitivity analysis of a roofing system, concluded that the quality of the vapor barrier has no influence on controlling interstitial condensation if the quality of the air barrier is uncertain. So, it is important the building envelope has some control measures to prevent severe moisture problems due to inevitable air leakages (Janssens & Hens, 2003).

Although having a single element able to solve all the problems with condensation would be desirable, the physics behind the problem does not work like that. Effective management of moisture is the result of controlling heat, air and moisture transfer through the careful choice of material properties; failure on managing one of these three factors may cause serious problems, e.g., premature deterioration, mould growth, drop in performance, high energy costs, among others (Rousseau, 2003).

The NBC requires that air barrier systems provide a continuous barrier to air leakage from the interior of the building into the wall assembly to prevent excessive moisture condensation during the cold season. For that, the system shall possess "characteristics necessary to provide an effective barrier to air infiltration and exfiltration under differential air pressure due to stack effect, mechanical systems or wind" (item 9.25.3.1).

Since the word "effective" for a complex system raises some questions about what is an effective air barrier system, Lux & Brown (1989) comment that "channel flows" happen when air goes through channels and passages in the building envelope. Usually, air enters the wall due to the presence of some orifices (which may be hard to find) and exits somewhere on the façade; unfortunately, the path between interior and exterior openings cannot be easily determined. However, since the air barrier is a system composed of an assemblage of simple materials (Figure 2.9), it is likely that the air leakage path is in between the joints of many single components.
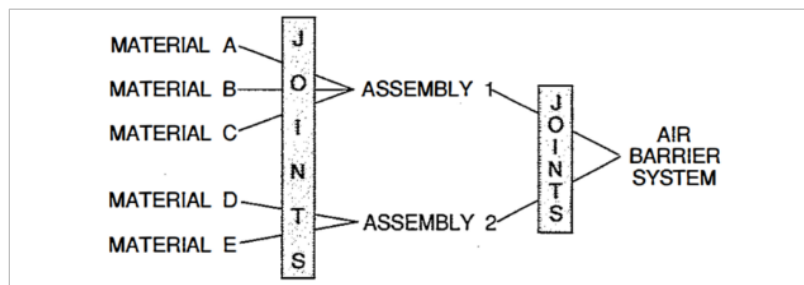
Figure 2.9. Many elements make up the air barrier and proper detailing of joints is critical to its effectiveness (Lux & Brown, 1989).

The NBC also emphasizes this detail saying that (item A-9.25.3.1.(1)):

> *Openings cut through this membrane, such as for electrical boxes, provide opportunities for air leakage into concealed spaces, and special measures must be taken to make such openings as airtight as possible. Attention must also be paid to less obvious leakage paths, such as holes for electric wiring, plumbing installations, wall-ceiling and wall-floor intersections, and gaps created by shrinkage of framing members.*

One relevant aspect of air leakage is that at low rates, the heat flux is also low and there is almost no influence on the temperature of the leakage path; therefore, the only practical effect is the undesirable moisture accumulation, comparatively higher than with high leakage rates. This happens because at higher air leakage rates, heat flux has a greater contribution and the path becomes so warm the condition for condensation cease to exist: higher temperatures mean lower relative humidity for the same rate of moisture of the warm indoor air (Ojanen & Kumaran, 1992). Bomberg & Onisko (2002) and Kumaran & Haysom (2000) cite this behavior to explain the absence of moisture problems in old and leaky walls: the wall is so warm that condensation cannot occur; even though the warming effect dominates the propensity for condensation, there will be a price to pay related to energy efficiency.

Moisture accumulation also varies according to outdoor temperature (geographical locations) since water vapor needs temperature below the dewpoint to produce liquid water or ice. For instance, Figure 2.10 shows the values of moisture accumulation and outdoor temperature in different cities (nine in Canada and three in Finland) for the same air leakage rate (0.98 L/s.m^2 at 21°C and 30% RH): in general, the colder the city, the higher the amount of moisture, but this might vary a little because of other factors, such as winter duration (Ojanen & Kumaran, 1992). In very cold cities like Resolute Bay, Winnipeg and Sodankylä, the moisture accumulated at the end of the period does not go back to the initial amount, which means there will probably be moisture accumulation along time and deterioration of the system when comparing to the cities where there is no moisture accumulation.
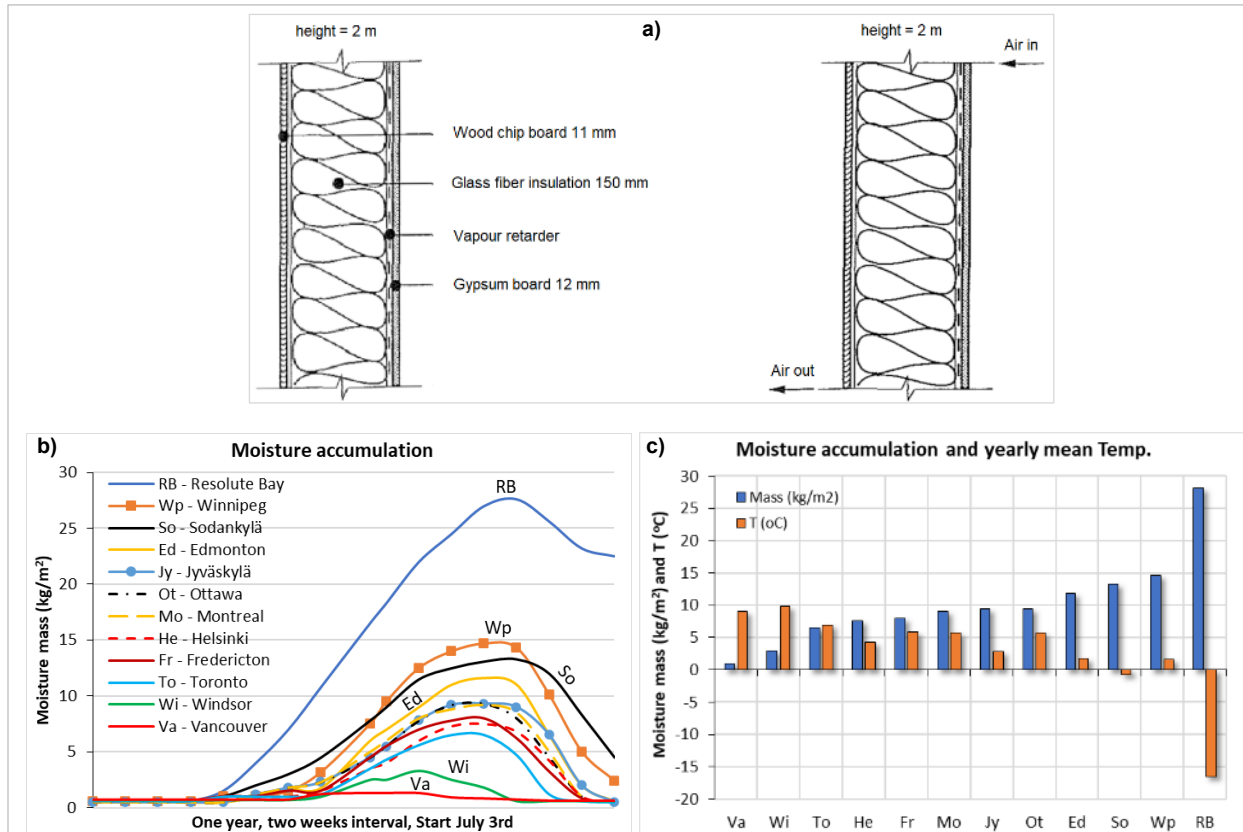
Figure 2.10. a) wall configuration; b) mass of moisture per surface area as a function of time; c) moisture accumulation and outdoor temperature for different cities (adapted from Ojanen & Kumaran, 1992).

In an experiment with a 2" x 4" residential wall with a type II vapor barrier inside, evenly distributed exfiltration was induced by a pressure difference of 50 Pa. When comparing different indoor conditions, 36% RH at 21°C and 48% RH at 21°C, Figure 2.11 shows that moisture accumulation at 48% RH is higher than at 36%. This means the tolerable air leakage rate will strongly be related to the humidity level of the indoor air (Ojanen & Kumaran, 1996).
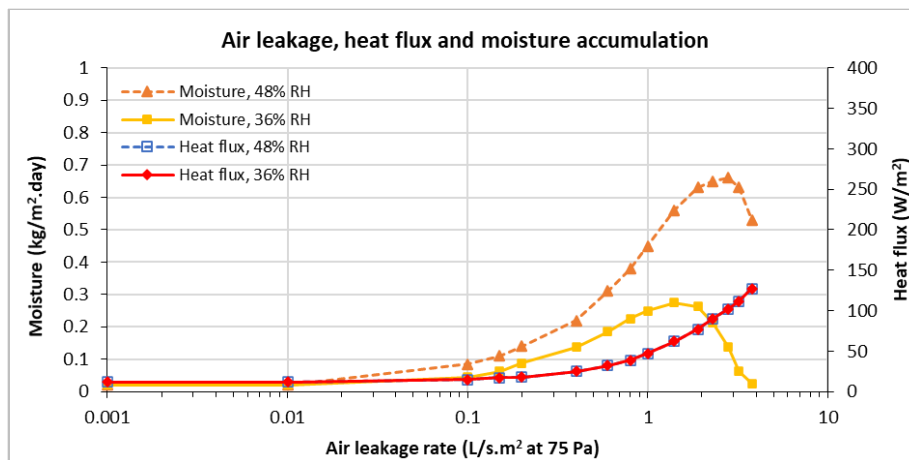
Figure 2.11. Correlation between air leakage rate, heat flux and moisture accumulation, indoor conditions at 21°C, 36% RH and 21°C, 48% RH (adapted from Ojanen & Kumaran, 1996).

In another study, Ojanen & Kumaran (1996) varied the properties of either the materials or the whole system, like air leakage rate. Indoor temperature was 21°C and the cavity was 140 mm deep. After performing a sensitivity analysis, the results in Figure 2.12 show that:

- Moisture accumulation increases as air leakage increases (Figure 2.12a) as long as the assembly is not warmed up because of very high air leakage rates.

- For the same air leakage rate, moisture accumulation decreases as the vapor permeance of the exterior layer increases (Figure 2.12b). This means greater air leakage rates may be tolerated with more vapor permeable sheathing.

- For the same air leakage rate, the higher the indoor RH, the higher the moisture accumulation; also, exterior insulation keeps the OSB temperature at higher levels and decreases the accumulation of moisture (Figure 2.12c).
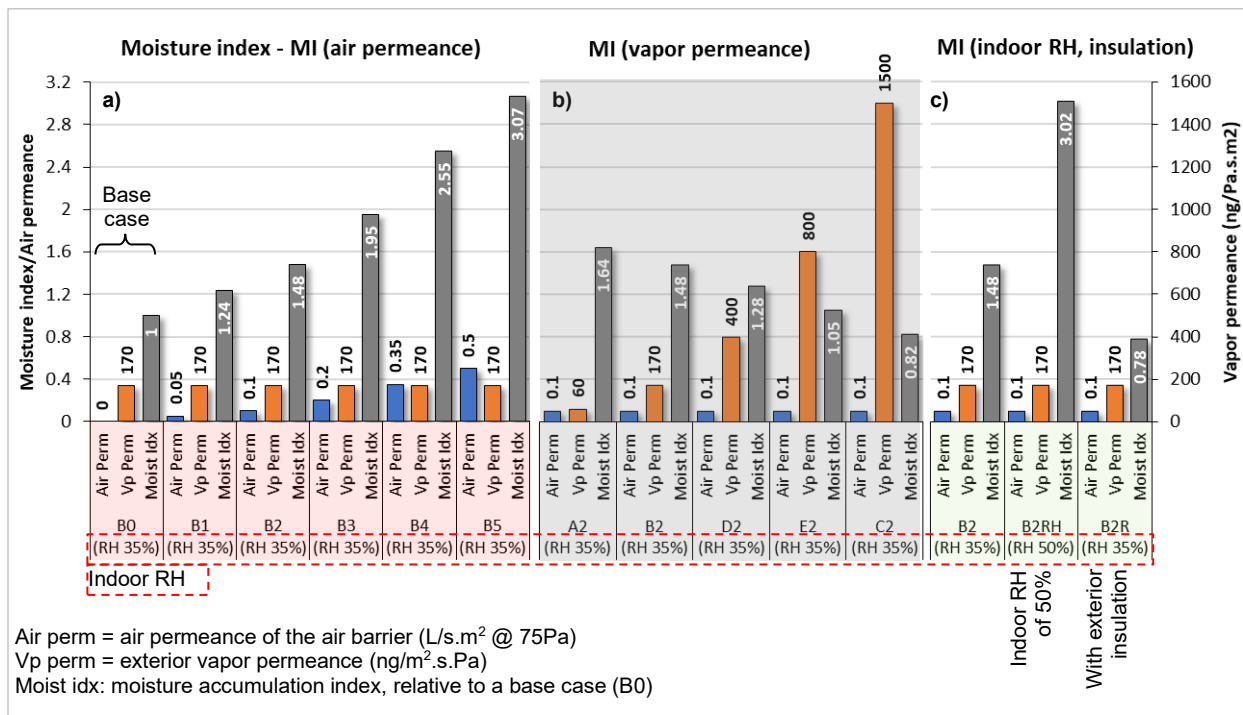
Figure 2.12. Sensitivity analysis of moisture index as a function of a) air permeance, b) exterior vapor permeance and c) interior RH and exterior insulation (adapted from Ojanen & Kumaran, 1996).

In a correlated study, Kumaran & Haysom (2000) analyzed the influence of air leakage and exterior insulation on moisture accumulation by performing another set of simulations: when comparing to the base case (B0, diffusion only), air leakage of 0.1 L/s.m^2 @ 75 Pa increased the moisture content about 70%; adding external insulation (RSI 0.75) with the same leakage rate, accumulated moisture decreased by about 50%. The rate between exterior to in-cavity insulation was 0.75/3.52 = 0.214 (roughly 0.20) and this value was enough to control moisture accumulation in Ottawa-area climate with indoor RH of 36%. Figure 2.13 shows the configuration of the walls and the accumulated moisture profiles over one year.

Figure 4. Wall B0   Figure 5. Wall B2   Figure 6. Wall B2R
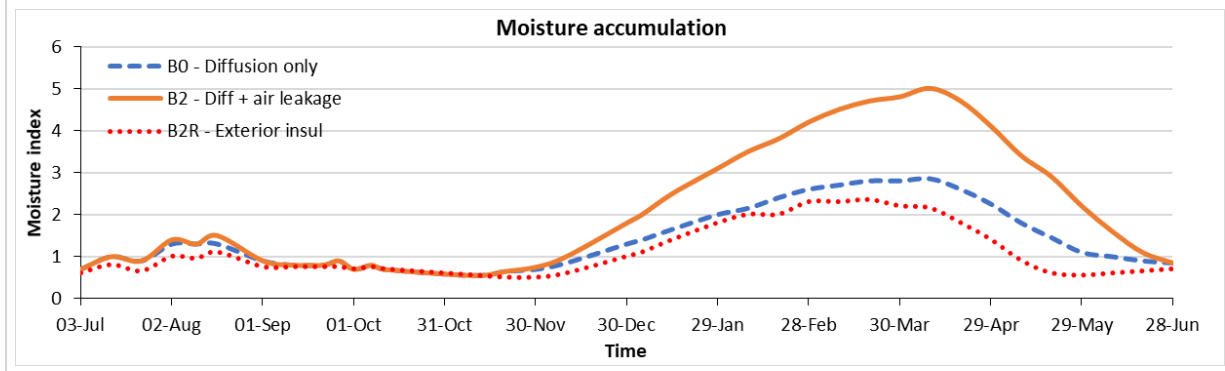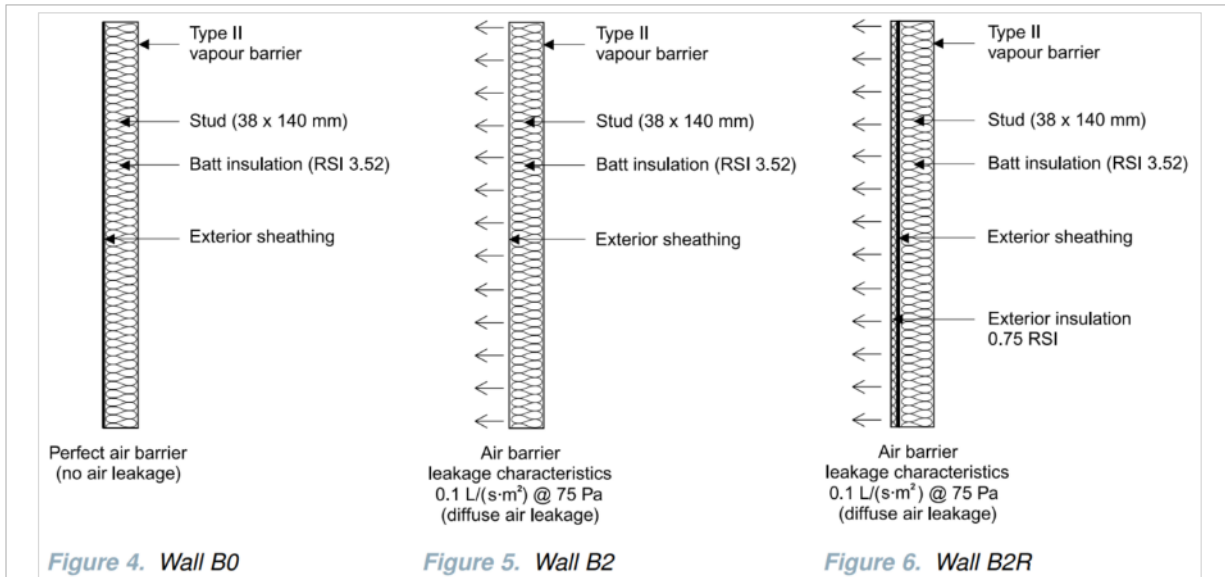
**Figure 2.13. Effect of air leakage and exterior insulation on moisture accumulation
(adapted from Kumaran & Haysom, 2000).**

Zarling et al (1982) described several problems in subarctic climates (Alaska) in a field study with 9 cases and a variety of moisture-related problems were found: ice dams, insulation freezing, frost melting, water dripping etc. In some cases, the buildings needed heating for more than 10 months throughout the year and the mild season was not enough to dry the accumulated moisture. So, any little amount of vapor counted and ended up accumulating moisture month after month in form of ice; during a milder season, even short, part of this ice melted and caused a lot of troubles. Robinson (1992) mentions that cold and damp climates like in the Atlantic provinces and northern areas with very low temperature and short drying season were most affected by moisture-related problems.

The maximum acceptable air leakage rate for the air barrier system ultimately depends on the warm and cold side temperature and relative humidity conditions, and table 5.4.1.1 of the NBC proposes some values of maximum air leakage rates for the air barrier system: 0.05, 0.10, 0.15, 0.20 and 0.50 L/sm^2 @ 75 Pa. Those values are related to the likelihood of condensation on the cold side: the higher the relative humidity inside, the lower should be the air leakage rate (assuming the same temperature for both values of RH).

The threshold of 0.20 L/s.m^2 (@ 75Pa) for housing and small buildings (Part 9 of the NBC) was adopted by the National Energy Code of Canada for Buildings (NRCC, 2017, para. 3.2.4.2) as a maximum permissible air leakage rate due to energy loss reasons (Hershfield, 1997, p. 10). It is important to note that energy loss is intrinsically linked to finances and time and each part of Canada may have different variables when assessing that; for instance, evaluating the influence of energy and gas bills and construction costs results in distinct overall results. When there was an attempt to produce a national energy code back to the 80s, this issue was on the table (Sander et al., 1995).

Knowing that it is practically impossible to build a flawless air barrier, the results from Figure 2.12 and Figure 2.13 show that keeping the cold side of the assembly a little warmer than the outdoor air decreases the accumulated moisture, which in practice means to have part of the insulation towards the outside of the sheathing. Then, after another set of simulations, it was found that the accumulated moisture was proportional to the degree-days (Figure 2.14) and so was the rate of outboard to inboard insulation: the colder the location, the higher the amount of external insulation required to control moisture accumulation (Kumaran & Haysom, 2000).
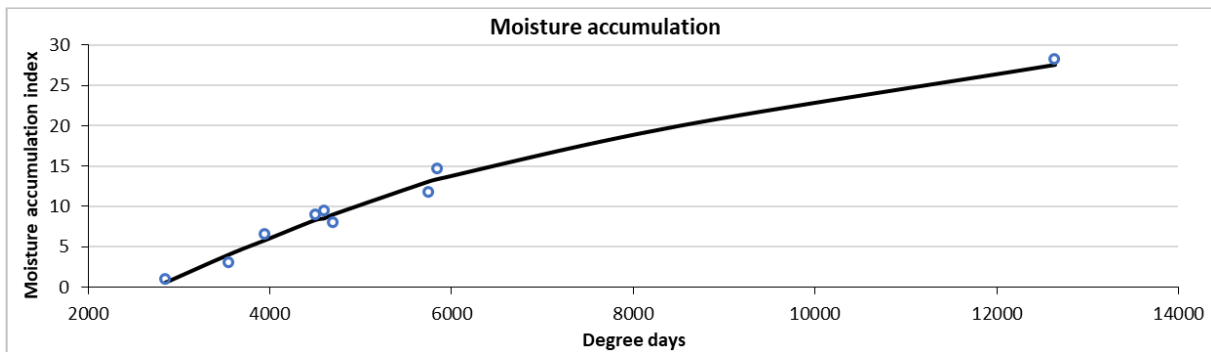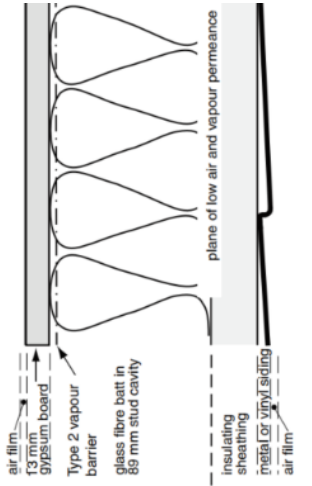
Figure 2.14. Effect of air leakage on moisture accumulation for different values of HDD (adapted from Ojanen & Kumaran, 1996).

To address the influence of different climate regions across Canada, the values in Table 2.1 were incorporated in the 1995 version of the NBC. As previously mentioned, the lowest ratio of 0.20 was adequate to control condensation for an interior RH of 36% at 21°C in Ottawa area (60% RH at -15°C); higher indoor RH levels may require adjustments in the value used, though (Kumaran & Haysom, 2000).

As a summary of the assumptions when calculating the values in Table 2.1, the list below shows the relevant aspects (Brown et al., 1998; Chown & Mukhopadhyaya, 2005; Kumaran & Haysom, 2000, 2001; NRCC, 2020, sec. A.9.25.5.2):

- Outdoor conditions: Ottawa climate, 60% RH at -15°C.
- Indoor conditions: 35% RH at 21°C.
- Mechanical ventilation system operating with an ACH between 0.3 and 0.5.
- Indoor vapor barrier type II: 60ng/Pa.s.m^2.
- Air barrier throughout the assembly: 0.024 to 0.1 L/s.m^2.
- Moisture generation rate: between 7.5 and 11.5 L per day.
- No thermal bridging effects are accounted for.

Table 2.1. Example of calculation and ratio of outboard to inboard thermal resistance, adapted from the NBC (NRCC, 2020, sec. 9.25.5.2).

Example of calculation	Heating Degree-Days of Building Location, Celsius degree-days	Minimum Ratio of Total Thermal Resistance Outboard of Material's Inner Surface to Total Thermal Resistance Inboard of Material's Inner Surface (example of cities)
	up to 4 999	0.20 (Vancouver, Toronto, Ottawa, Montreal, Halifax, Charlottetown, Moncton)
	5 000 to 5 999	0.30 (Calgary, Quebec, Edmonton, Saskatoon, Winnipeg, Thunder Bay)
	6 000 to 6 999	0.35 (Whitehorse, Teslin)
	7 000 to 7 999	0.40 (Smith River, Island Falls, Lynn Lake)
	8 000 to 8 999	0.50 (Yellowknife, Kuujjuak, Dawson)
	9 000 to 9 999	0.55 (Iqaluit, Inuvik, Fort McPherson)
	10 000 to 10 999	0.60 (Baker Lake, Nottingham Island)
	11 000 to 11 999	0.65 (Cambridge Bay, Arctic Bay)
	12 000 or higher	0.75 (Isachsen, Eureka, Alert)

The limit of 35% indoor RH raised some questions in regions of the coastal climate of British Columbia: higher indoor RH levels are the real case and can be tolerated due to the higher outdoor temperature over the heating season. Then, a short research project was initiated as an attempt to characterize the limits for mild and damp climates and the respective indoor RH levels. The results showed that the cities of most concern are the ones with high moisture load together with a milder winter, which means the ventilation might not be enough to keep the indoor RH below 35%. Due to time constraints, the results were not conclusive and further work is needed to confirm the extrapolation of the results (Chown & Mukhopadhyaya, 2005).

Janssens & Hens (1998) also mention this approach (outboard/inboard ratio) as a successful practice to lessen the risk of condensation, even when the outdoor thermal resistance is as small as the one of an air layer. When studying locations in Finland and Canada, Ojanen (1998) mentions that the drying efficiency of a wall with a 150 mm thick insulation could be increased by 7.5 times by installing 30 mm of this insulation at the exterior side of the sheathing. Straube (2011), using the concept of dew point at the sheathing layer, explores the idea of avoiding condensation by adjusting the outboard/inboard insulation ratio taking into consideration the monthly average temperatures.

Mild and warm cities may be able to get rid of the accumulated moisture during the cold season and the risk of biodeterioration is low. On the other hand, in very cold cities in the North, with high HDD values, the summers may be so short and cool that the water accumulated during the previous winter cannot dry out and it is carried over into the following winter, causing a progressive

buildup of water in the building envelope. Also, even if there was not air leakage in these cities, vapor diffusion itself should not be neglected, since the cold period is much longer than in mild cities (Latta, 1985).

An extensive experimental study (Armstrong et al., 2009, 2010; Maref et al., 2010) performed in a FEWF (field exposure of walls facility) in Ottawa corroborated the concepts behind Table 2.1 and explored the implications of adding exterior insulation to a wood frame wall. Some of the findings are:

- The sheathing layer (OSB) was kept at higher temperature when compared to the base case without exterior insulation; hence, RH levels were lower. When comparing an insulation with high air and vapor permeance (mineral fiber) against one with low permeance (XPS), RH levels at OSB were higher with low permeable insulation since it "trapped" the moisture by impairing the diffusion of water vapor towards the outside.
- Strong wind pressures can cause infiltration even when the indoor environment is pressurized, and this may increase the drying capability of the insulated cavity and reduce the risk of condensation. At least, it can avoid the warm indoor air of getting inside the insulated cavity.
- High indoor RH, pressure difference, air leakage and a cold surface are simultaneously necessary conditions for the condensation to happen (elements in Figure 2.3). Eliminating one of them changes the dynamic of the system and may reduce the risk of interstitial condensation.

Thue & Skogstad (1996), when studying vapor barriers requirements, found that there might be some relation between the vapor permeance of the interior and exterior parts of a wall so that it becomes "moisture safe" in cold climates. Provided that the interior barrier has a maximum vapor permeance, an exterior barrier 10 times more vapor-permeable avoids moisture accumulation inside the cavity. That ratio can go up to 25 or 50, depending on the indoor permeance, but if the indoor is too vapor-permeable, there will be moisture accumulation no matter how high the exterior permeance is. Simonson et al (2005), after monitoring a single-family house in Helsinki, found that the ratio should be at least 3 (three) so that mould issues are unlikely to happen.

In a case study related to the TriState Homes with thousands of prefabricated houses built in a very cold region (HDD exceeds 8500) in the rural northern parts of Wisconsin, many of them presented severe problems with mold and decay after the company went bankrupt. The study found that, among other minor factors, a vapor barrier with low permeance at the cold side of the wall together with high moisture content of the air leakage led the problems many years after the construction; in some cases, the problem took as many as 20 years to get noticed, which means the moisture accumulation increased year after year. A good agreement was found between the problems and the number of occupants: the higher the number of people inside, the greater the problem; the indoor moisture generated is proportional to the number of occupants (Merill & Tenwolde, 1989; TenWolde, 2000; Tsongas & Olson, 1995).

In United States, different types of walls were evaluated under the conditions of different climates using computerized simulations to calculate the relative humidity level of the layers. It was found that, while vapor barriers at the warm side are important for preventing moisture issues in cold climates, they may have the opposite consequence under hot and humid climate (Burch et al., 1995).

2.3. Summary of the air leakage issue

Air leakage issues are a complex problem and sometimes not as intuitive as they seem. They are a complex balance among material properties, insulation, leakage rate, indoor and outdoor RH and T, vapor permeance of the layers; most of the time sensitivity analyzes are required to identify the importance of each variable over the global behavior of the assembly. However, some key points can be drawn:

- The amount of moisture transferred into the insulated cavity due to diffusion alone is negligible when compared to moisture due to air leakage.

- Up to a certain rate of air leakage, moisture accumulation increases as the leakage rate increases. After a threshold, the rate is so high that it can warm up the whole assembly and moisture accumulation decreases.

- The maximum air leakage rate for the same city and assembly design is related to the properties of the warm indoor warm. Considering a constant temperature, the higher the RH of indoor air, the lower the tolerable air leakage rate.

- Vapor barriers with small holes or cuts may work as well as flawless barriers as long as there is no pressure difference which induces forced convection.

- Installing part of the insulation of the assembly on the outer side of the sheathing layer keeps it warmer and reduces the risk of moisture accumulation due to air leakage.

2.4. Review of air leakage simulation

2.4.1. Air leakage paths

The mechanism which explains air leakage may become very complex and it is related to wind pressures, stack effect, indoor and outdoor conditions, shape/size/height of the building, HVAC systems, type of assembly etc. Some inactive paths under low pressures may become "active" when the pressure difference increases, inducing more non-linearity to an already complex problem. This situation is extensively discussed by Lstiburek (2000), theoretically and with practical examples using a single-family house in Minneapolis, MN and a school facility in Westford, MA. More information was added later (Lstiburek et al., 2002), but a main guideline from both studies is that to control the pressure inside a building one must: 1) get rid of openings and holes and 2) when the air is enclosed, control the HVAC system.

As explained by Ojanen & Kohonen (1989), changing the path may change the expected hygrothermal performance of the whole assembly; Torp & Graee (1971) say that condensation and ice formation vary both in intensity and position inside the wall because the water vapor which enters the cavity is related not only to the flow rate, but also to the distribution of the air currents: while a distributed air leakage may cause uniform condensation, a concentrated one may cause moisture-related problems to a very specific spot only.

Kunzel et al. (2012) add that exfiltration is a multidimensional effect and cannot be captured by one-dimensional calculation. Moreover, even if a 3D approach was applicable, it would still be inaccurate because the configuration of the air leakage paths remains unknown, and simplifications are needed. Figure 2.15 shows two simple examples: a) the path is a straight line between the interior and the exterior side of the assembly, the air flow resistance is very low and the warm air exfiltrates easily, mostly leading to energy loss; b) in this case, the tortuosity of the path is high

and so is the resistance to the flow, leading to a low air leakage rate; as the warm air moves through the assembly, it gets cooled down and there may be concentration of moisture and condensation, which might lead to bio-deterioration.
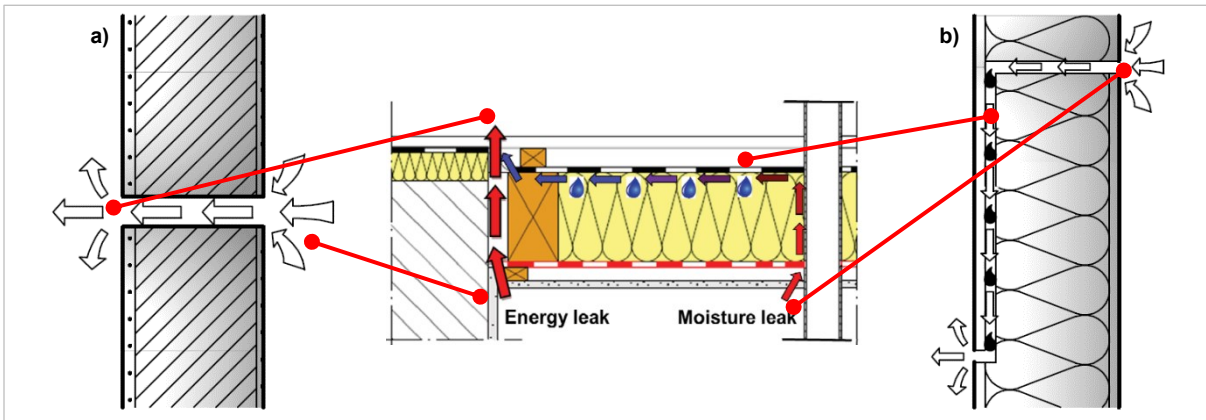
Figure 2.15. Flow channels in construction: a) energy leak and b) moisture leak,
(adapted from H. M. Künzel, 2014; Künzel et al., 2012).

When analyzing the correlation between air leakage paths and hygrothermal performance, Ojanen & Kumaran (1996) came up with Figure 2.16, with five possibilities: path number 5 is one of the worst cases in terms of moisture accumulation and conveys the idea of air leakage entering through a crack/slot ate the bottom of the wall, diffusing through the insulated cavity and managing its way out at the top of the wall. To the right side of each path there is a bar showing the relative moisture accumulation: paths 1 and 5 are the worst cases, 3 and 4 are in between and 2 is the best case.
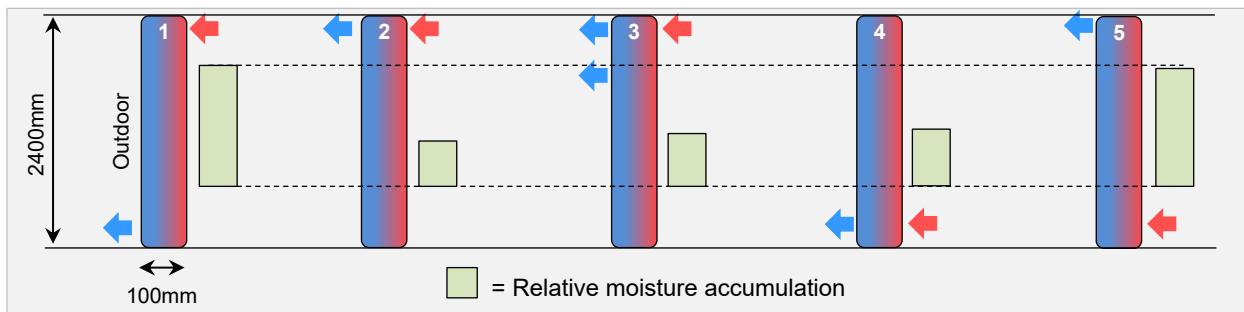
Figure 2.16. Five possible paths for exfiltration and relative moisture accumulation,
(adapted from Ojanen & Kumaran, 1996).

Figure 2.16 assumes the exfiltrated air leaves a warm environment (indoors) and travels towards a cold environment (outdoors). So, the longer it stays close to the cold side of the assembly, the higher the risk for condensation as long as the air leakage rate does not warm up the path (Figure 2.11). While in paths 2, 3 and 4 the air crosses only the insulation thickness, in paths 1 and 5 the way is roughly 24 times longer, about the height of the wall (2400 mm). So, path number 5 has been adopted in other studies as the worst-case scenario (Bunkholt et al., 2021; Chown & Mukhopadhyaya, 2005; Defo & Lacasse, 2020; Junginger et al., 2020; Kayll et al., 2020; Saber, 2014).

In-cavity moisture accumulation maps for different wall configurations (Figure 2.17) were obtained by Desmarais (2000) and Desmarais et al. (2000, 2001) in a lab experiment using a 2.4 m high wall assembly: a continuous gap at the bottom (Figure 2.17a), a localized hole (Figure 2.17b) and distributed exfiltration (Figure 2.17c). By means of gravimetric samples, it was possible to weigh the moisture accumulation close to the air entry and in many other positions of the sheathing board. The paths shown in Figure 2.17a,b are similar to path 5 in Figure 2.16 and the results of the experiment show that the bottom part of the wall was wetter than the rest of it due to the effect of air leakage. For the distributed leakage path (Figure 2.17c), moisture accumulation was less critical and sparser.
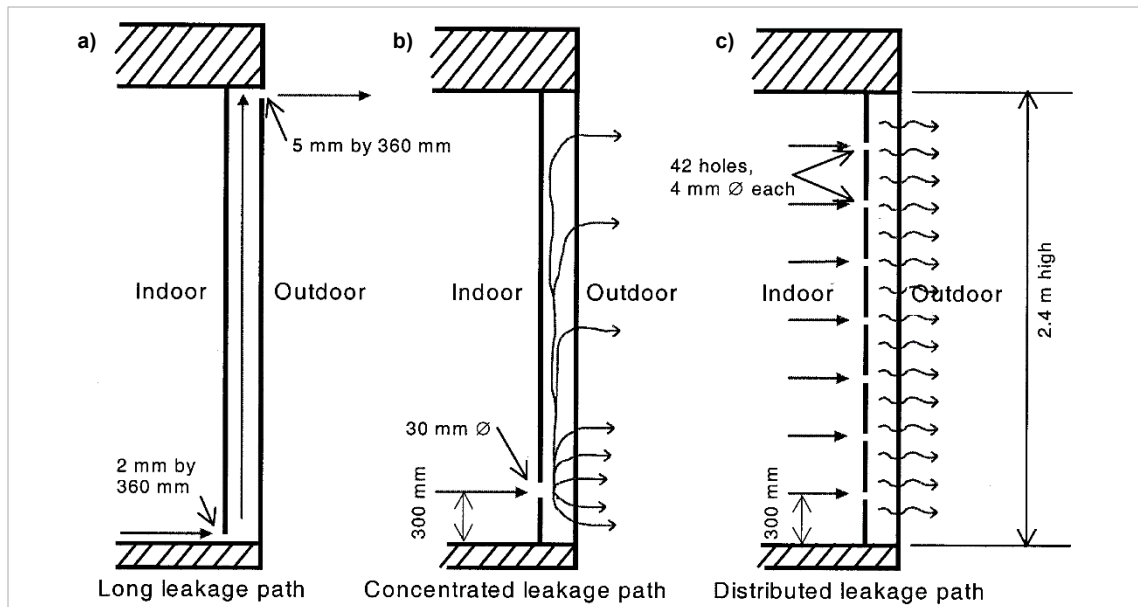
Figure 2.17. Three different air leakage paths: a) long, b) concentrated and c) distributed, (Desmarais et al., 2000).

Pallin et al. (2015) and Hun et al. (2016) also analyzed different exfiltration paths (Figure 2.18) according to the likelihood of having moisture-related problems. The authors mention that, among the countless number of possibilities, a previous analysis must be done to identify where the exfiltrated air may induce moisture accumulation and practical experience from the field is valuable in this moment. After selecting the most plausible possibilities, simulations can be performed.

This aspect is also discussed by Kölsh et al (2016) during an experiment where they vary the number, size and position of the air entries, the permeability of the insulation, and the pressure difference. The main conclusions are: high density insulations retain more moisture than low density ones and then reduce the condensation at the sheathing; different arrangements of holes change completely the moisture profile; holes close to the studs lead to a higher airflow because of the recess of the insulation at the corner. Figure 2.19 shows moisture distribution diagrams according to the air leakage configuration.
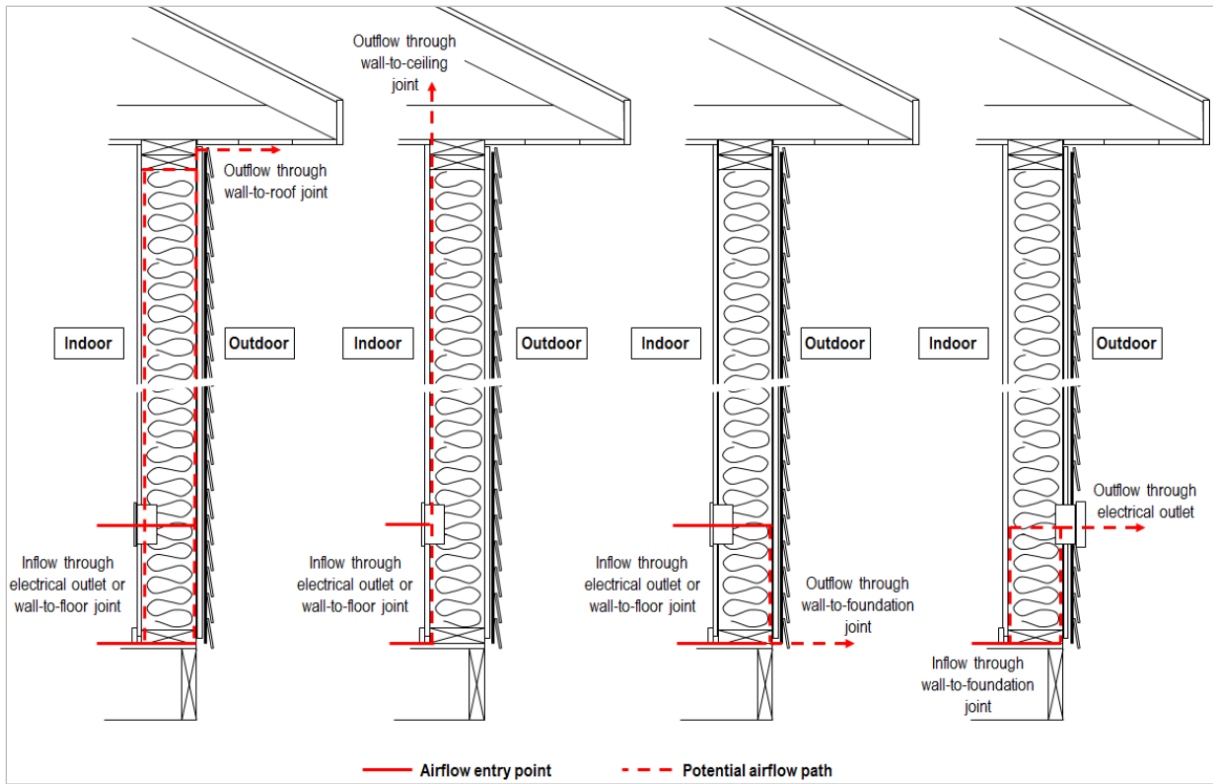
Figure 2.18. Possible moisture leaks in a wall due to exfiltration (Pallin et al., 2015).
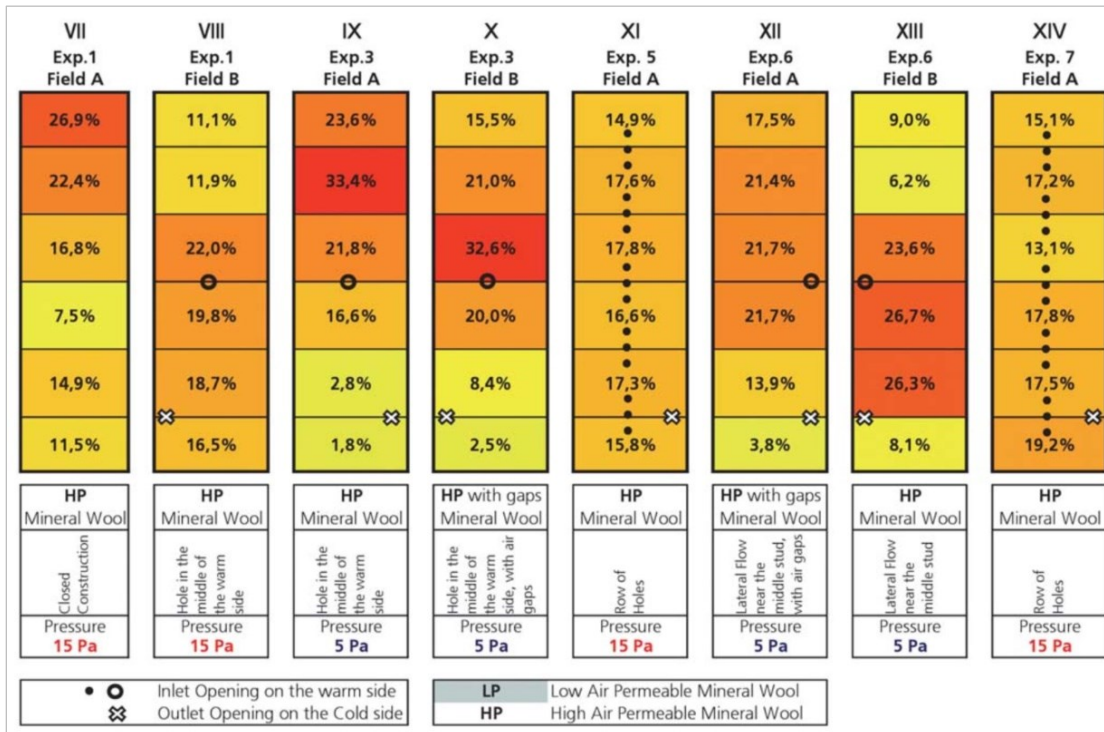
Figure 2.19. Moisture distribution in the paper sheets for the experiments with high air permeable mineral wool, view from the cold side (Kölsch et al., 2016).

In another experimental research, Bunkholt et al. (2021) tested moisture accumulation in the insulated cavity due to forced convection for different air leakage paths (Figure 2.20). Although the aim of the study was to compare the performance of wood fiber and mineral wool insulations, the highest moisture accumulation was at the bottom of the assembly for the long path (Figure 2.20a) and at the top for the short path (Figure 2.20b).
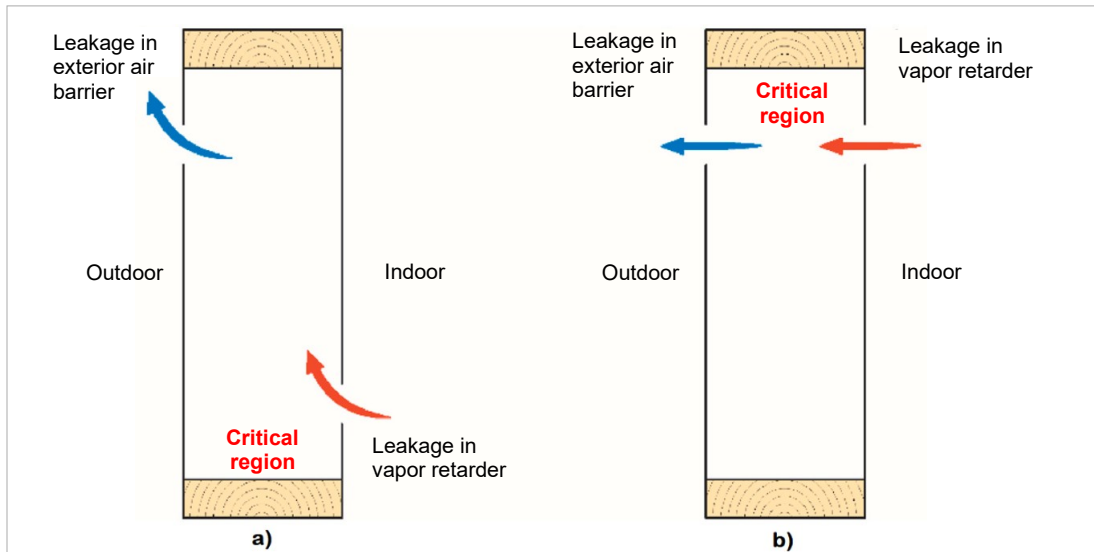
**Figure 2.20. Cross section showing the intended leakage path for moist indoor air
(adapted from Bunkholt et al., 2021).**

Regarding insulation permeability, a very compact layer of mineral wool is less prone to air movement than a light one since the porosity is affected by how compact the material is and the flow direction. This means that, for the same pressure difference, a cavity filled with dense mineral wool will probably have a lower air leakage rate than a cavity filled with a less dense mineral wool. Other factors also play a role and the air leakage rate and path are more or less influenced by them (Boardman & Glass, 2020; Hurel et al., 2017).

In conclusion, warm air from inside the building can exfiltrate through cracks, joints, unintentional openings, electrical boxes etc. All these possibilities lead to many different paths for the air to exfiltrate through the assembly and it is impossible to determine the exact one. There might be a preferable path due to constructive reasons, which does not mean many others do not exist. So, like with any other complex problem, some simplifications are necessary to be able to perform computational analysis. Usually, the best approach is to get results from the worst case and from the best-case scenarios; it is likely that the real solution falls in between. Otherwise, Wang (2018) shows the number of simulations increases exponentially when analyzing stochastic variables and time may become a real hurdle, impairing the desirable flux of work.

2.4.2. 1D models: infiltration and ventilation approaches

When using 1D models, there are two ways of simulating the effect of air leakage: a) applying a moisture source calculated from the indoor air to the surface where condensation is likely to happen (infiltration approach) or b) converting the air leakage rate to ACH and apply it the insulated cavity (ventilation approach).

To explain the infiltration approach, Figure 2.21 represents the 1D model of an assembly with brick cladding; interior conditions are 50%RH at 20°C, and exterior conditions are 60%RH at -15°C, which means a moisture content of 8.5 g/kg and 0.9 g/kg respectively. In case of air leakage, the warm indoor air goes inside the cavity and reaches the inner surface of OSB, which is assumed to be at -5°C. As the maximum amount of moisture air at -5°C can hold is 3.4 g/kg, all the excess of moisture from the warm air will condense on the OSB surface: 8.5 – 3.4 = 5.1 g; this amount of liquid water should be applied on the OSB surface.
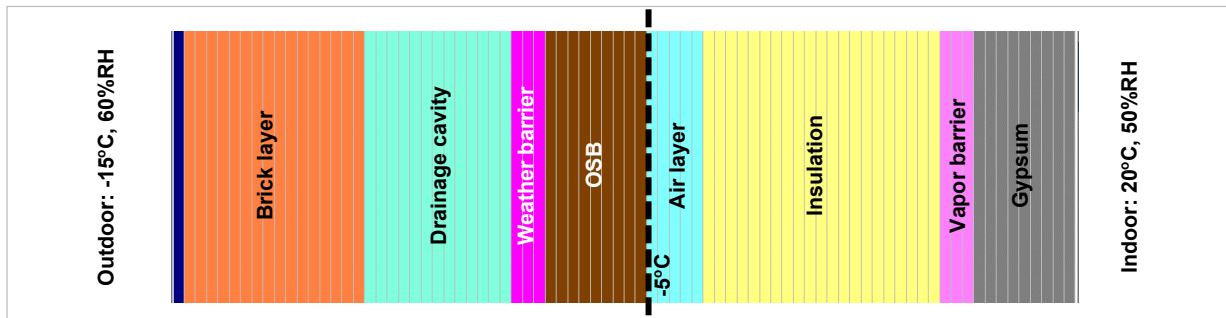
Figure 2.21. 1D discretization of a brick cladding wall with the condensation layer at the inner side of OSB.

The rationale behind the previous calculation is the *infiltration approach*, proposed by Kunzel et al. (2012): as long as the air leakage rate and the temperature of the condensation plane are known, the amount of moisture to be applied (as moisture source) during the simulation is easily calculated. Before the simulation begins, though, one must know where the critical surface inside the geometry is, i.e., where the water vapor is likely to condense. Also, any changes in the indoor air during its trajectory towards the OSB are neglected. Moreover, the layer where the moisture is applied to should be split in at least two parts to avoid any numerical problems: one with the moisture source and another with the remaining thickness (Antretter & Pallin, 2019).

Another approach, known as the *ventilation model* (Künzel et al., 2012), considers a thin air layer close to the condensation plane and applies to this layer as many air changes (ACH) as necessary to represent the air leakage rate, which is more straightforward than the infiltration model. According to the authors, the major difference between the two models is the convective effect, which may lead to convective drying as soon as the temperature of the condensation plane rises above the dew point of the indoor air. A ventilated cavity (which means convective effect), dries out much faster than an unventilated one and this effect is discussed elsewhere (Kalamees & Kurnitski, 2010; Karagiozis & Kuenzel, 2009; Salonvara et al., 2007; Van Belleghem et al., 2015).

Wang & Ge (2017) analyzed the relative position of the air layer inside the cavity by comparing the simulation results from both 1D models with the results from laboratory experiments. A constant air leakage rate of 0.315 L/s was imposed by means of a pump at the bottom of the assembly and two types of cavity insulation were used: fiberglass and cellulose fiber. The results show that both 1D models can be used to evaluate the effect of air leakage provided that the position of the air layer and the air leakage rate are previously benchmarked. When comparing the models, the infiltration approach is more conservative and tends to overestimate the moisture content of the OSB sheathing because convective drying is neglected. More details about the experimental part of this study can be found in Fox (2014) and Wang (2018).

Since air entry position, gravity and buoyancy effects induce different results for different heights, 1D simulations cannot represent top and bottom plates and they assume any output variable to have the same value along the height of the wall (Desmarais et al., 2000; Ge et al., 2019; Saber, 2014). So, 1D models can give a first indication of the hygrothermal performance of a wall, which might be enough; if not (because important effects would be lost), following up with 2D models or even field monitoring is the next step (Dalgliesh et al., 2005).

Palin et al. (2015, 2016) proposed a correction factor "η" to be applied to the air leakage rate (or ACH) so that 1D results mimic 2D results. This factor is calculated considering the thermal conductance of the materials surrounding the air leakage path and also the distance between the point of evaluation and the air entry. Simulations were undertaken using Wufi 1D and Wufi 2D and the results from both approaches are in good agreement (Figure 2.22). The authors emphasize that the factor was focused on temperature analysis since the length of the path has a greater effect on heat exchange than on moisture exchange. Moreover, mould index is usually an important performance factor for hygrothermal evaluation and the combination of relative humidity and temperature may have to be analyzed as well.
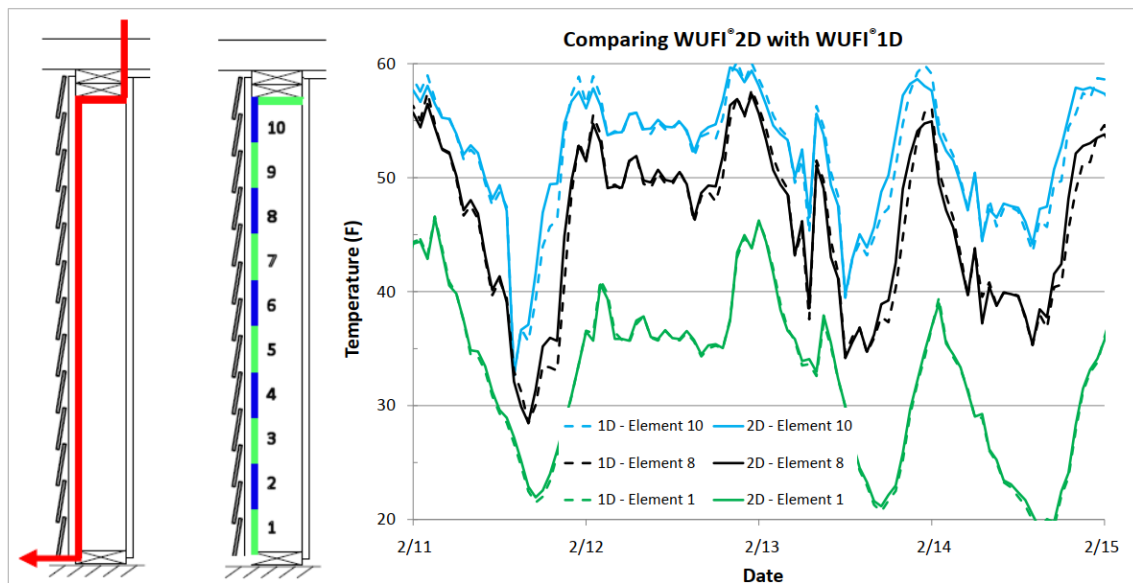
Figure 2.22. A comparison between WUFI 2D and WUFI 1D reveals that the 1D tool is capable of simulating air leakage at any location inside the air leakage path (Pallin et al., 2015).

2.4.3. 2D models: ACH and air pressure approaches

In Figure 2.23, there is a representation of the same assembly using 1D and 2D models: in 1D (Figure 2.23a), bottom and top plates cannot be incorporated; however, they have a strong influence on their surroundings and the outputs taken at their level from the 2D model do not match the values from the 1D model, which has the same output regardless of the height of the wall. To avoid this problem, 2D models should be used so that the air entry can be placed at any height on the gypsum board or even many air entries can be modelled at the same time, like the examples in Figure 2.17.
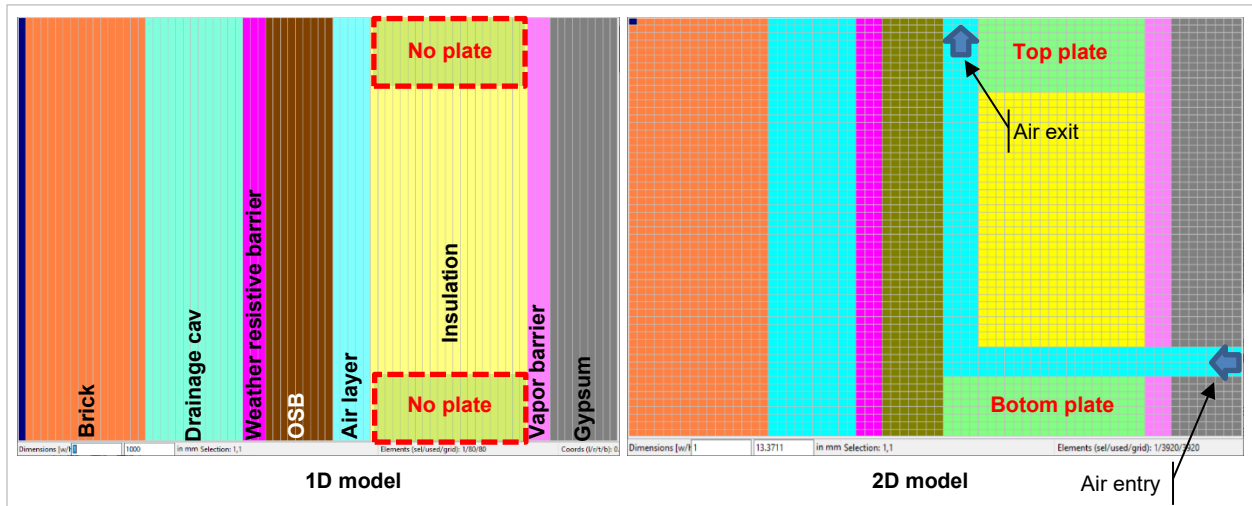
Figure 2.23. 1D and 2D models of the same wall assembly: 1D cannot represent the plates and the horizontal part of the air leakage path.

The *ACH approach* in 2D models is the same as the ventilation model in 1D: knowing the air leakage rate, the number of air changes can be calculated and applied to the whole insulated cavity or parts of it. Unless the model is built to apply different ACH to different parts of the geometry, it will be evenly distributed all over the selected region. This is not realistic, though, because the air flux is influenced by pressure losses along the path.

In this case, the *air pressure approach* can be used: applying a pressure difference between the air entry and the air exit, the solver calculates the air flux through each cell considering the properties of the insulation. For example, if the insulation is airtight (Figure 2.24a), the airflow passes through the air channel only; if the insulation is air permeable (Figure 2.24b), the flow spreads unevenly all over the insulation.
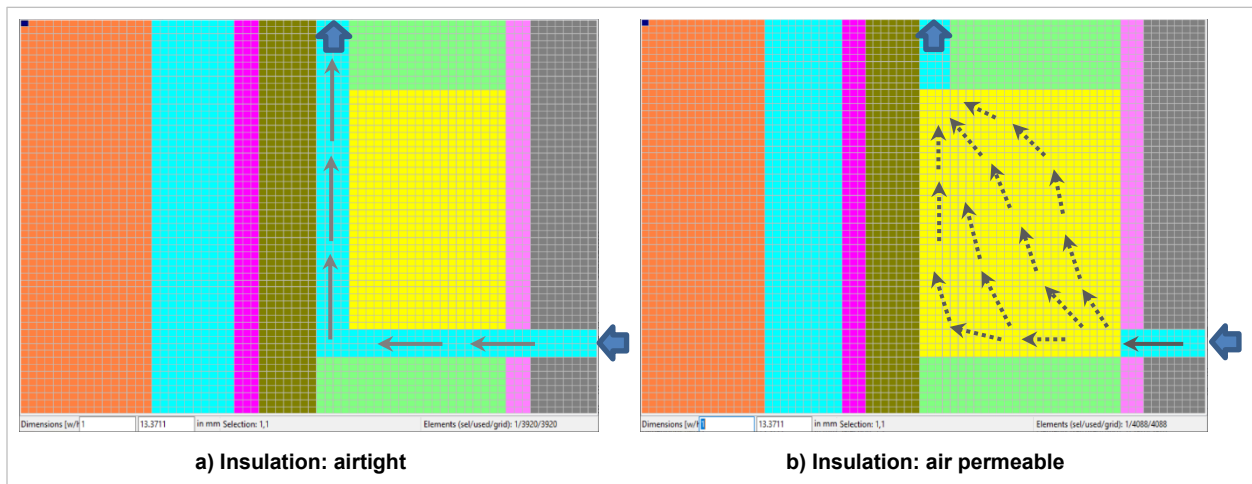
Figure 2.24. Exfiltration through the insulated cavity: a) airtight insulation; b) air-permeable insulation.

The user must be aware of the relation between pressure difference and air leakage rate, though, since it varies according to the properties of the materials and the geometry itself. For the same pressure difference, different geometries result in different air leakage rates. For instance, the

cavity insulation in Figure 2.25a is 140 mm thick. If the type of insulation is changed or its thickness is increased to 184 mm (Figure 2.25b) or the air entry is moved to a higher position, the new air leakage rate will be different because the resistance between the air entry and the air exit is not the same anymore.
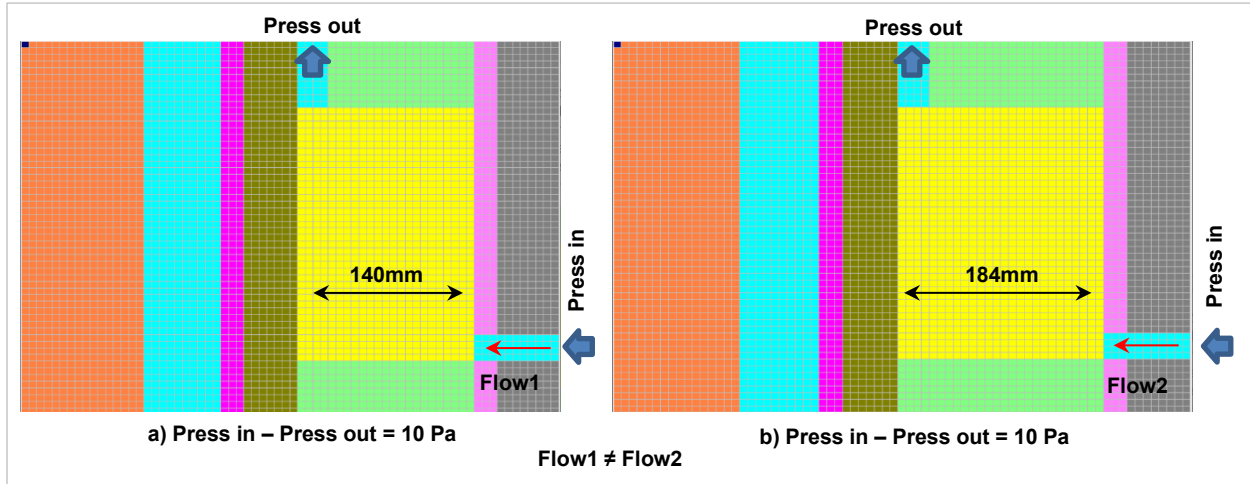
Figure 2.25. Exfiltration through insulated cavities with different thicknesses:
the air flow rate is not the same for the same pressure difference.

This approach was used during a laboratory experiment varying the number, size and position of the air entries, the permeability of the insulation, and the pressure difference (Kölsch et al., 2016). The authors concluded that high density insulations retain more moisture than low density ones and then reduce the condensation at the sheathing; different arrangements of holes change completely the moisture profile; holes close to the studs lead to a higher airflow because of the recess of the insulation at the corner.

In a set of simulations using Delphin, the air entry position, stretching factor, air permeability of the insulation and pressure difference were considered. The results show that the air permeability of the insulation and the air pressure difference were the two most important factors which drive the dry air mass flow through the structure, whereas the details of the discretization had a smaller impact (Laukkarinen et al., 2021).

Using a pump to impose an air flux through an opening into an insulated ceiling, Belleudy et al. (2015) measured the temperature along the path in the cellulose insulation and compared the experimental results with the outputs from a 2D numerical model using Comsol Multiphysics. The authors found that considering heat, air and moisture transfer produce more accurate results than considering only heat and air transfer in the model. A similar study is described by Kalamees & Kurnitski (2010).

The decision about using 1D or 2D models relies mostly on the assumption of the air leakage path. While 1D models may produce good results for distributed paths, concentrated paths require the use of 2D models because the results vary along the height of the assembly. When comparing the two models, some general aspects can be drawn:

- Using 1D models, the major difference between infiltration and ventilation approaches is the convective effect, which may lead to convective drying as soon as the temperature of the condensation

plane rises above the dew point of the indoor air. With the infiltration model, the critical surface in-side the geometry must be assumed and the changes in the indoor air during its trajectory towards the OSB and any water absorption at the OSB surface are neglected. With the ventilation model, the position and thickness of the air layer must be assumed.

- Due to the intrinsic absence of vertical discretization in 1D models, they cannot consider top and bottom plates or any other singularity along the height of the assembly, which is an important draw-back when dealing with different air leakage paths.
- 2D models with ACH approach require the same ACH for the whole insulated cavity unless different inputs are created for different portions of the geometry. The pressure approach better represents the reality since the flux distribution is automatically calculated by the solver.
- While 2D models give more details, they require much more time to run; 1D models are faster and can be used as a first screening, but they provide fewer details.

2.4.4. Implementation details

Most of the information in this section is related to Delphin HAM (Heat, Air and Moisture transfer) modelling and an overview of this tool is given in section 3.4.1.

Also, with the objective of avoiding confusion when referring to the 2D model, Figure 2.26 shows the terms used to identify parts of the geometry:

- Element or cell: any single element of the whole model.
- Mesh or grid: the group of all the cells which make the model.
- Layer: any subset of cells that belong to the same material, for instance OSB, insulation, gypsum.
- Surface grid thickness (SGT): the thickness of the first column (or row) of cells which defines the surface of a layer.
- Stretching factor (STR): also known as expansion factor, it is the relation between the thickness of two subsequent rows/columns of cells: if the first column is 2 mm thick, the second will be 4 mm thick with a stretch factor of 200%. The values can be shown as a percentage or a number: for in-stance, 150% and 1.5 have the same meaning. The minimum allowable stretch factor is 101%.
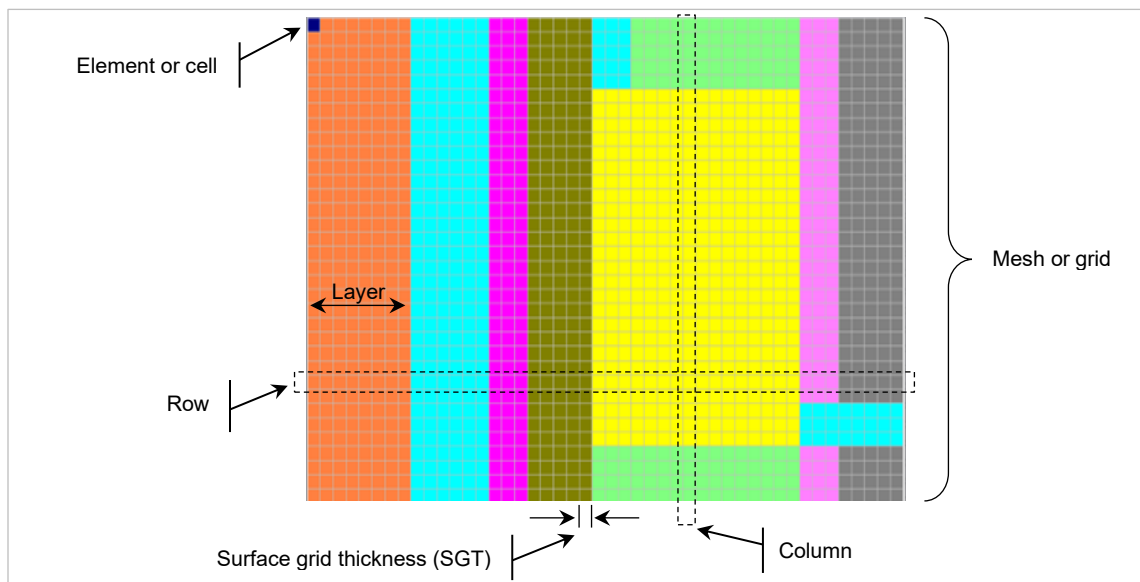
Figure 2.26. Terminology related to the 2D model.

2.4.4.1. Discretization

ASHRAE (2017) explains that the first step when modelling a geometry for computational analysis is:

> *to divide the region of interest into a large number of smaller elements called **cells**. The collection of cells that makes up the domain of interest is typically called the **mesh or grid**, and the process of dividing up the domain is called **meshing, gridding, grid generation, or discretization** of the computational domain.*

Although many different types of grids exist, the irregular ones are more useful when dealing with complex structures. In building engineering, however, usually the fluxes coincide with the x,y co-ordinates of the cartesian plane and a rectangular grid becomes the obvious selection (Ferziger et al., 2020). Rectangular grids are described as orthogonal grids by ASHRAE (2017).

The grid size is unknown when modelling a geometry and usually the software does the discretization automatically, starting with a minimum SGT and creating the other ones based on the STR. However, different values of SGT and STR may output different results. Defo et al. (2021 a; 2021 b) mention that different tools present different grid generation and they might affect mould results in more than 100%. Hirsch (1988) showed that the best numerical solution is given by the discretization which best represents the continuum, i.e., a grid size which tends to zero. Very fine grids, however, are related to much more computational requirements and, therefore, the strategy is to use a grid as coarse as possible so that the required accuracy is reached.

Generally, minimum and maximum widths for any element should be 1 mm and 50 mm respectively, either for 1D or 2D simulations. For the STR, 1.2 to 1.4 are suitable values for 1D projects whereas 1.5 is recommended for 2D projects to avoid long simulation times. Those values should be adopted at the beginning but they may require adjustments under very strong gradients; in these cases, a finer grid may be required and the best one must be selected based on a sensitivity analysis (Bauklimatik, 2022).

At the beginning of a sensitivity analysis, a coarse mesh should be applied to the geometry because it allows the user to evaluate computer requirements and running time; besides, coarser meshes run faster and many "test runs" can be performed to get a general view of the solution to the problem. Later, the grid may be refined and must be sufficiently fine to provide an adequate resolution of the important flow features; mesh concentration may be required in the vicinity of layer boundaries and a grid which works well for a given variable does not necessarily produce the same level of accuracy for another variable (Tu et al., 2013).

According to Ferziger (2020), the grid should be finer when strong gradients are expected because more elements are needed to adequately represent the flow, keeping the errors at acceptable levels. This fact was also observed by Cornick (2009): coarse grids may not capture the correct profile of the variable being assessed because grid size have a considerable effect on the results.

Figure 2.27 shows an example of this effect: the shaded region of Figure 2.27a and Figure 2.27b represents the same physical portion of a given homogeneous body subjected to a temperature difference of 20°C between its opposite faces. According to Figure 2.27a, the whole region is at 27.5°C (taken as the average of its two faces); according to Figure 2.27b, part of the region is at 28.7°C and part is at 26.7°C. Since the body is homogeneous, Figure 2.27b best represents the

real situation and Figure 2.27a gives the greatest error. For a stronger gradient, the error would be even higher if the grid was kept the same.
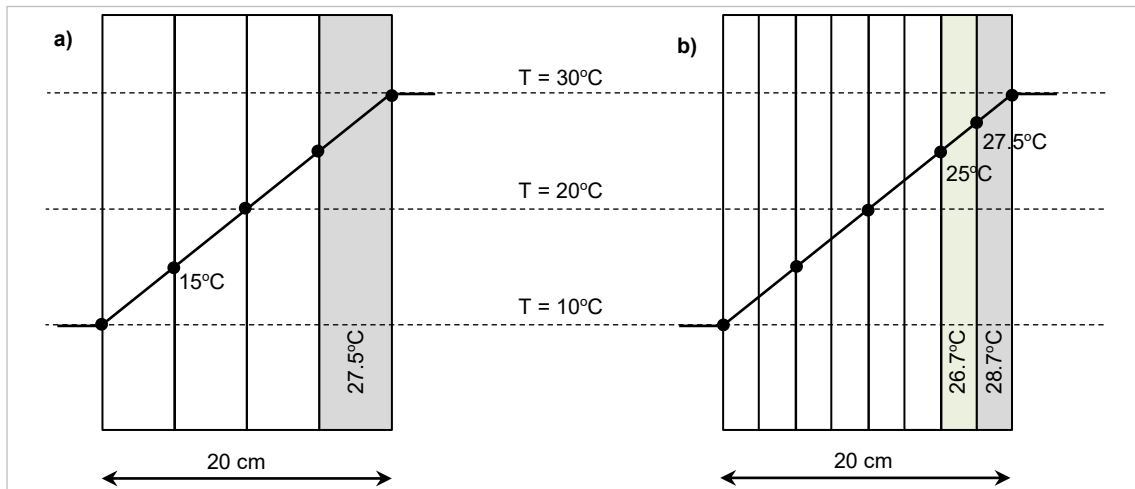
Figure 2.27. Calculated temperature distribution varies according to the grid resolution.

Figure 2.28 shows the differences between the temperatures obtained by the simulation and the reference temperatures (for six positions in a given geometry) when varying: a) the STR and b) the SGT (Bauklimatik, 2022). In this case, STR from 1.15 to 1.51 (Figure 2.28a) shows straight lines for all the six cases, meaning that it does not have a significant influence on the temperature difference. On the other side, SGT (Figure 2.28b) has a strong influence when varying from 10 mm to 1 mm, but it shows no further improvement for values below 1 mm. Since smaller values mean a significant increase in the total number of elements in the grid and computational requirements, one can assume 1 mm provides sufficient accuracy.
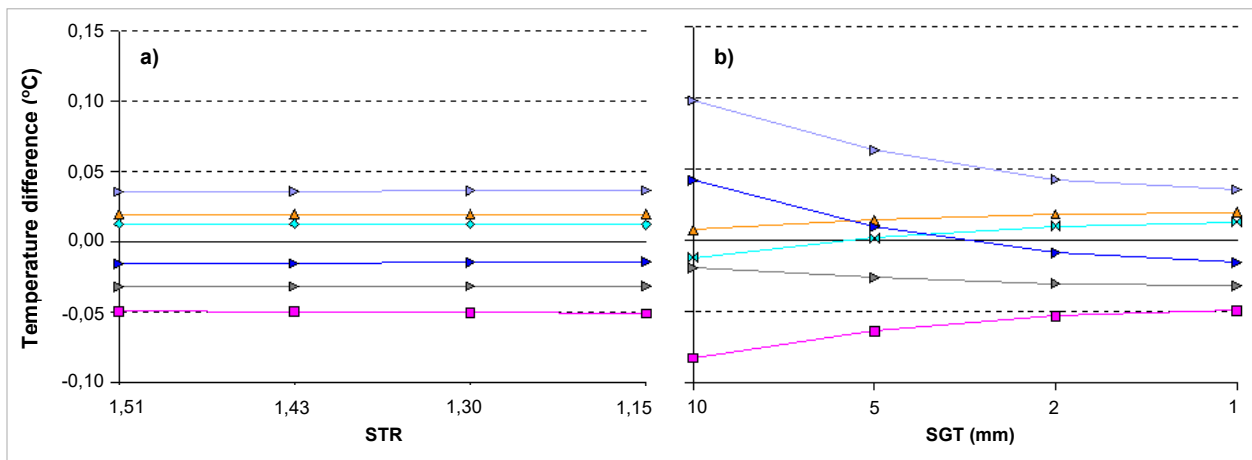
Figure 2.28. Temperature differences for six positions as a function of a) STR and b) SGT. (Bauklimatik, 2022).

Paepcke & Nicolai (2020) present a grid sensitivity study using coarse, medium and fine meshes. Their conclusion indicates that fine grids produce the best results, but medium discretization might be acceptable in terms of accuracy. The grid may be different for the same geometry depending

on the variable being studied, for instance energy balance or moisture storage. Hence, the hygrothermal analysis can be done by evaluating two sets of results, one for each variable, as long as they are assumed to be independent of each other.

A set of simulations using Delphin was performed by Laukkarinen et al (2021), varying the air entry position, STR, air permeability of the insulation and pressure difference. The results show that the air permeability of the insulation and the air pressure difference were the two most important factors for the dry air mass flow through the structure, whereas the details of the discretization had a smaller impact. Aggarwal (2023) also did a mesh analysis before performing simulations of a wood frame wall with brick and stucco cladding: varying the SGT among 0.1, 0.5 and 1.0 mm, the results for moisture accumulation varied about 5% after 2 years of simulation.

In any case, the user should have a good understanding of the problem and what the solution might be, since very small errors accumulating over millions of iterations might lead to wrong results without any notice. Ferziger (2020) emphasizes that having a good understanding of the goal of the simulation and of the physics which govern the solution enable the user to promptly detect any weird output. Cornick (2009) mentions that having a good understanding of the capabilities and limitations of the tool and confidence through benchmarking is also important. Kunzel & Karagiozis (2010) say that the results should be checked for plausibility and compared to experimental data when possible; if they inspire confidence, the resulting hygrothermal conditions should be interpreted within the building envelope system: temperature, relative humidity and moisture content should not exceed the limits specified for each material.

2.4.4.2. *The relation between air flux and air leakage rate*

The air flux through an opening is a consequence of the pressure difference and of the resistance along the path; however, this resistance cannot be analytically calculated because it depends on the balance of pressure losses inside the whole cavity, which is related to the geometry itself and to the property of the materials. If the position of the air entry (or air exit) is changed, the flux will also change even though the pressure difference is kept constant; the same happens when either the thickness of the insulation or the height of the air entries change. As a general principle, though, the closer the air entry and exit are, the higher the flux since the resistance between them is lower.

The air flux through the opening is an output of the Delphin solver, which takes into consideration the materials properties and calculates how much air goes through each cell. Fechner (2021, 2022) mentions that Delphin works with two independent solvers:

- The first solver calculates the air flux through each cell for both directions according to the geometry, pressure difference and air permeability of the materials. The air mass balance is evaluated at each time step.
- The second solver uses the outputs from the first solver as part of the inputs when solving the balance equations for heat and moisture transfer.

Figure 2.29a shows the Delphin model of a wall assembly and Figure 2.29b shows an air channel as a ventilated layer behind the cladding; the analogy of the layers in both cases is given by the solid lines. The example considers an air flow passing through a 2 cm opening and traveling inside

a 4 cm thick and 5 m long vertical channel. The air flow through a single channel inside the assembly can be analytically calculated using Eq. 2.1 (Fechner (2021)):

$$Flux = \frac{\Delta P}{R\ddot{u} + R_1 + R_2 + R_3} \rightarrow \frac{Pa}{\frac{Pa.s}{kg}} = \frac{kg}{s}$$

Eq. 2.1

$$R\ddot{u} = \frac{1}{\delta.A} = \frac{1}{2\frac{kg}{m^2.s.Pa} * 0.02m * 1m} = 50\frac{Pa.s}{kg}$$

$$R1 = R3 = \frac{\Delta x}{K_{air}.A} = \frac{0.02m}{0.1\frac{kgm}{m^2.s.Pa} * 0.02m * 1m} = 10\frac{Pa.s}{kg} \quad R2 = \frac{\Delta x}{K_{air}.A} = \frac{5m}{0.1\frac{kgm}{m^2.s.Pa} * 0.04m * 1m} = 1250\frac{Pa.s}{kg}$$

Where:
Rü: surface resistance at the air entry (2-cm high)   δ =   surface exchange coefficient (set to 2)
R1, R3: resistance in the gap (2-cm high) K_{air} =   air permeability (K_g from the material file)
R2:   resistance in the channel (5-m high)
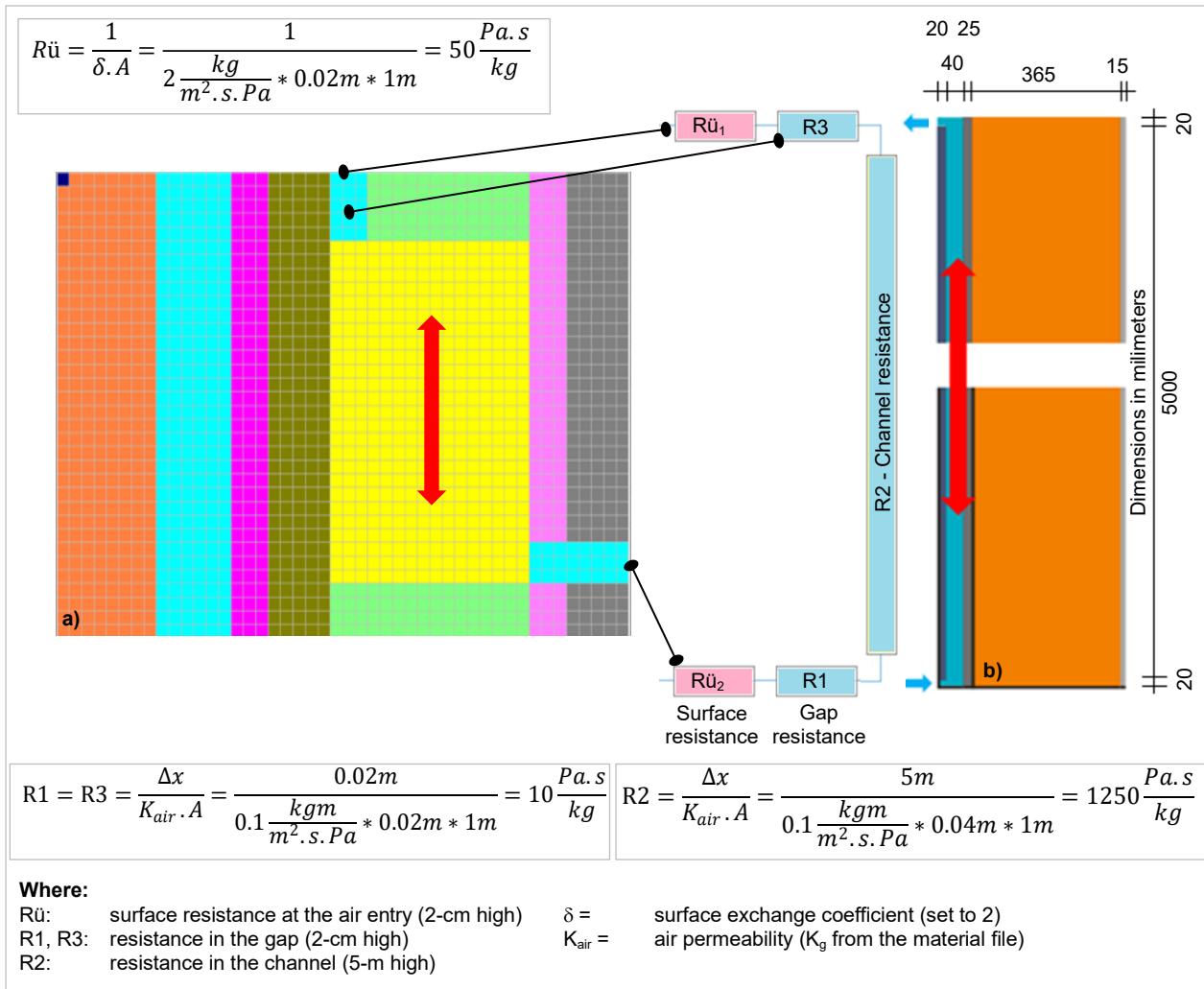
Figure 2.29. a) modelled assembly; b) example of air flow calculation through a ventilated air space (adapted from Fechner, 2021).

The Rü value is related to the surface exchange coefficient, which was set to 2 when configuring the model. In the modelled assembly, R3 is the resistance of the 72 mm long air channel which connects the insulation with the exterior surface of the top plate and R1 is the resistance of the 12.5 mm long air channel which connects the insulation with the exterior surface of the gypsum board. R1 and R3 are just an analogy of how the model works and they are not set up in the model. They are automatically evaluated when the solver calculates the air flux according to the geometry and material properties.

This is an example of a simple and uniform channel, but for a situation like Figure 2.24b (air-permeable insulation), the flow cannot be analytically calculated, and a solver is necessary.

Regardless of the way the air travels inside the assembly, the maximum volumes of exfiltrated air per m^2 of wall are suggested in the section A-5.4.1.2.(1) of the NBC, which states:

> *These values are for air barrier systems in opaque, insulated portions of the building envelope. They are not for whole buildings, as windows, doors and other openings are not included. The table is provided for guidance when testing air barrier systems as portions of an envelope.*

So, the values are related to opaque walls without any intentional openings (windows, doors etc.). When simulating air leakage, however, it is assumed the exfiltrated air passes through one or a couple of intentional openings in the model. This means the flux is concentrated in one single opening so that the worst-case scenario can be evaluated. Figure 2.30 shows two possibilities with the same area: one slot of 50x1 cm and another one of 10x5 cm; the arrows show the direction of the flow through those sections.
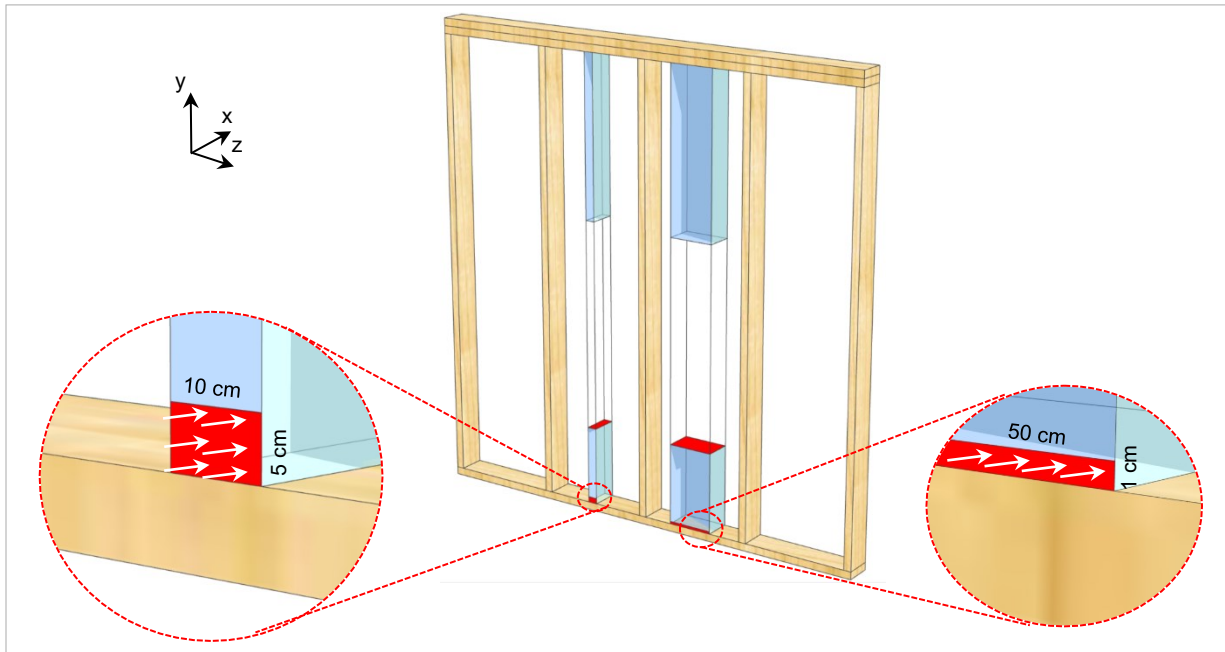
Figure 2.30. Different shapes of the air leakage entry; the arrows indicate the flux direction.

For a 2.4m^2 wall and an air leakage rate of 0.05L/s at 75Pa, this airflow must pass through these two openings and the flux for each one is calculated according to Eq. 2.2 and Eq. 2.3:

$$Flux_{1x50cm} = \frac{flow\ rate}{area} = \frac{0.05\frac{L}{s.m^2} * 2.4m^2}{0.01m * 0.5m} = 24\frac{L}{s.m^2}\ (at\ 75Pa) \qquad \textbf{Eq. 2.2}$$

$$Flux_{5x10cm} = \frac{flow\ rate}{area} = \frac{0.05\frac{L}{s.m^2} . 2.4m^2}{0.05m * 0.1m} = 24\frac{L}{s.m^2}\ (at\ 75Pa) \qquad \textbf{Eq. 2.3}$$

Those values are for pressure differences of 75 Pa and therefore they need to be converted to air leakages under pressures of about 10 Pa; this can be done by using the power law equation:

$$Q = c(\Delta P)^n$$

<div align="right">**Eq. 2.4**</div>

Where:

- Q: air flow through opening, m^3/s
- c: flow coefficient, $m^3/s.Pa^n$
- n: pressure exponent, dimensionless

According to ASHRAE (ASHRAE, 2017), a typical value for n is about 0.65, but values for "c" and "n" can be determined for a specific building by using fan pressurization testing. Hens (2007) mentions that the power law equation may be used to describe air flow in cavities, air layers, cracks, joints, holes, voids etc., but this requires air permeability and flow exponent "n" to be known, which is complicated when dealing with a very complex hydraulic network. Then, "n" was adopted as 0.65 and the conversion between pressures is written as:

$$\frac{Flow_{10Pa}}{Flow_{75Pa}} = \frac{c(10)^{0.65}}{c(75)^{0.65}} \rightarrow Flow_{10Pa} = Flow_{75Pa} * \left(\frac{10}{75}\right)^{0.65}$$

<div align="right">**Eq. 2.5**</div>

$$Flow_{10Pa} = Flow_{75Pa} * 0.3$$

<div align="right">**Eq. 2.6**</div>

While the area and the air flux are the same for both openings, the volume subjected to the air flow is proportional to the width of the opening (the depth of the model, z-axis). The volume related to the 10x5 cm air entry is 10*18.4*232.8 cm^3, five times smaller than with an air entry of 50x1 cm^2, i.e., 50*18.4*232.8 cm^3 (Figure 2.31a). Even though simulating air leakage through a 10x5 cm^2 box is possible, the results ignore what happens in reality: the air spreads all over the insulation between two studs instead of traveling only through a hypothetical volume defined by [width of the opening * depth of the cavity * height of the cavity]. Therefore, the results overestimate the effect of the air leakage by concentrating the flow in a smaller volume, which does not exist. The consequences of this on the hygrothermal performance are discussed when setting up the model (Chapter 4).

This hypothetical volume is just an analogy to explain the physical concept related to the width of the opening; all the simulations are always run in 2D (x and y). Delphin only takes into consideration the depth of the model (z axis) when calculating results for variables integrated over the space, like moisture content in kg/m^3.

Focusing on the wider opening, Figure 2.31 shows three possible cross sections (A, B and C) to analyze the hygrothermal performance. Section C is closer to the wood stud than section A and it is plausible to assume the hygrothermal performance differs in each of them. Although this is true in real life, it is not true when running 2D simulations because they do not consider what is happening towards the z-axis (there is no way to "tell" Delphin there is a stud close to section C). Therefore, the three sections output the same results.
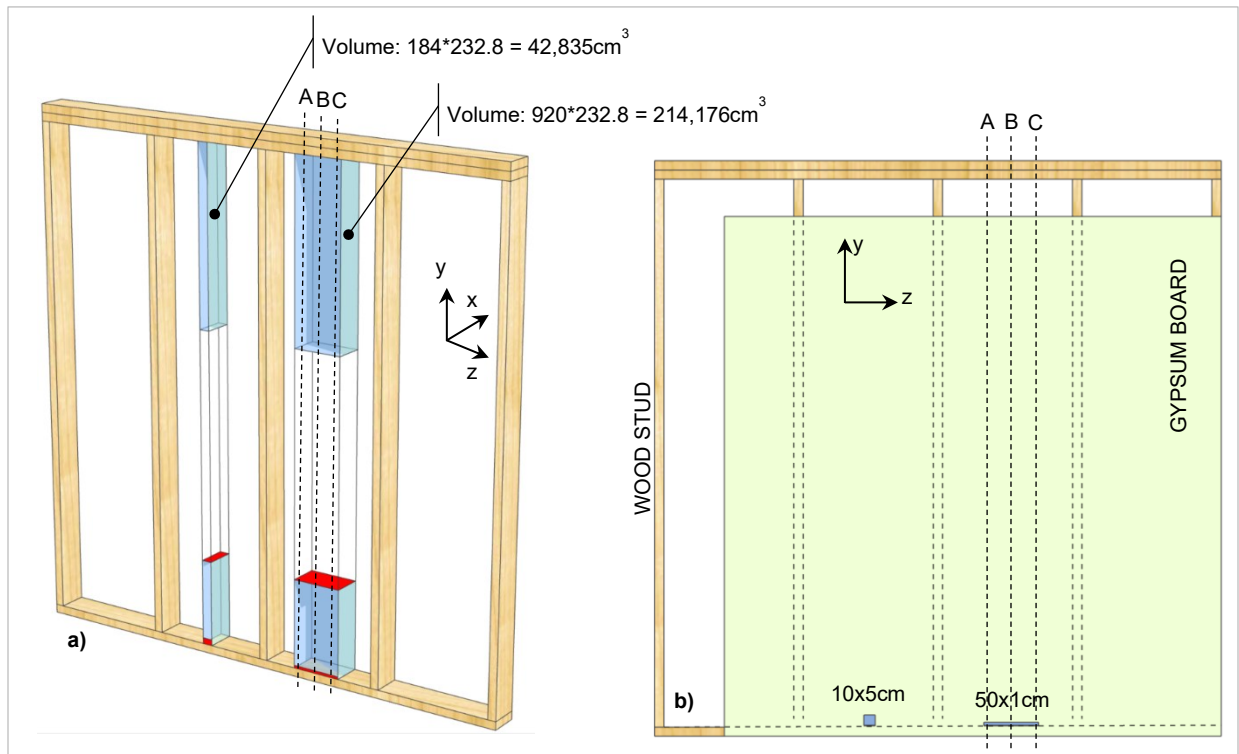
Figure 2.31. a) the volume subjected to air leakage varies with the opening; b) three possible sections (A, B and C) to analyze the hygrothermal performance of the assembly.

2.4.4.3. The relation between air flux and air permeability of the insulation

As discussed previously, the flux at the entry is an output of the Delphin solver and the relation with other variables is given by Eq. 2.7:

$$Flux = f(pressure, materials\ properties, air\ entry, path)$$ **Eq. 2.7**

After establishing the path, the air entry height and the pressure difference, the solver calculates the dispersion of the air through the cavity insulation according to the air permeability of the materials. If the required flux is not obtained, two strategies can be used:

- For a given geometry, the pressure difference must be adjusted until the flux is obtained.
- For a given pressure difference, the air permeability of the insulation must be adjusted so the desired flux is obtained as an output of the solver.

Changing the properties of the materials is a technique that can be used to better match simulation and experimental results, and it may require a sensitivity analysis for complex situations, like the experiments from Boardman & Glass (2020): the authors adjusted the properties of many materials in the assemblies as a way of improving the accuracy of the simulation results when compared to the experiments in the lab.

ASTM C 522 (ASTM, 2016) prescribes a method for measuring air permeability of porous materials with an apparatus like the one shown in Figure 2.32: air is forced through a section of the material due to a pressure difference provided by an air supply or vacuum mechanism. For mineral wool, the fibers of the specimen are mostly perpendicular to the air flow since this is the orientation

of the matts when installed in the cavity. The whole experiment is based on the idea that the flux is unidirectional and homogeneous.
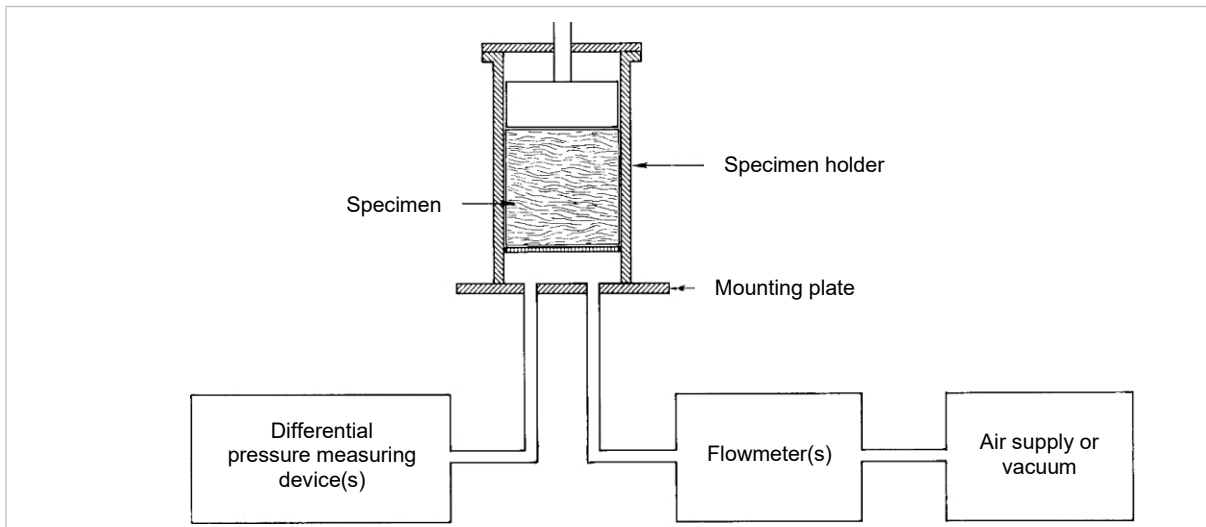
Figure 2.32. Schematic diagram of airflow apparatus to measure air flow resistance (ASTM, 2016).

However, air leakage through an assembly is the result of many irregular channels with different sizes and paths and the flux is neither unidirectional nor homogeneous. They cannot be simply condensed in a single channel without simplifications and losses, which means the permeability values found in the laboratory test are not directly applicable. The solver calculates the air flux through each cell for both directions according to the geometry, pressure difference and air permeability of the materials (Fechner, 2021, 2022).

Also, Gellert (2010) emphasizes the insulation itself is not homogeneously placed in place, it might settle with time and the permeability varies with its moisture content. Harreither et al (2015) found that the air flow resistance and density of each specimen among a set of 300 varies because of the inherent non-homogeneity of the material itself and also because of installation techniques and size of the specimen. After considering all these aspects, the air permeability of the insulation in the cavity may vary more than 100%. Hens (2007) adds:

> *Mass transfer properties do not characterize the material but the porous system, which may be quite variable between samples of a same batch of material samples and interacts intensively with the relative humidity in the surrounding air, giving rise to adsorption and capillary condensation … Things even become more complicated when looking to real envelope parts. They do not behave as the idealized constructions, models simulate, composed of homogeneous materials, with ideal diffusion and suction contacts in between. Simulating their heat, air, and moisture response with the models available today may show results which deviate largely from the actual response. Blaming the quality of the material data for these discrepancies is not correct. One should instead critically scrutinize the models and work on upgrades which include material heterogeneity, account for air transport, consider gravity and external pressure induced flow through cracks, voids, and air layers, take real initial conditions into account and evaluate probability and risk.*

In a study to determine the best building practice for Greenlandic conditions, Friis et al. (2023) undertook many simulations using Delphin and the material properties were iteratively calibrated to get the best fit between the model output and experimental data. So, varying the air permeability of the insulation in the model is a plausible strategy towards the goal of imposing an air flux at the air entry. Watt et al. (2014, 2015), when simulating air leakage due to natural convection using COMSOL Multiphysics, adjusted the air permeability of the interior fiber board so that the required values for air leakage rate could be attained.

Computer models must be adjusted to reflect the real assembly, accounting for heterogeneity, cracks, voids and other factors that make the material properties not directly applicable (Hens, 2007). Sometimes a sensitivity analysis might be required and material properties must be adjusted as a way of improving the correlation of the model with the experiment (Boardman & Glass, 2020). This sensitivity analysis is discussed when setting up the model in Chapter 4.

Different authors use different simulation tools and each one has its own engine to solve the balance equations related to heat, air, and moisture transfer. So, it is plausible to expect that those tools react differently to the same simplification and produce different results. This concept is explored by Defo et al. (2021) for four different tools (Delphin, Wufi, Comsol and hygIRC) and, even though there is no explicit citation to air leakage, the idea is applicable to it.

2.5. Summary of air leakage simulation

For a given air leakage rate, the paths of the air inside the insulated cavity vary because of material properties, constructive details, and unpredictable flaws; therefore, decisions on this subject are very difficult to make and the worst-case scenario is usually assumed due to the absence of more reliable information.

Even more simplifications are needed when practical assumptions must be transferred to a computer program and either 1D or 2D models have inherent limitations because air leakage is a spatial phenomenon and cannot be represented in only one or even two directions. Between 1D and 2D models, the latter can consider the height of the assembly, an important detail when assessing air leakage, but a much greater computational demand is implied when comparing to a 1D model.

During the 2D model implementation, the first step is to build the best grid in terms of time demand and accuracy, which may require a sensitivity analysis. After that, the relation between pressure difference, air leakage rate and air flux must be determined so that the assembly is subjected to the correct exfiltration rate. Also, adjustments of the air permeability of the insulation may be required to get the air leakage rate prescribed by the Canadian code or any other standard.

After reviewing the literature, the most important gap is the absence of details about how the air leakage simulations were implemented: most of the papers about the subject do not mention important details, which makes impossible for a third party to repeat the same work. To address this gap, this section clarified all the necessary details to implement air leakage using Delphin: the discretization process, accuracy and convergence, relations between air leakage rate, air permeability and air flux, and different air leakage paths. With those details, anyone´s simulations can be reproduced and compared to other studies.

2.6. Mould index as a performance indicator

Mould growth is a complex mechanism which is mostly influenced by relative humidity, temperature, material susceptibility, surface quality and duration (Ojanen et al., 2010). Different models are available in the literature for computing mould growth on building materials, for instance Nofal (1998), Sedlbauer (2001), Nofal and Kumaran (2010), Vereeken et al. (2011), Gradeci et al. (2017).

In this study, the VTT mould growth model (Lähdesmäki et al., 2011; Ojanen et al., 2010; Viitanen et al., 2015, 2011) was adopted and it is described by ASHRAE 160 (ASHRAE, 2016). It returns a number between 0 (no mold growth) and 6 (surface fully covered with mould), called Mould Index (MoI), by considering hourly values of relative humidity and temperature. As the algorithm can be easily implemented with the help of some equations (Eq. 2.8 to Eq. 2.14), processing the simulation results becomes a simple task; Table 2.2 provides all the necessary coefficients.

Table 2.2. Parameters for MoI calculations (adapted from ASHRAE, 2016).

Sensitivity class (examples)	k_1		W	A	B	C
	M < 1	M ≥ 1				
Very sensitive (Untreated wood; includes lots of nutrients for biological growth)	1	2	0	1	7	2
Sensitive (Planed wood, paper-coated products, wood-based boards)	0.578	0.386	1	0.3	6	1
Medium resistant (Cement or plastic based materials, mineral fibers)	0.072	0.097	1	0	5	1.5
Resistant (Glass and metal products, materials with efficient protective compound treatments)	0.033	0.014	1	0	3	1

Starting from zero, the MoI should be accumulated for each hour using Eq. 2.8:

$$M_t = M_{t-1} + \Delta M$$

Eq. 2.8

Where:

- M_t: MoI for the current hour
- M_{t-1}: MoI for the previous hour
- ΔM: change in MoI calculated according to the conditions specified below

If M_t yields a negative number at any time step, it shall be automatically set to zero.

If the surface temperature (T_s) is greater than 0°C, the relative humidity for mould initiation (RH_{crit}) shall be calculated according to Eq. 2.9 (very sensitive or sensitive material) or Eq. 2.10 (medium resistant or resistant material):

$$RH_{crit} = \begin{cases} -0.00267T_s^3 + 0.160T_s^2 - 3.13T_s + 100 \text{ when } T_s \leq 20°C \\ 80 \text{ when } T_s > 20°C \end{cases}$$

Eq. 2.9

$$RH_{crit} = \begin{cases} -0.00267T_s^3 + 0.160T_s^2 - 3.13T_s + 100 \text{ when } T_s \leq 7°C \\ 85 \text{ when } T_s > 7°C \end{cases}$$

Eq. 2.10

If the relative humidity at the material surface (RH_s) is greater than RH_{crit}, an increase in MoI shall be calculated as shown in Eq. 2.11:

$$\Delta M = \frac{k_1 k_2}{168exp(-0.68lnT_s - 13.9lnRH_s + 0.14W + 66.02)}$$

Eq. 2.11

Where:
- k_1:   mould growth intensity factor
- k_2:   mould index attenuation factor
- W: parameter from material sensitivity class

The mould index attenuation factor (k_2) shall be calculated according to Eq. 2.12:

$$k_2 = max\{1 - exp[2.3(M - M_{max})], 0\}$$

Eq. 2.12

Where M_{max} is the maximum MoI at the current hour (Eq. 2.13):

$$M_{max} = A + B\left(\frac{RH_{crit} - RH_s}{RH_{crit} - 100}\right) - C\left(\frac{RH_{crit} - RH_s}{RH_{crit} - 100}\right)^2$$

Eq. 2.13

Coefficients A, B and C are selected according to the sensitivity class.

If $T_s \leq 0°C$ or $RH_s \leq RH_{crit}$, a decline in the MoI shall be calculated according to Eq. 2.14:

$$\Delta M = \begin{cases} -0.00133k_3 \text{ when } t_{decl} \leq 6 \\ 0 \text{ when } 6 < t_{decl} \leq 24 \\ -0.000667k_3 \text{ when } t_{decl} > 24 \end{cases}$$

Eq. 2.14

Where:
- K_3:   decline coefficient specific to material surface
- t_{decl}:   number of hours from the moment when conditions for mould growth changed from favorable ($T_s > 0$ and $RH_s \geq RH_{crit}$) to unfavourable ($T_s \leq 0°C$ or $RH_s \leq RH_{crit}$)

Chapter 3. Methodology

3.1. Wall configuration

A wood frame wall of a 3.5-storey (10-m high) residential building located in suburban areas was considered. Figure 3.1 shows the typical composition of a brick cladding wall, Figure 3.2a shows the configuration of the assembly for hygrothermal simulations and Figure 3.2b shows the equivalent cross section.
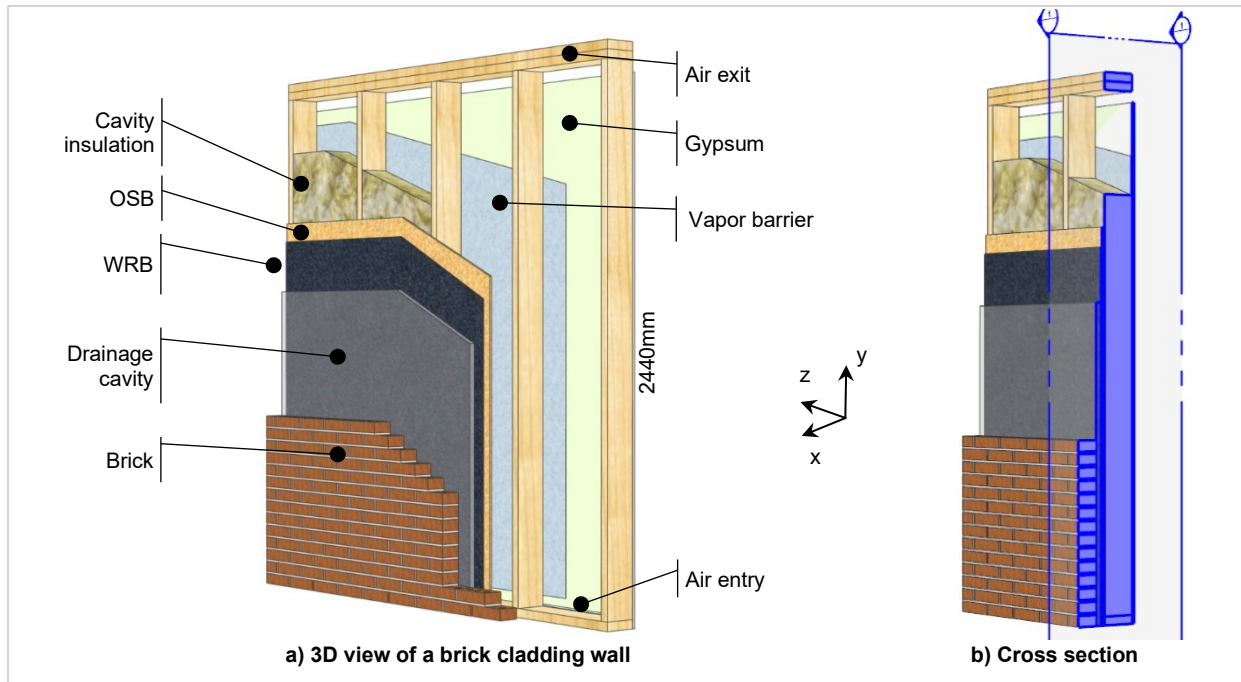
Figure 3.1. a) Typical composition of a brick cladding wall with the air entry at the bottom and air exit at the top; b) cross section.

1. Gypsum board (12.7 mm)
2. Polyethylene (6 mil = 0.15 mm)
3. Stud with mineral wool insulation
4. OSB (11.1 mm)
5. Sheathing membrane: 30' paper
6. Air layer
7. Brick veneer
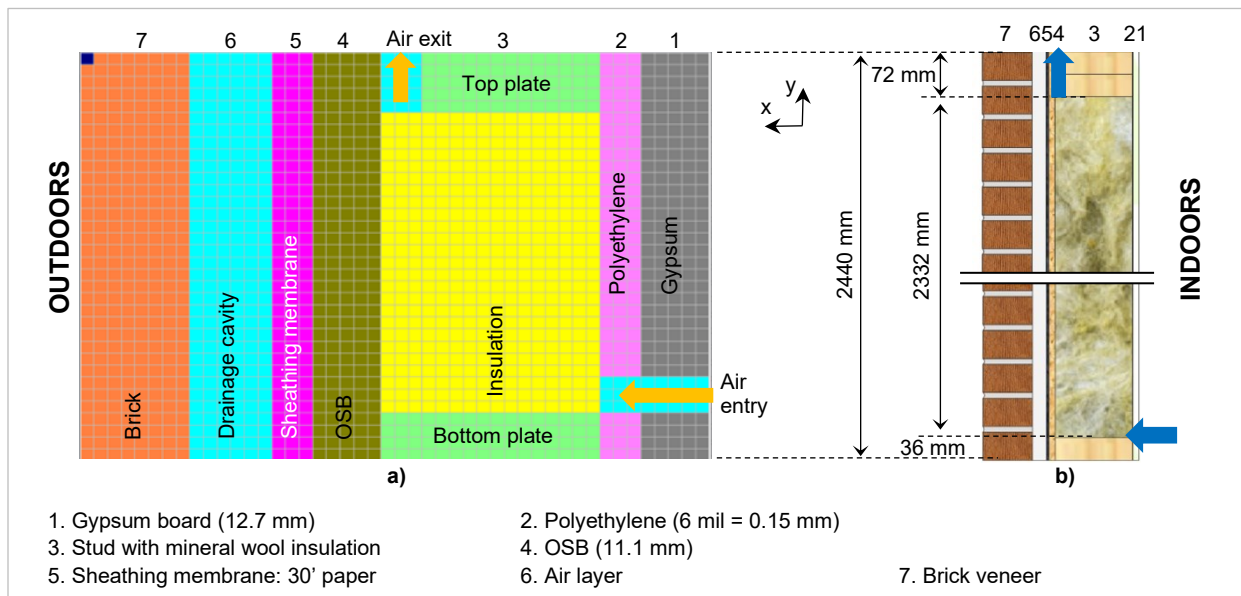
Figure 3.2. Brick veneer wall configuration (not to scale): a) Delphin model; b) cross section.

From the sheathing membrane (also called WRB – weather resistive barrier) to the indoor side of the assembly (from layer 5 to 1), all the layers are the same for all walls. Also, a capillary break (drainage cavity) is required by the NBC (NRCC, 2020, provision 9.27.2.2.(5)) when:

- HDD < 3400 and MI > 0.9 or
- HDD ≥ 3400 and MI > 1.0.

With brick cladding, a 25 mm thick capillary break is the same for all cases. With direct applied stucco (Whitehorse and Ottawa), there is no capillary break, and a 1.5 mm thick air layer was created so that the ACH could be applied to it. In Vancouver, which requires a capillary break, the air layer is 10 mm thick.

Figure 3.3 shows a 3D view and the description of the layers of each cladding type: brick, stucco, and vinyl.

A) **BRICK VENEER**
1. Gypsum board (12.7 mm)
2. Polyethylene (6 mil = 0.15 mm)
3. Plates & mineral wool
4. Sheathing board: OSB (11.1 mm)
5. Sheathing membrane: 30' paper
6. Air layer (drainage cavity).
7. Brick veneer cladding

B) **STUCCO**
(with drainage cavity)
1. Gypsum board (12.7 mm)
2. Polyethylene (6 mil = 0.15 mm)
3. Plates & mineral wool
4. Sheathing: OSB (11.1 mm)
5. Sheathing membrane: 30' paper
6. Furring
7. Lath
8. Basecoat
9. Finishing

Figure 3.3. Description of the layers of the assemblies.

3.2. Geographic locations

Appendix C of the NBC has a list with hundreds of cities across Canada and for each one some information is given, for instance: annual rain, design temperature, moisture index (MI), HDD, among others. MI is a measure of the overall risk to the development of possible moisture issues in a wall assembly; it is calculated as a function of wetting and drying indices: while the wetting index is basically related to the amount of rain, the drying index is related to the degree of vapor saturation of the air, a more complex phenomenon related to the temperature of the air. Those two indices are better explained in Cornick et al (2002) and Cornick and Dalgliesh (2003).

Three cities were selected for analysis, based on their geographic location and HDD (climatic zone): Ottawa (ON), Whitehorse (YT) and Vancouver (BC). From now on, these cities will be referred to as Ott, Van, and Whe, respectively; the city of Toronto with vinyl cladding was used only when setting up the model. Table 3.1 shows some climate details of the selected cities and Figure 3.4 shows the climatic regions of Canada.

Table 3.1. Geographic location and climate details of the selected cities (NRCC, 2020).

City (Province)	Latitude (°)	Longitude (°)	HDD [1] (h)	Zone [2]	RSI_{min} (W/m²K) [3]	Moisture index (MI) [4]	Annual rain (mm)
Whitehorse (YT) – Whe	60.71	-135.07	6580	7B	3.85	0.5	170
Vancouver (BC) – Van	49.28	-123.12	2825	4	2.78	1.4	1325
Ottawa (ON) – Ott	45.32	-75.67	4440	6	3.08	0.8	750
Toronto (ON) – Tor	43.68	-79.63	3800	5	3.08	0.9	730

(1) HDD: Heating degree days below 18°C.
(2) Zone: Climatic zone, inferred from the HDD value.
(3) RSI: Effective thermal resistance (without heat-recovery ventilator, Table 9.36.2.6.-A).
(4) MI: Moisture index (refer to Appendix C of the National Building Code for explanations about MI).
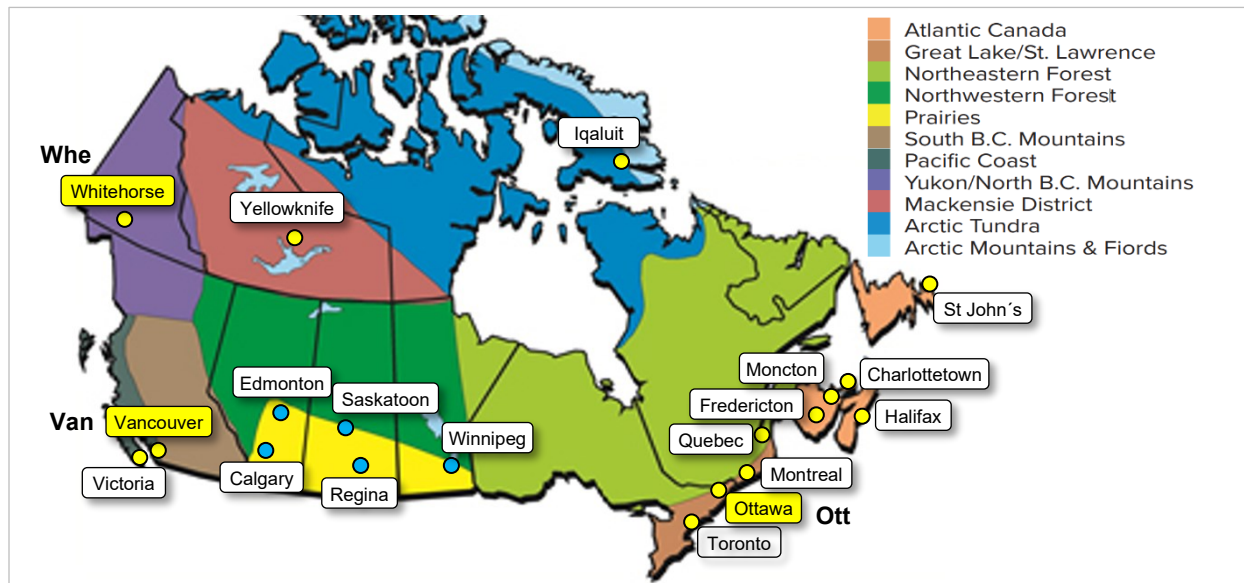
Figure 3.4. Climatic regions of Canada and location of the major cities (ECCC, 2020).

3.3. Climate data

Two sets of climate data were used: historical (H) and future (F7, when a global warming of 3.5°C is expected to be reached by the end of the 21st century). Both sets were obtained as described by Gaur & Lacasse (2022) and encompass 15 realizations having 31 consecutive years, from 1991 to 2021 and from 2064 to 2094. Figure 3.5 to Figure 3.7 show the profiles for RH, T, WDR and wind speed and pressure difference for each city.

For hygrothermal simulations, the 31 years were sorted in descending order of average winter temperature (from January to April and from October to December); then, the 3rd coldest year was selected and repeated three times.

The default wall orientation was the one which has the highest total pressure difference between inside and outside. However, when the pressure outside happened to be higher than the pressure inside the building, it was set equal to indoor pressure, which means only exfiltration was considered in all cases.
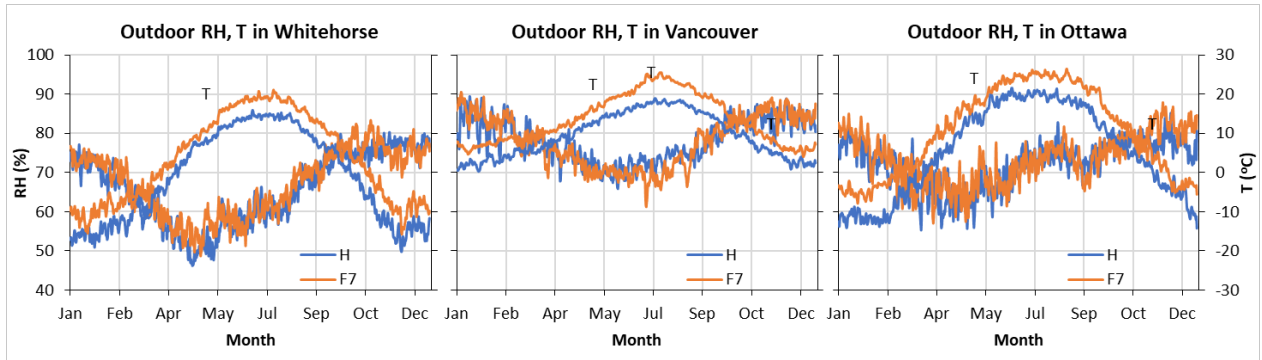
Figure 3.5. Outdoor RH and T profiles (15 Runs combined) for the three cities, historical (H) and Future (F7) periods.
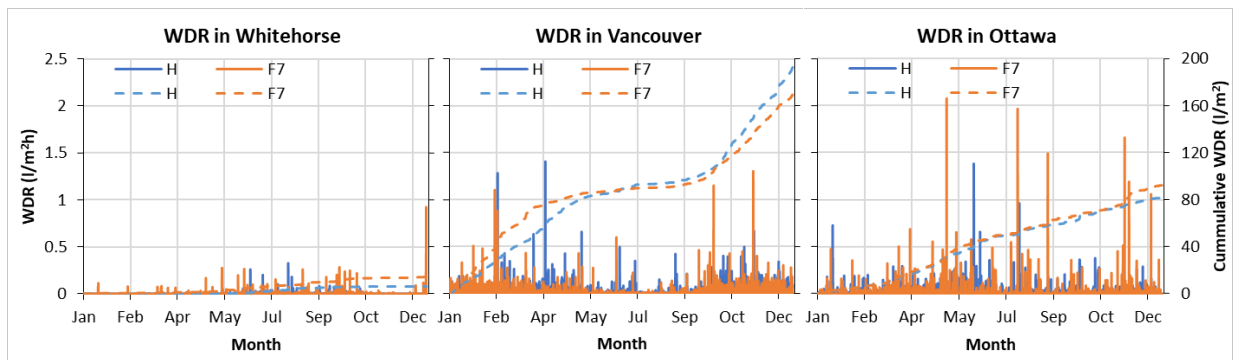
Figure 3.6. Hourly WDR (solid lines) and cumulative WDR (dashed lines) for the three cities, historical (H) and Future (F7) periods.
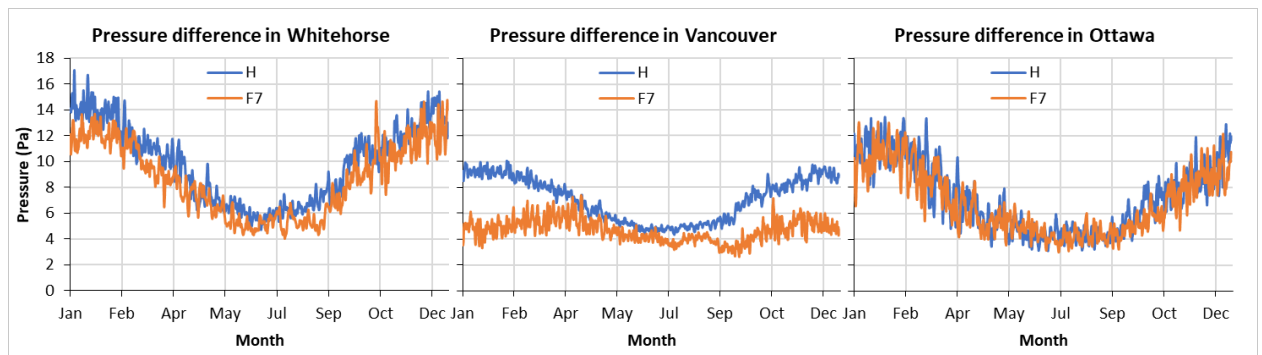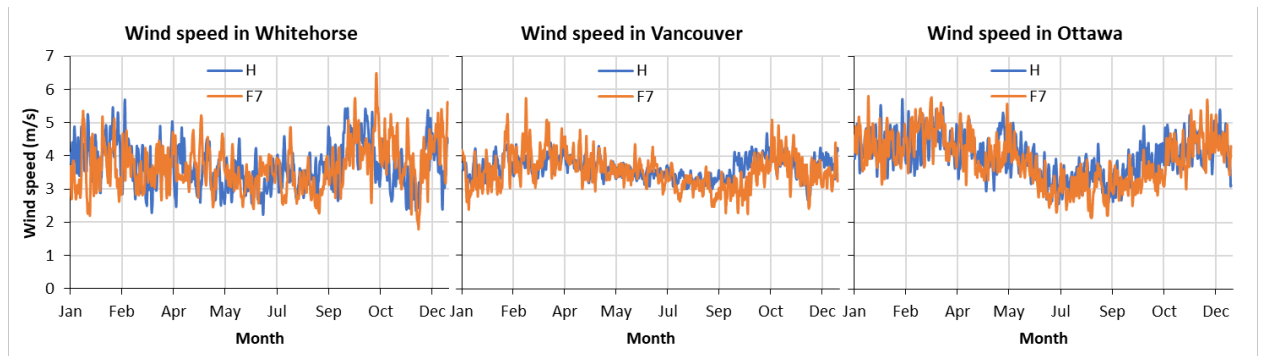
Figure 3.7. Wind speed and pressure difference for the three cities, historical (H) and Future (F7) periods.

Indoor and outdoor air pressures were derived from the combination of indoor mechanical ventilation, wind, and stack pressures. In this study, the ventilation pressure was set to 3 Pa.

Stack pressure is due to the temperature difference between indoor and outdoor and is calculated as follows:

$$\Delta P_{stack} = z(\rho_{out} - \rho_{in}) * g$$

Eq. 3.1

Where:

- ΔP_{stack}:   stack pressure (Pa)   z: height (m)
- ρ_{out}:   outdoor air density (kg/m^3) ρ_{in}:   indoor air density (kg/m^3)
- g: gravity (9.81 m/s^2)

For a 3.5-storey residential building, it was considered the neutral plane is in the middle of the 2nd floor, at about 5 m. The pressure was calculated at the bottom of the 1st floor, which means z = - 5 m.

Wind impinges directly on a wall and flows around or over a building, creating a distribution of pressures on the building´s exterior surfaces; these pressures are related to the wind direction and speed, air density, wall orientation and surrounding conditions. The value is calculated using the Bernoulli equation (Eq. 3.2):

$$P_w = C_p * \rho * \frac{U^2}{2}$$

Eq. 3.2

Where:

- P_w: wind pressure (Pa)
- C_p :   surface pressure coefficient (dimensionless)
- ρ: outdoor air density (kg/m^3)
- U: wind speed (m/s)

The air-pressure coefficient is related to the angle between the wind direction and the wall. In this study, the harmonic trigonometric function developed by Walker and Wilson (1994) was used (Eq. 3.3):

$$C_p = \frac{1}{2}\left\{[C_p1 + C_p2](cos^2\emptyset)^{\frac{1}{4}} + [C_p1 - C_p2](cos\emptyset)^{\frac{3}{4}} + [C_p3 + C_p4](sin^2\emptyset)^2 + [C_p3 - C_p4]sin\emptyset\right\}$$

Eq. 3.3

Where:

- C_p1:   pressure coefficient when wind is at 0°
- C_p2:   pressure coefficient when wind is at 180°
- C_p3:   pressure coefficient when wind is at 90°
- C_p4:   pressure coefficient when wind is at 270°
- Φ: wind angle

Typical values for C_p1 to C_p4 for low-rise buildings are 0.6, -0.3, -0.65, -0.65, respectively.

3.4. HAM configuration

3.4.1. Overview of the simulation tool

According to DELPHIN documentation, the program (Coupled Heat, Air, Moisture and Pollutant Simulation in Building Envelope Systems) was first developed in 2004-2006 with funding support from research grants from U.S. Environmental Protection Agency, U.S. Department of Energy, Syracuse Center of Excellence in Energy and Environmental Systems, EQS-STAR Center/New York State Office of Science, Technology and Academic Research, and Syracuse University. It is an outcome of a joint effort between BEESL/Syracuse University (USA) and the Institute for Building Climatology/University of Technology Dresden (TUD), Germany. One of the first applications of this tool is described by Kalamees & Kurnitski (2010) when assessing the performance of exterior walls and roofs under forced moisture convection.

The development of the code first started around 1988 and it was called DIM; under this name it was further developed to version 3.1. Around 2000, a graphical user interface was added, and the name was changed to DELPHIN. This was the beginning of DELPHIN 4 and the first try for coupling with air transport was implemented in the tool. Around 2004, Andreas Nicolai started to develop DELPHIN 5 while working at Syracuse university, where he managed to get the fundings. He also wrote his PhD dissertation focusing on salt and VOC transfer (Nicolai, 2007) and a summary for this can be found elsewhere (Nicolai et al., 2009). The development of DELPHIN 6 started in 2015 and the current development is under the frame of his own company: Bauklimatik Dresden Software GmbH.

The tool has been validated for the heat, moisture and air transport for one- and two-dimensional problems with five HAMSTAD[3] benchmarks, two cases using ISO 10211 (ISO, 2017), one case using EN 15026 (BSI, 2007) and one suction-drying test. All validation cases could be mapped and recalculated with different versions of Delphin and the results were always within the specified tolerance range or in the range of the other numerical solutions. The benchmarks include (among others): one-dimensional insulated roof, a two-layer wall under dynamic climatic conditions and a brick wall with internal insulation attached with mortar (Sontag et al., 2013).

An important feature of DELPHIN is its ability to handle wind-driven rain deposition, solar radiation, air leakage and moisture/heat sources as individual files.

3.4.2. Material properties

The properties of the materials used in this study were taken from NRC material database.

3.4.3. Initial conditions

Initial conditions were set to 15°C and 60% RH for all layers.

---

[3] The HAMSTAD project (Heat, Air and Moisture Standardization) dealt with the numerical simulation of heat, moisture, and air transport mechanisms in building materials.

3.4.4. Boundary conditions

3.4.4.1. Wind-driven rain (WDR)

All cases were simulated with and without wind-driven rain so that it was possible to see the influence of the air leakage alone. When WDR was considered, 1% of it was applied to the outer layer of the sheathing membrane.

3.4.4.2. Indoor conditions

Indoor temperature was calculated using the ASHRAE method with the "Heating Only" approach (ASHRAE, 2016) as shown in Table 3.2.

Table 3.2. Details of the method for calculating indoor temperature, heating only (ASHRAE, 2016).

24-hour running average of outdoor temperature	Indoor design temperature, °C (°F)	
	Heating only	Heating and air conditioning
$T_{0,24h} \leq 18.3°C$ ($T_{0,24h} \leq 65°F$)	21.1°C (70°F)	21.1°C (70°F)
$18.3°C < T_{0,24h} \leq 21.1°C$ ($65°F < T_{0,24h} \leq 70°F$)	$T_{0,24h} + 2.8°C$ ($T_{0,24h} + 5°F$)	$T_{0,24h} + 2.8°C$ ($T_{0,24h} + 5°F$)
$T_{0,24h} > 21.1°C$ ($T_{0,24h} > 70°F$)		23.9°C (75°F)

The European Class model (class 3 – moderate moisture generation) described in ISO 13788 (ISO, 2012) was used to calculate indoor relative humidity (Eq. 3.4).

$$RH_i = \frac{(P_e + \Delta P)}{P_{sat,i}} * 100 \qquad \text{Eq. 3.4}$$

Where:

- RH_i: indoor RH (%)
- P_e: outdoor vapor pressure at the mean monthly temperature (Pa)
- ΔP: vapor pressure difference (indoor – outdoor) for the selected class (Pa)
- $P_{sat,i}$:   indoor saturation vapor pressure (Pa)

The value of ΔP is related to the selected moisture generation class and to the temperature difference between indoor and outdoor as well (Figure A.2 from ISO 13788).

The Class model was selected because it performs well for such a simple model and can be used when reliable data regarding moisture generation rates and air changes is not readily available (Cornick & Kumaran, 2007, 2008). Figure 3.8 shows the profiles for indoor RH an T.
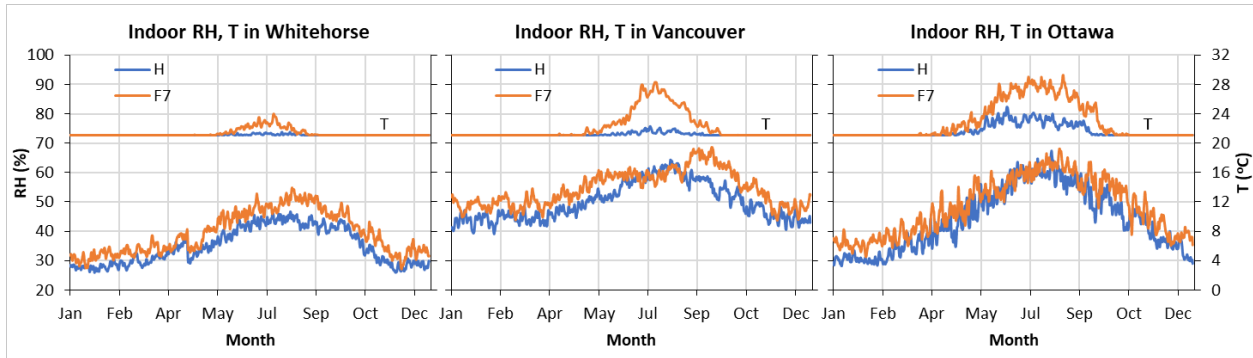
Figure 3.8. Indoor RH and T for the three cities, historical (H) and Future (F7) periods.

3.4.4.3. Other boundary parameters

Coefficients and parameters used to configure the simulations were adopted as follows:

- outdoor convective heat transfer: $4+4v$ W/m²K, (v = wind speed in m/s)
- outdoor vapor transfer: $2.44*10^{-8} + 2.44*10^{-8}$ v s/m, (v = wind speed in m/s)
- indoor heat transfer: 8 W/m²K
- indoor vapor transfer: $1.52*10^{-8}$ s/m
- ground shortwave reflection: 0.2
- ground longwave emission: 0.9
- surface shortwave absorption: 0.6 for red brick and 0.35 for all others
- surface longwave emission: 0.9

3.4.5. Simulation parameters

All the simulations were set to start on Jan 1st. The solver parameters were set as: initial time step = 0.01 s; maximum time step = 60 min; relative tolerance = 10^{-6}; smallest time step = 10^{-5} s.

3.5. Assumptions when configuring the hygrothermal simulations

During the creation of the computational model, some assumptions were made as follows:

- Simulations were run for three consecutive years using the third coldest year selected among the 31-year period and this was assumed to be the worst-case scenario for air leakage.
- The bottom and top part of the assembly were considered adiabatic, which means there is no HAM flux through those sections.
- All layers are supposed to be in perfect contact with each other. In the case of air leakage, gaps between the insulation and the frame may form preferable and unpredictable paths.
- The hygrothermal results do not take into consideration the wood studs. The scrutinized section is in the middle of the insulated cavity and only the presence of top and bottom plates was considered.
- Material properties are assumed to be the same regardless of the material´s thickness.
- Material properties are assumed to be the same in both x and y axes.
- The air permeability of the insulation was considered an independent variable.

- Buoyancy was disabled in all cases, which means the natural convection inside the cavity was not considered. It was assumed its influence would be minor when compared to the effect of air leakage.

- The orientations of the walls were selected based on the greatest air leakage rate and the simulations were performed with and without WDR. The direction with the worst-case scenario for WDR may not be the same, though.

- WDR infiltration was assumed to be 1% regardless of the cladding. This means a direct applied stucco has the same moisture load as brick cladding with a drainage cavity of 25 mm. In practice, this cannot be true.

- WDR is applied homogeneously from bottom to top of the sheathing layer. However, when using 2D models, some specific portions of OSB could be subjected to liquid water due to constructive reasons. This would require even more assumptions, though, and homogeneous distribution was adopted.

- ACH values were assumed constant during the simulation, but it varies according to the hourly wind speed, and this may affect the drying potential of the assembly. This effect was neglected and assumed to be minor when dealing with moisture due to air leakage coming from indoors.

3.6. Performance assessment

The mould index (MoI) was calculated assuming a sensitive class for both material and surface, and 0.1 as decline factor (there is no suggestion for OSB in ASHRAE and then 0.1 was adopted as a conservative value[4]).

3.6.1. Locations of interest

The spots highlighted in red/black (Figure 3.9) are the monitored positions where the simulation results were extracted from. The length of each position is also shown, and they are not the same because they are related to the number of cells in the grid.
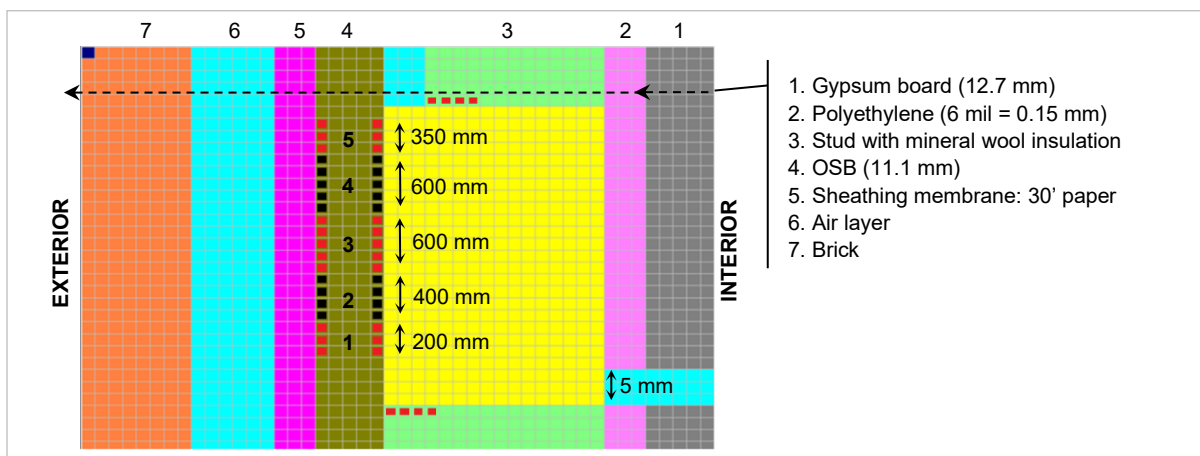
Figure 3.9. Brick veneer wall configuration (not to scale), monitoring positions (dashed lines in red/black) and the five locations of interest due to air leakage: "1" to "5".

---

[4] Table B-2 and comment B-25 of ASHRAE 160.

Chapter 4. Set up of the model

4.1. Configuring the air leakage path

A set of 3 year long simulations using the model in Figure 3.9 was performed varying the air permeability of the insulation and the height of the opening; the air permeability of the air in the channels at the air entry and at the air exit was adjusted to the same value of the air permeability of the insulation for each case. North orientation in Whitehorse was assumed for all cases.

The target was to obtain air leakage rates in the range of the values suggested by NBC, converted to values at 10 Pa. This pressure was used to calibrate the model and find the relation between flux, opening height and air permeability. The hourly pressure for each city, however, is given by the climate files. Figure 4.1 shows the results for five different values of K_g and 10 different opening heights. Based on that, one can create any other relation by adjusting the pressure difference or the value of K_g, whichever is more convenient.
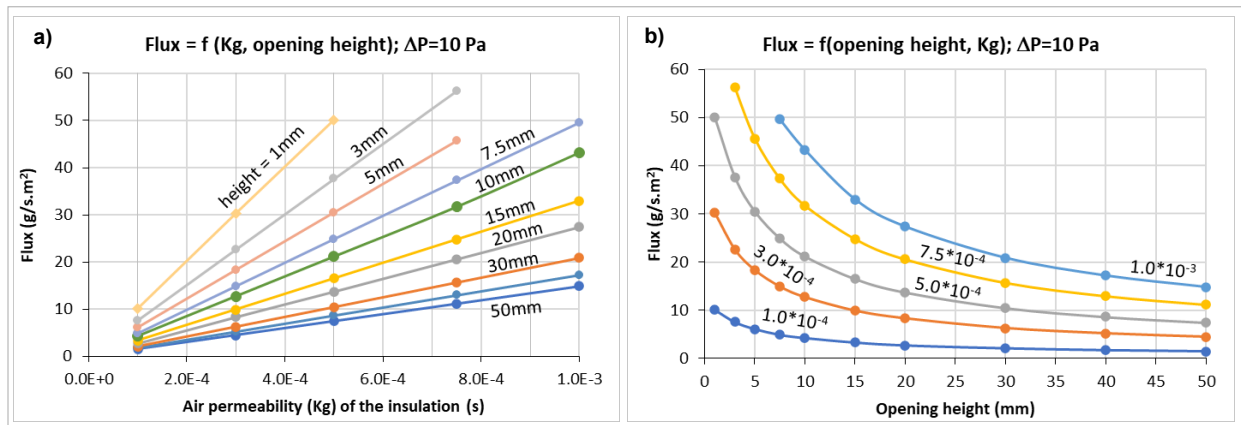
Figure 4.1. Flux at the air entry (@10 Pa) for different values of
a) insulation air permeability (K_g) and b) opening height.

Table 4.1 shows the values extracted from Figure 4.1; the flux is proportional to the value of K_g for a given opening height. This happens because R2 is much bigger than Rü, R1 and R3 (Figure 2.29) and the permeance is mostly related to R2, which has a linear relation with K_g. This is very useful since any desired flux can be obtained by interpolating the values in Table 4.1; moreover, the value of Rü has negligible effect over the results, either using δ=2 or δ=1000; so, δ=2 was used in all simulations.

Table 4.1. Flux at the air entry for different values of insulation air permeability (K_g) and opening height

K_g (s)	Flux at 10 Pa (g/s.m^2)									
	Opening height at the bottom plate (mm)									
	50	40	30	20	15	10	7.5	5	3	1
$1.0*10^{-4}$	1.48	1.72	2.10	2.70	3.30	4.24	4.90	6.11	7.55	10.10
$3.0*10^{-4}$	4.45	5.17	6.28	8.30	9.90	12.71	14.90	18.31	22.62	30.23
$5.0*10^{-4}$	7.42	8.61	10.46	13.71	16.50	21.17	24.90	30.49	37.64	50.00
$7.5*10^{-4}$	11.13	12.92	15.68	20.56	24.78	31.73	37.30	45.67	56.35	-
$1.0*10^{-3}$	14.84	17.22	20.90	27.39	33.00	43.26	49.60	-	-	-

The value for δ, the exchange coefficient, was kept constant at its default value of 2.0.

Figure 4.2 show the results at 360 h[5] in terms of RH and T maps when the geometry was subjected to an air leakage rate of 0.05 L/sm^2 @ 75 Pa (flux of 8.5 g/s.m^2 @10 Pa, according to Eq. 2.3). Even though the air leakage rate is the same in both cases, the opening 1x50 cm^2 is five times wider than 5x10 cm^2, which means the same amount of air passes through different volumes (Figure 2.31) of the insulated cavity at the same time. Therefore, the smaller the volume, the higher the effect of the leakage rate.

RH (%) of the geometry at 360 h (ΔP = 10 Pa)　　　　T (°C) of the geometry at 360 h (ΔP = 10 Pa)
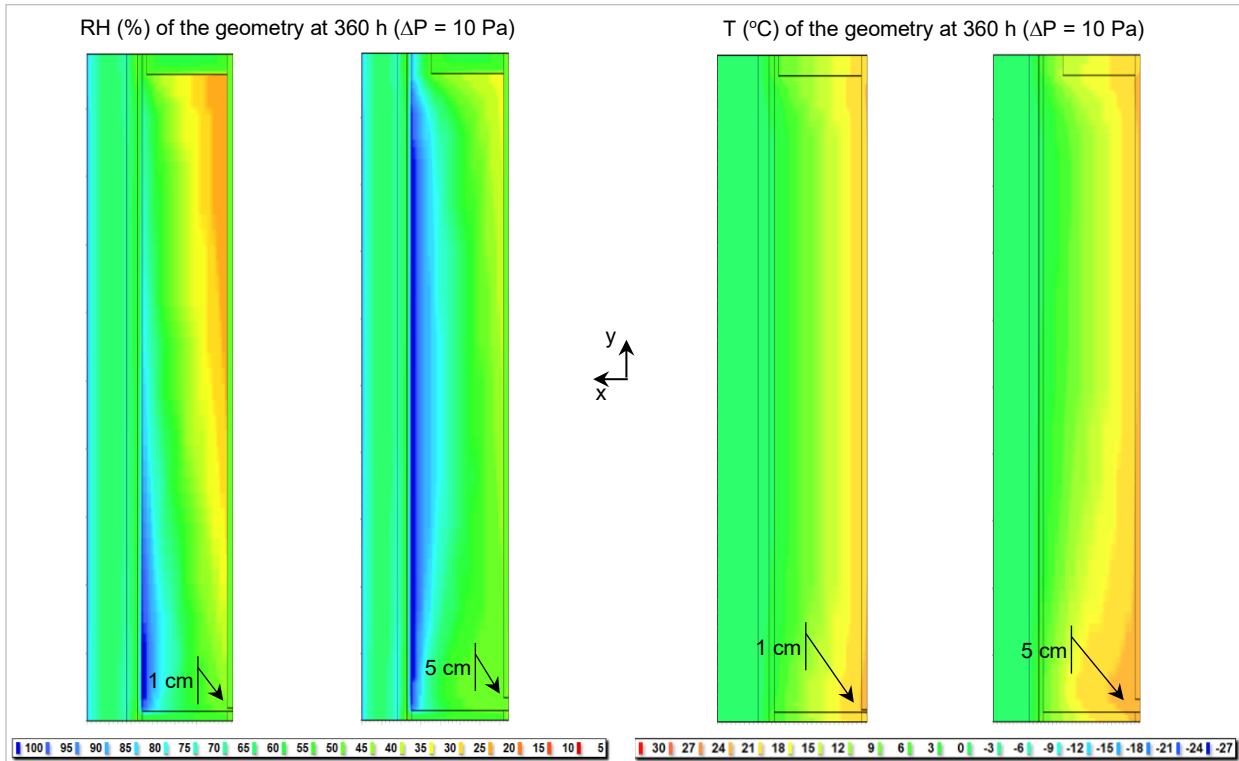
Figure 4.2. RH and T maps inside the geometry for two different opening heights (1 and 5 cm) subjected to the same air leakage rate.

Varying the air permeability of the insulation could have an impact on buoyancy effect since permeable insulations have air-filled porosity. However, buoyancy is only considered if explicitly activated in the configuration window (Figure 4.3).
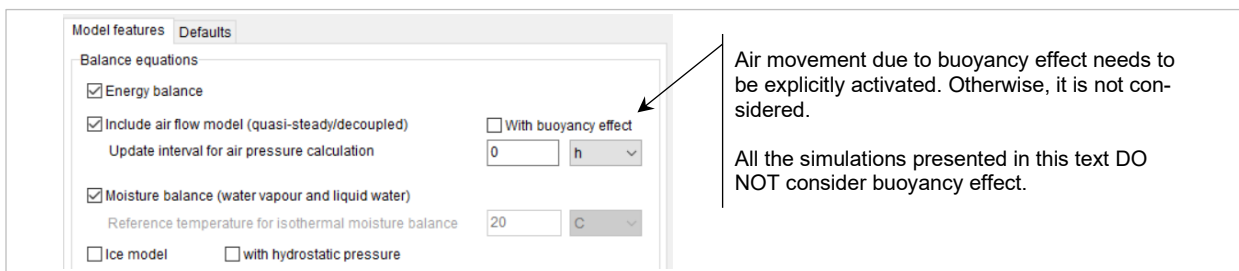
Figure 4.3. Simulation settings showing the option to activate buoyancy effect.

---

[5] The value of 360 h was selected because the differences at this time were evident enough to show using colorful maps.

With the buoyancy effect disabled, Figure 4.4 shows the maps for RH and T and Figure 4.5 shows the profiles for moisture content of OSB (whole layer) and RH of OSB (close to the bottom plate): regardless of the K_g, the results are the same. Therefore, no differences in the hygrothermal results are expected when changing the air permeability of the cavity insulation, which means that adjusting this property as a way of getting the desired air flux is doable and has no unintended consequences.
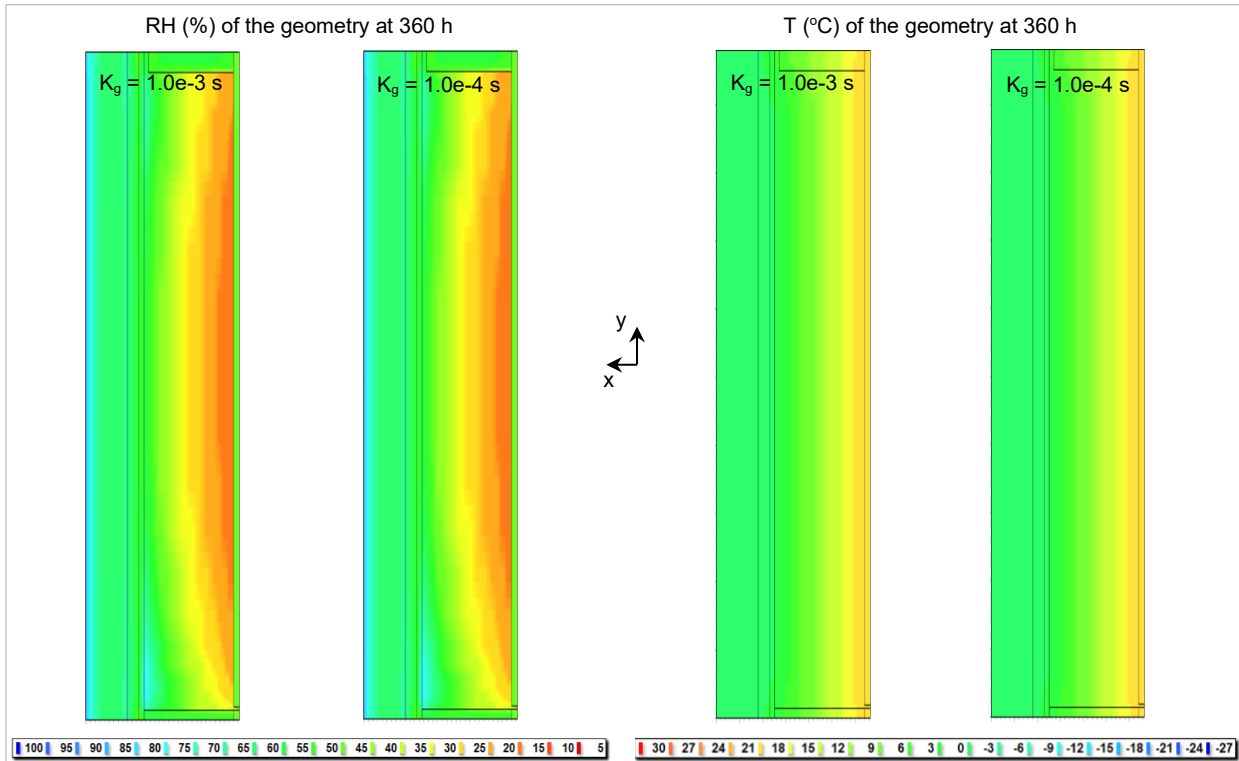
Figure 4.4. RH maps inside the geometry for an opening height of 10 mm for two air permeabilities of the cavity insulation: 10^{-3}s and 10^{-4}s. Buoyancy effect is disabled.
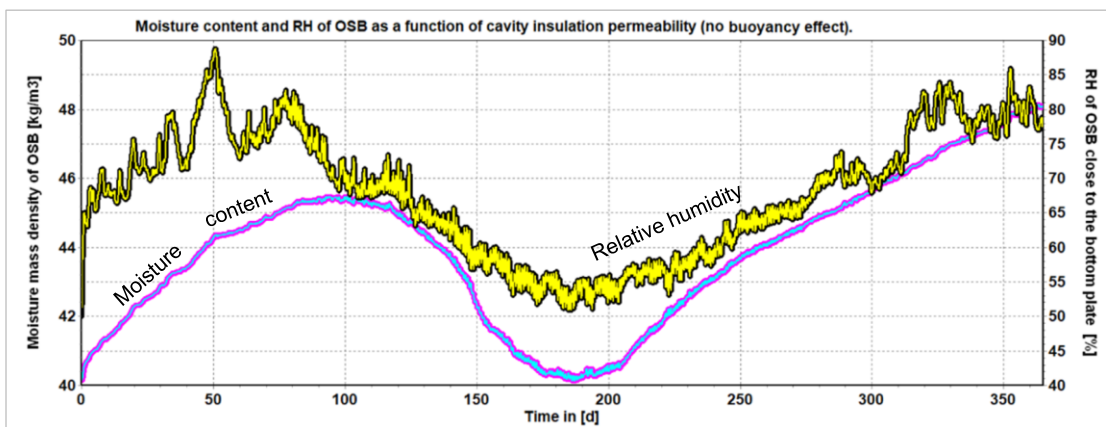
Figure 4.5. MC of OSB (whole layer) and RH of OSB (close to the bottom plate) for two air permeabilities of the insulation: 10^{-3}s and 10^{-4}s. Buoyancy effect is disabled.

Lastly, Figure 4.6 and Figure 4.7 emphasize the importance of defining how the air openings are modeled and their influence on the hygrothermal results. Figure 4.6 shows that the effects of air leakage are concentrated at the same level of the openings, which agrees with the results shown in Figure 2.17. Also, for the same opening size and position, the hygrothermal results vary if the airflow changes from horizontal to vertical. The maps of RH (Figure 4.6a,b) are slightly different and may not be so obvious, but the profiles of RH and MC over one year (Figure 4.7) make this difference clearer. The horizontal opening, whose flow is oriented towards OSB, shows greater RH and MC during the cold season.
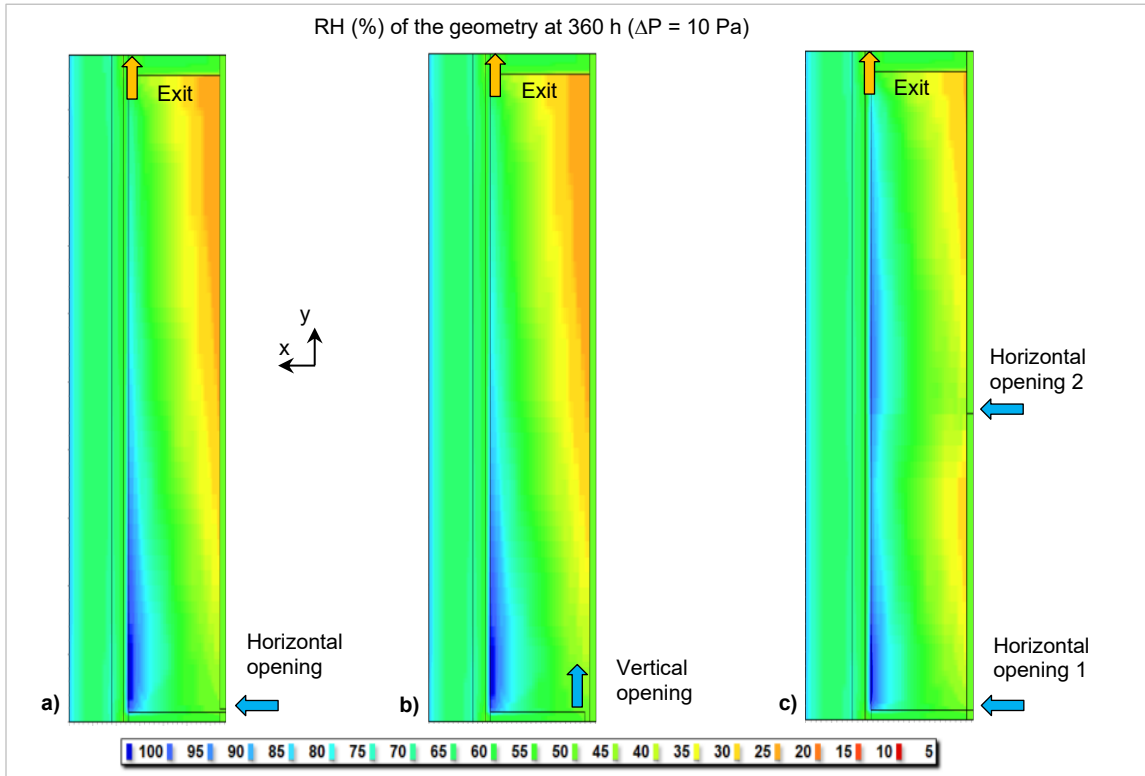
Figure 4.6. RH maps inside the geometry for three cases: a) one horizontal opening; b) one vertical opening; c) two horizontal openings.
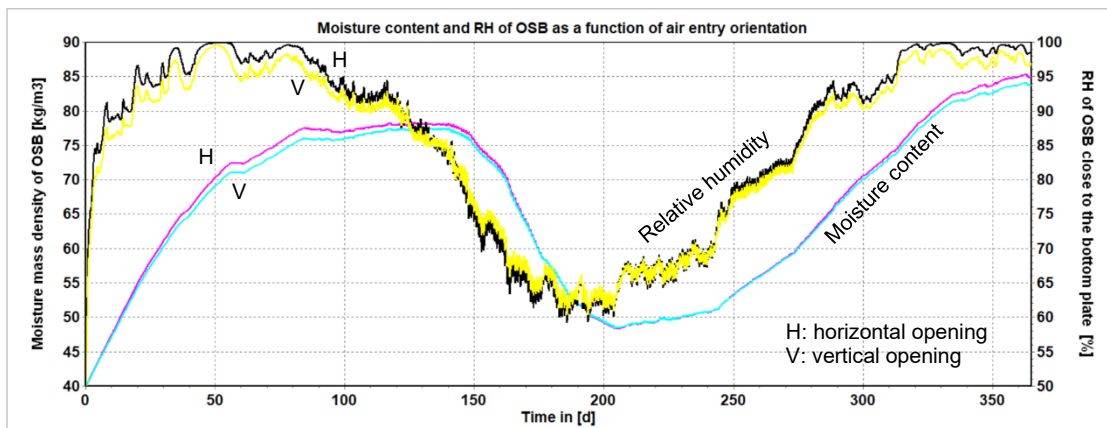
Figure 4.7. MC of OSB (whole layer) and RH of OSB (close to the bottom plate) for two cases: one horizontal opening at the bottom and one vertical opening at the bottom.

4.2. Impact of the mesh size

After establishing the relation among air flux, opening height and pressure difference, a 5 mm high continuous horizontal opening was assumed at the bottom of the assembly. Position "1" (Figure 3.9) was selected to assess the hygrothermal results and a set of simulations was performed for the sensitivity analysis. An air leakage rate of 0.10 L/s.m² at 75 Pa was adopted, which represents an air flux of:

$$Flux_{5mmx1m} = \frac{0.10 \frac{L}{s.m^2} * 2.4m * 1m}{0.005m * 1m} * 0.3 = 14.4 \frac{L}{s.m^2} \cong 17 \frac{g}{s.m^2} \ (at \ 10Pa)$$

Eq. 4.1

As a way of deciding the best grid to use, the set of simulations used five SGT: 0.25 mm, 0.5 mm, 1.00 mm, 2.00 mm, and 3.00 mm. Starting from each of these SGT, three STR were used to generate the final mesh: 1.5, 2.0 and 3.0. The combination of these two variables will be shown using the following format: [SGT; STR]. For example [0.25; 1.5], [1.0; 3.0], [2.0; 2.0] and so on.

The city of Whitehorse (HDD = 6580, climate zone 7B) was selected because it is very cold and prone to problems with moisture accumulation due to air leakage. Brick cladding was selected because it is thicker than stucco and, thereafter, it is a better option for analyzing the discretization. All the cases were simulated with two pressure differences: constant at 10 Pa and with the values from the climate file (Figure 4.8).
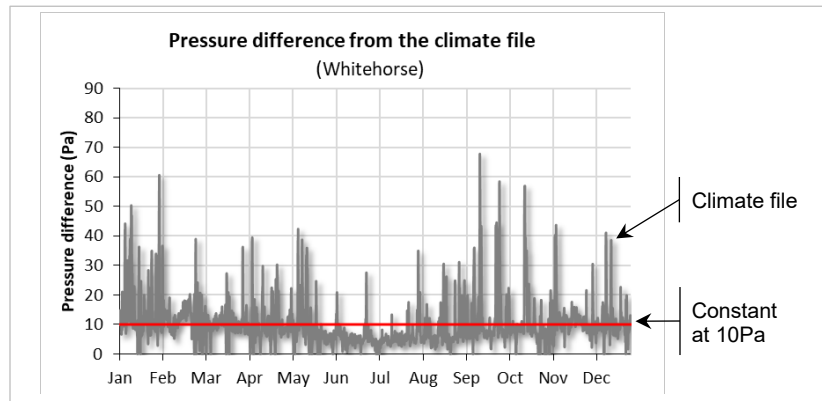
Figure 4.8. Profile of the pressure difference when compared to 10 Pa.

Figure 4.9 shows the final grid for an SGT of 0.25 mm when the discretization is done considering three STR: 1.5, 2.0 and 3.0; while the finest grid has 6468 cells, the coarse one has only 2772. The shaded region was not modified so that the outputs at position "1" were extracted from the same physical portion of the assembly, regardless of the mesh.
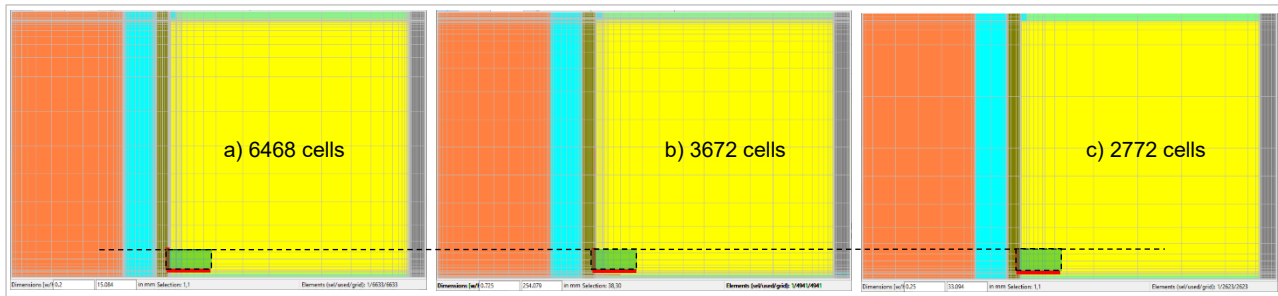
Figure 4.9. Final discretization and number of cells for SGT of 0.25 mm and STR of a) 1.5; b) 2.0 and c) 3.0. Grid inside the shaded region kept constant for the three cases.

Table 4.2 and Figure 4.10 show some relevant data about each case: SGT, STR, number of cells and simulation time[6]. Regardless of the pressure difference, constant at 10 Pa and from the climate files (Figure 4.8), the simulation time is similar.

Table 4.2. Time required (average per year) to run the simulations in Whitehorse with brick cladding with two pressure differences: constant at 10 Pa and from the climate files.

SGT (mm)	STR	Cells	Time (h)		SGT (mm)	STR	Cells	Time (h)	
			ΔP = 10 Pa	ΔP = datafile				ΔP = 10 Pa	ΔP = datafile
0.25	1.5	6468	23.3	24.2	2.00	1.5	2520	5.0	5.4
0.25	2.0	3672	8.7	9.0	2.00	2.0	2142	3.8	4.1
0.25	3.0	2772	5.9	6.5	2.00	3.0	1564	2.3	2.4
0.50	1.5	4941	12.9	13.8	3.00	1.5	2548	4.1	4.4
0.50	2.0	3300	7.0	7.2	3.00	2.0	1927	2.7	2.8
0.50	3.0	2352	4.0	3.9	3.00	3.0	1720	2.4	2.1
1.00	1.5	4389	8.5	11.9					
1.00	2.0	2726	4.4	5.8					
1.00	3.0	2132	3.0	3.2					

Figure 4.10a shows the simulation times are proportional to the total number of cells. Figure 4.10b shows the simulation time for each SGT when varying the STR: the variation is similar for each SGT and the time is lower for greater STR since the total number of cells is lower. During the discretization, care was taken to keep the flux in the range of 17 ± 0.5 g/s.m² because this has a significant impact on the hygrothermal results.

---

[6] Simulation time is deeply related to the computer used but the proportion among them should be similar. These values were obtained using a Laptop Dell Inspiron, 8Gb RAM, CPU Intel i7 @ 2.2Mhz (8 cores), running Windows 10.
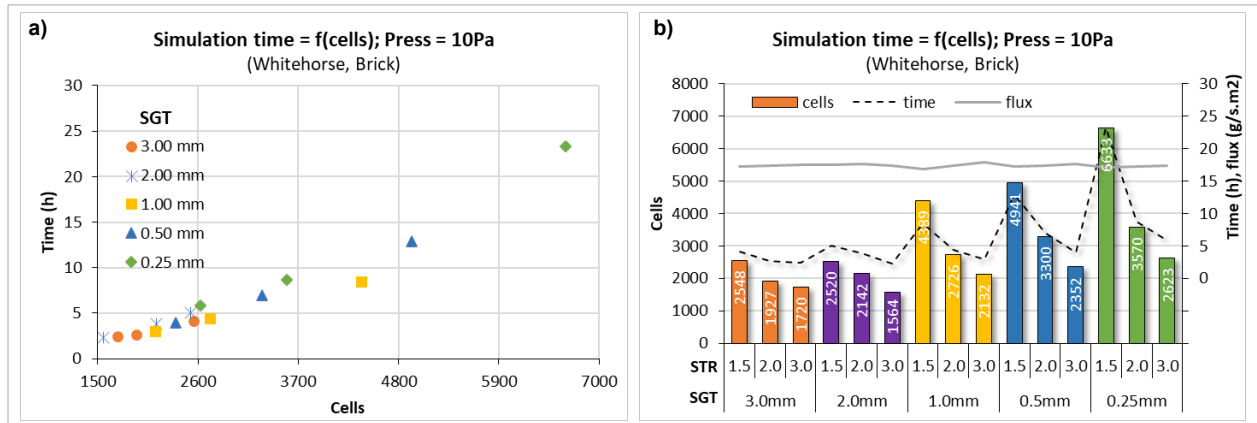
Figure 4.10. a) simulation time (average per year) as a function of number of cells and SGT; b) number of cells, simulation time and flux as a function of SGT and STR.

4.2.1. Accuracy

Figure 4.11a,b show the RH profile for variable SGT and two STR: 1.5 and 3.0. There is almost no difference between the profiles, which means using a STR of 1.5 or 3.0 leads to basically the same results.
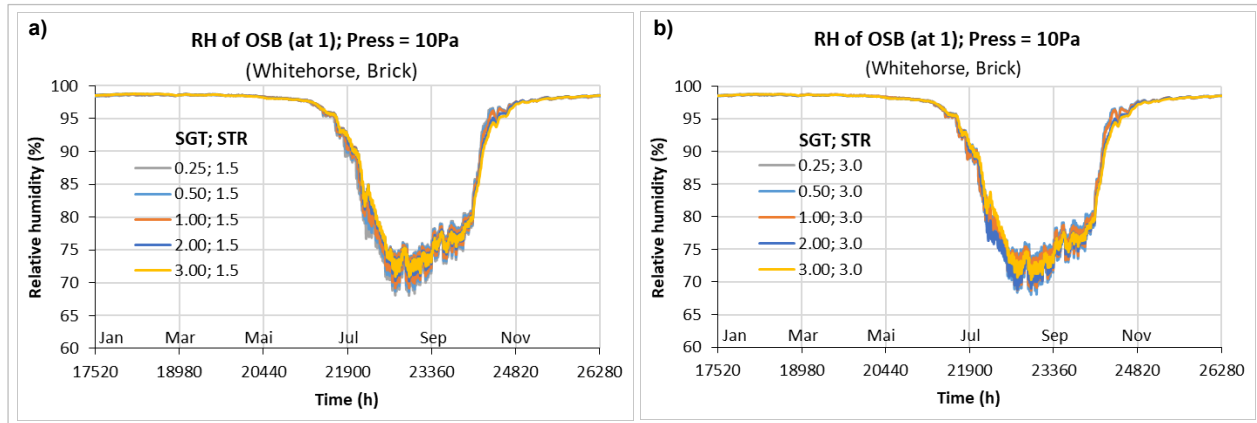
Figure 4.11. RH of OSB (at pos. 1) as a function of variable SGT and a) STR = 1.5; b) STR = 3.0.

Figure 4.12a,b show the RH profile for variable STR and two SGT: 0.25 mm and 3.0 mm. The first case is more sensitive to the variations of RH because the volume of material to reach equilibrium with the surrounding air is smaller and, therefore, it responds faster to the variations of RH. In both cases, though, the shape of the curve is the same.
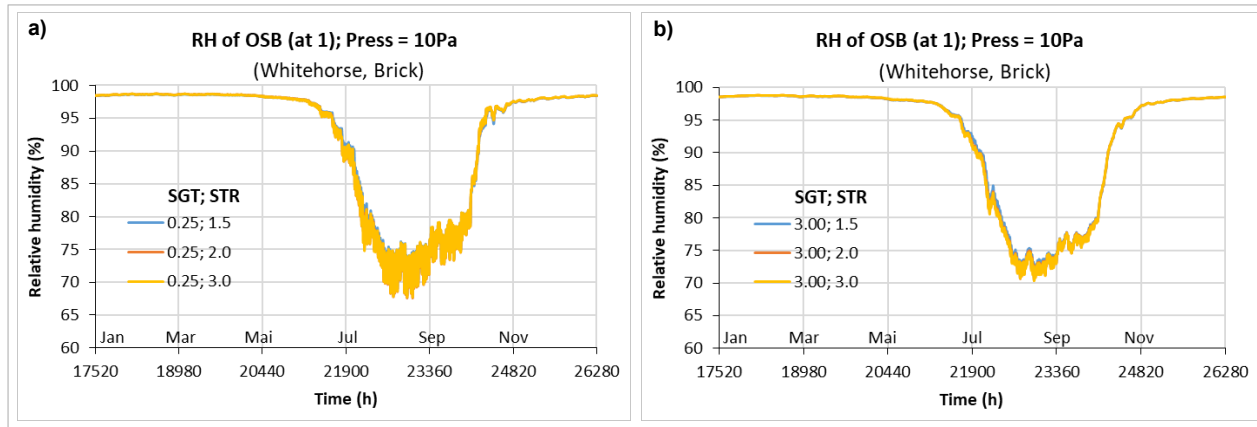
Figure 4.12. RH of OSB (at pos. 1) as a function of variable STR and a) SGT = 0.25; b) SGT = 3.0.

The hourly values of RH and MC profiles with SGT of 0,5; 1.0; 2.0 and 3.0 were compared to the outputs from the finest grid ([0.25; 1.5]) using the root mean square error evaluation (RMSE). Figure 4.13 exposes the comparisons: for a surface grid thickness of 3.00 mm, the RMSE of RH is 1.20%, 1.26% and 1.23% for STR of 1.5, 2.0 and 3.0 respectively (Figure 4.13a). When analyzing MC, these values are 0.95%, 0.97% and 1.00% (Figure 4.13b). Comparisons of the T profiles were intentionally omitted because the variation is minor (below 0.3°C).
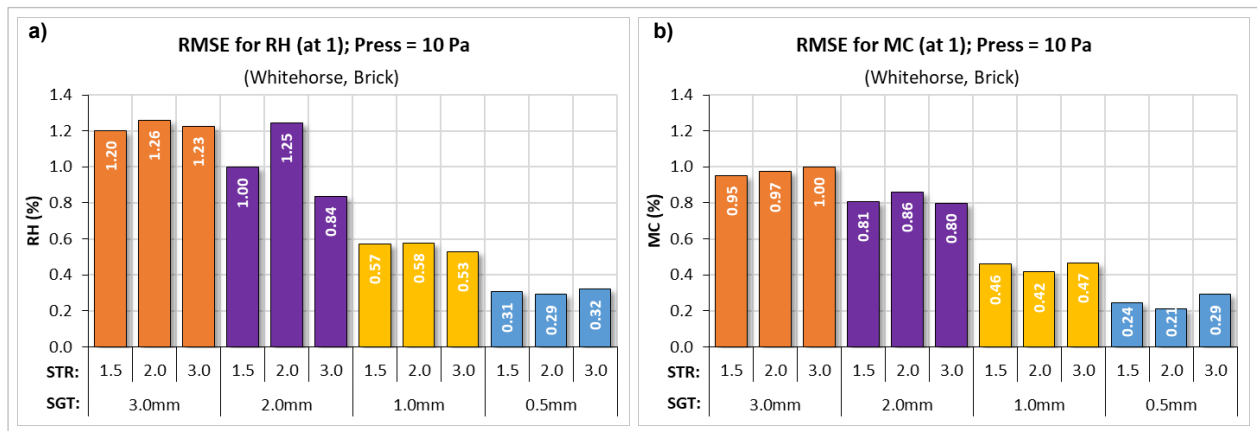
Figure 4.13. RMSE for a) RH and b) MC of OSB (at 1) when comparing to an SGT of 0.25mm.

All cases show that the coarser the SGT, the bigger the error and one must decide the highest tolerable value according to the situation being analyzed. Regarding simulation time, it varies from 2.3 h ([2.0; 3.0]) to 23.3 h ([0.25; 1.5]), which makes an SGT of 0.25 mm prohibitive.

Assuming a maximum RSME of 1% for RH and MC, only the case with SGT of 3 mm does not meet this criterion; if the threshold is raised to 1.5%, any option is acceptable. So, the option [2.0; 3.0] would be the best one because its simulation time is similar to [3.0, 3.0] but its results are more accurate in terms of RH.

Figure 4.14 shows the mould index profiles for all the combinations of SGT and STR: the variations in RH and T were not enough to introduce any significant difference in the mould index. However, it is important to emphasize that variations in the air flux greater than 5% may impact the results and compromise the accuracy.
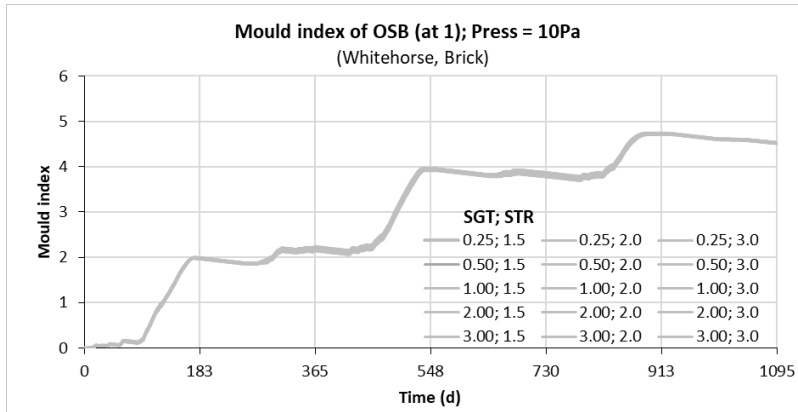
Figure 4.14. Mould index profiles for all the combinations of SGT and STR.

4.2.2. Convergence

To analyze the convergence of the model, RH and MC values from SGT of 0.5, 1.0, 2.0 and 3.0 were compared to the finest mesh by subtracting their values using STR of 1.5 (after subtraction, absolute values were taken to build the chart). Figure 4.15a,b show the results for RH and MC respectively for six positions in time taken from the profile in Figure 4.11a. As the SGT varies from 3.0 to 0.5 mm, RH and MC tend to converge to the values from the finest mesh. RH values in the range 20,000 h to 24,000 h fluctuate between 70 and 98% (Figure 4.11a), but the difference between [3.0; 1.5] and [0.25; 1.5] is only 1.0% at 22,000 h and 2.6% at 22,800 h (Figure 4.15a).

For the range 17,000 h to 21,000 h, Figure 4.11a shows that the differences in RH are much lower, almost negligible. This fact has important consequences when evaluating the mould index, since the VTT model considers mould growth only when RH is higher than 80%. If the RH values are similar regardless of the surface grid thickness, mould index will also be similar (Figure 4.14) since T is the same in all cases.

Figure 4.15b shows the differences when analyzing MC: the observations are the same as the ones for RH, but the absolute values are smaller: 0.25% at 22,000 h and 0,5% at 22,800 h. Considering all this and the simulation time, the option [2.0; 3.0] was taken as the **selected grid**.
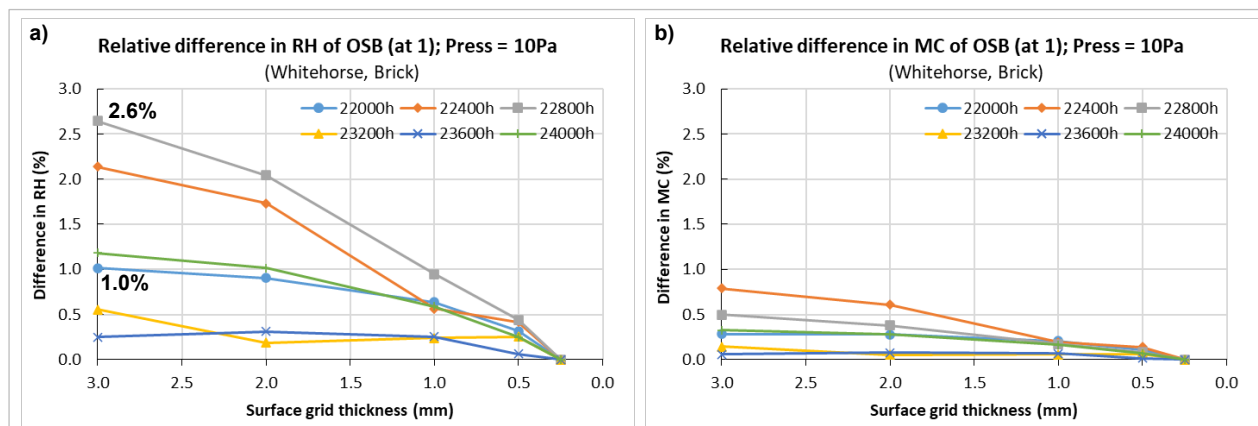
Figure 4.15. Differences in a) RH and b) MC of OSB (at 1) as a function of SGT at different times for STR = 1.5.

Accuracy and convergence were also analyzed in Toronto with brick cladding, Whitehorse with stucco cladding and Whitehorse with vinyl cladding; the results can be found in Appendix A.

4.3. Manual optimization

When the mesh is created, it is normal to start with an SGT (for instance 1 mm) and the simulation tool automatically creates the grid using a given STR. However, the thickness of any individual row/column can be modified manually, rows can be merged and so on. This is what is meant by "manual optimization" and it requires a good understanding of how the tool works and the consequences of these specific adjustments.

Once the selected grid has been defined, there still are some adjustments that can be made without compromising the accuracy of the results: firstly, the size of the cells far away from position "1" (for instance, the top plate is far from the bottom part of OSB) do not play a significant role on the outputs of that specific region; secondly, some cells in the middle of a component can be made bigger by using bigger STR. In both cases the goal is the same: reduce the number of cells in the grid.

Checking where the biggest gradients inside the whole geometry are helps when deciding what to do and where, since a fine mesh should be maintained at those positions. Figure 4.16 and Figure 4.17 show the RH field for two STR: 1.5 and 3.0. Apart from the number of cells, both fields are similar, and the biggest gradients are localized at: drainage cavity, OSB, brick cladding, and top and bottom plates.

In Figure 4.17, two columns in the middle of the brick layer were combined into one and two columns in the middle of the air layer were also combined into one, reducing the number of columns from 8 to 7 and from 6 to 5 respectively. The total number of cells varied from 1564 to 1496 (Figure 4.18). This task is done manually and generates a new optimized mesh. When downsizing even more other parts of the grid, it either introduces undesirable differences in the air flux, compromises the accuracy of the results (mainly RH and MC) or both.
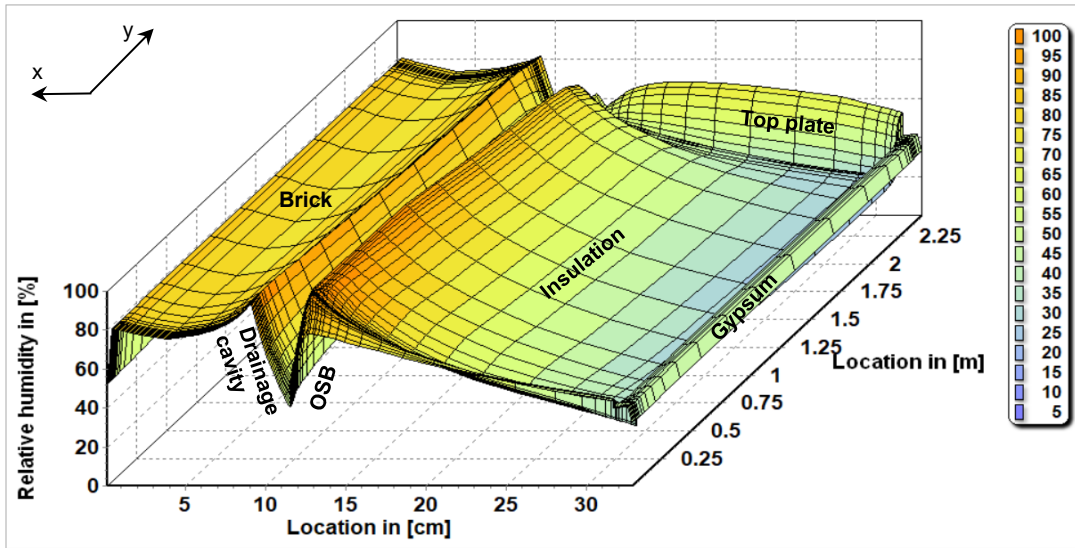
Figure 4.16. RH field of the assembly for [2.0; 1.5].
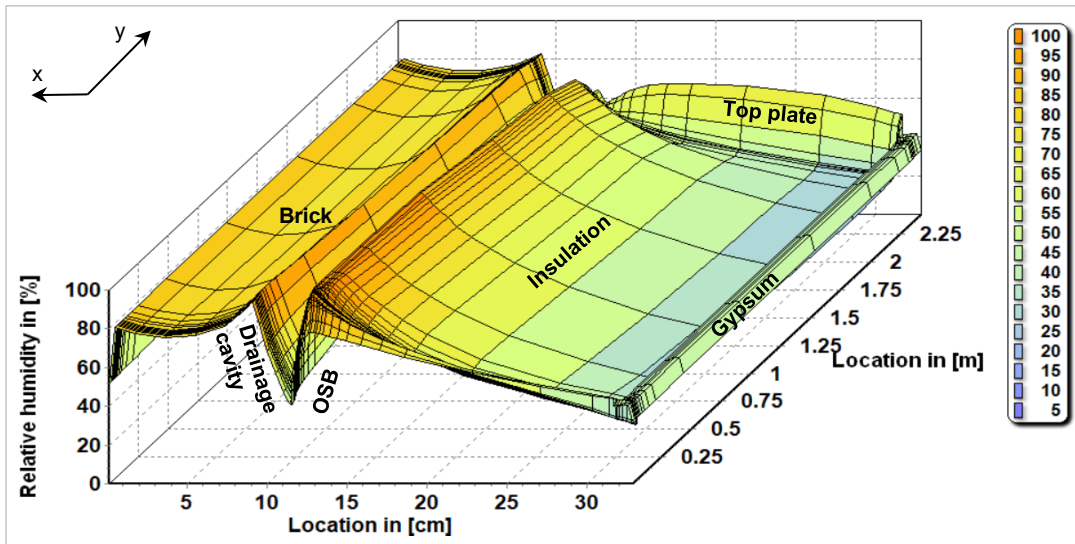
Figure 4.17. RH field of the assembly for [2.0; 3.0], the selected grid.
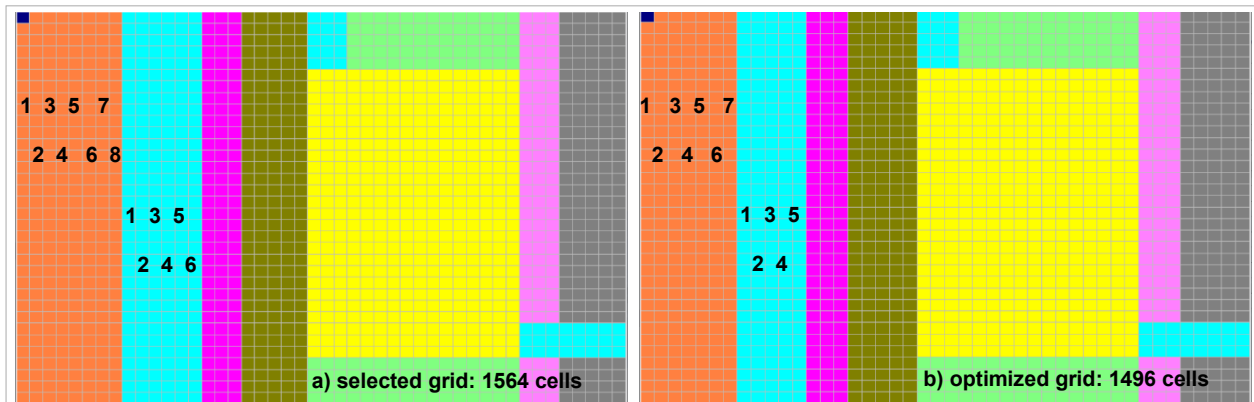
Figure 4.18. Number of cells for the a) selected grid and b) optimized grid.

Figure 4.19 shows RH and MC profiles for both meshes: the differences between the reference and the optimized mesh are negligible.

However, in this case the manual optimization was not able to reduce the simulation time because the number of cells is similar in the selected and optimized meshes. In any case, from the fine mesh [0.25; 1.5] to the selected mesh [2.00; 3.0], the simulation time was reduced from roughly 23h to 2.3h, which means getting the same results in only 10% of the time.
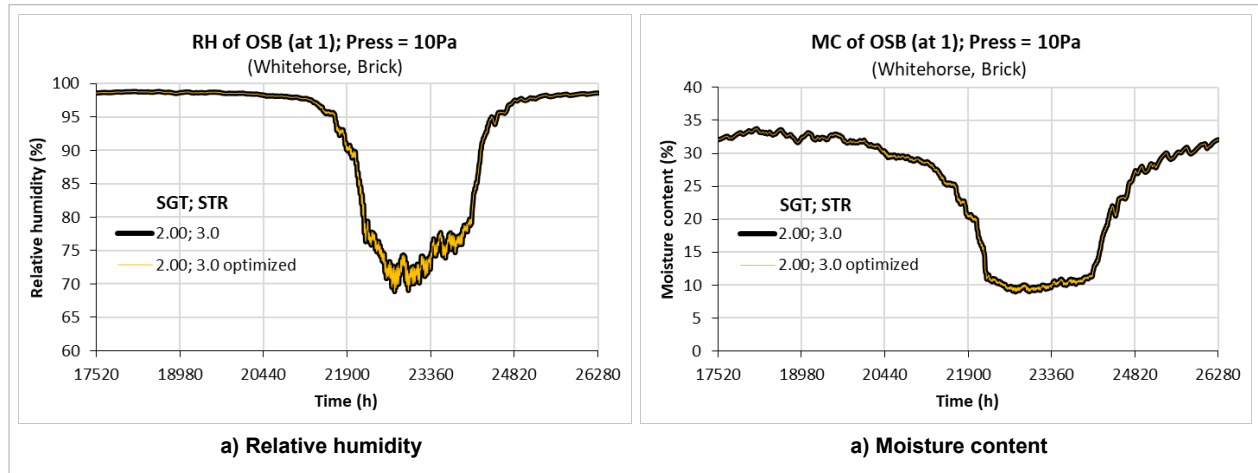
Figure 4.19. a) RH and b) MC of selected [2.00; 3.0] and optimized meshes [2.00; 3.0 optimized].

4.3.1. Simplification

If the outputs from any other region apart from position "1" are not necessary, the grid can be further optimized. This step includes its "deformation", keeping the focus only on the region of interest and making all the rest very coarse. Figure 4.20 and Figure 4.21 show this case: position "1" at the bottom part of OSB is 200 mm long in both selected and simplified meshes, even though it is 4 mm lower in the coarse mesh when comparing to the selected mesh.

Because of the considerable modification in the grid, the air permeability of the insulation had to be adjusted so that the airflow was the same in both cases: from $2.8*10^{-4}$ s in the selected grid, the air permeability of the insulation becomes $1.7*10^{-4}$ s in the simplified 2D (s2D).

Figure 4.22 shows a comparison of mould profiles from all the combinations of SGT and STR and from the simplified mesh: they all follow the same trend, although in Whitehorse with brick cladding there is a slightly higher deviation when using s2D. The most important factor, however, is the simulation time: while the selected grid took 2.3 h to complete, the simplified mesh took only 35 min. This means roughly 2% of the time required by the finest grid ([0.25; 1.5]) or 25% of the time for the selected grid ([2.0; 3.0]).

a) selected mesh: 1564 cells   b) simplified mesh (s2D): 430 cells

*dimensions in milimeters
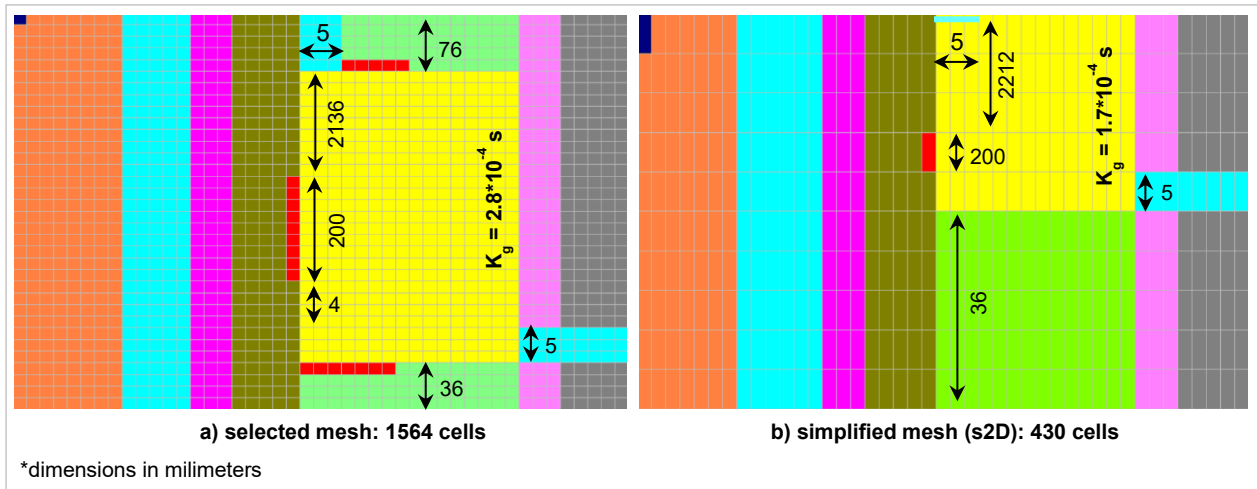
Figure 4.20. The selected mesh (a) was "deformed" to create the simplified mesh (s2D). Number of cells and distances are emphasized.

a) Selected mesh: 1564 cells   b) Simplified mesh (s2D): 430 cells
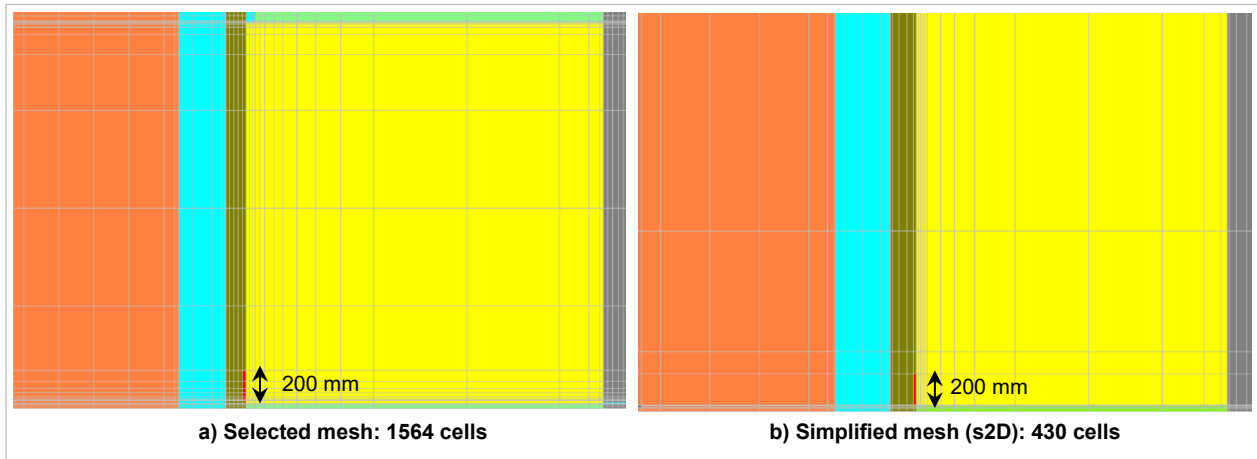
Figure 4.21. The selected mesh (a) was "deformed" to create the simplified mesh (s2D). Relative sizes of the cells are emphasized.
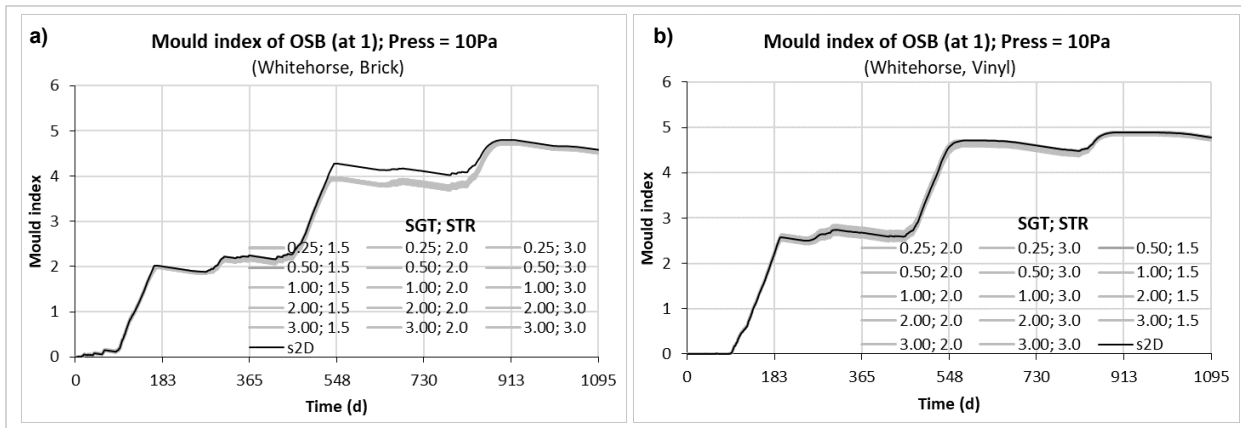
Figure 4.22. Mould index profiles for all the combinations of SGT and STR compared to the simplified grid (s2D) for a) brick and b) vinyl.

Chapter 5. Model application and simulation results

Hygrothermal simulations using the grid in Figure 4.18a were run for three cities across Canada: Whitehorse, Vancouver, and Ottawa. The assemblies were subjected to air leakage rates of 0.10 and 0.20 L/sm^2 at 75 Pa and brick (Bri) and stucco (Stu) claddings were considered under historical and future periods; Table 5.1 shows the configuration details for each city: insulation thickness, cladding type and thickness, drainage cavity and ACH.

Table 5.1. Main details of the brick and stucco assemblies for the three selected cities.

City	Insulation thickness (mm)	Cladding		Drainage cavity (mm)	ACH (/h)
		Type	Thickness (mm)		
Whitehorse	184	Brick	90	25	5, 10
		Stucco	19	1.5	0, 2
Vancouver	140	Brick	90	25	5, 10
		Stucco	19	10	5, 10, 50, 100*
Ottawa	140	Brick	90	25	5, 10
		Stucco	19	1.5	0, 2

* Vancouver has a 10 mm thick drainage cavity behind the stucco cladding. The ACH of 5 and 10 were simulated as the vented option (openings at the bottom only) and the ACH of 50 and 100 were simulated as the ventilated option (openings at bottom and top).

MoI is used as a performance indicator for the five positions inside the assembly. Figure 5.1 shows how the data is presented: it is organized in colors and each color is associated to a specific position in the assembly; also, the leftmost box plot is related to position 1 and the rightmost is related to position 5.
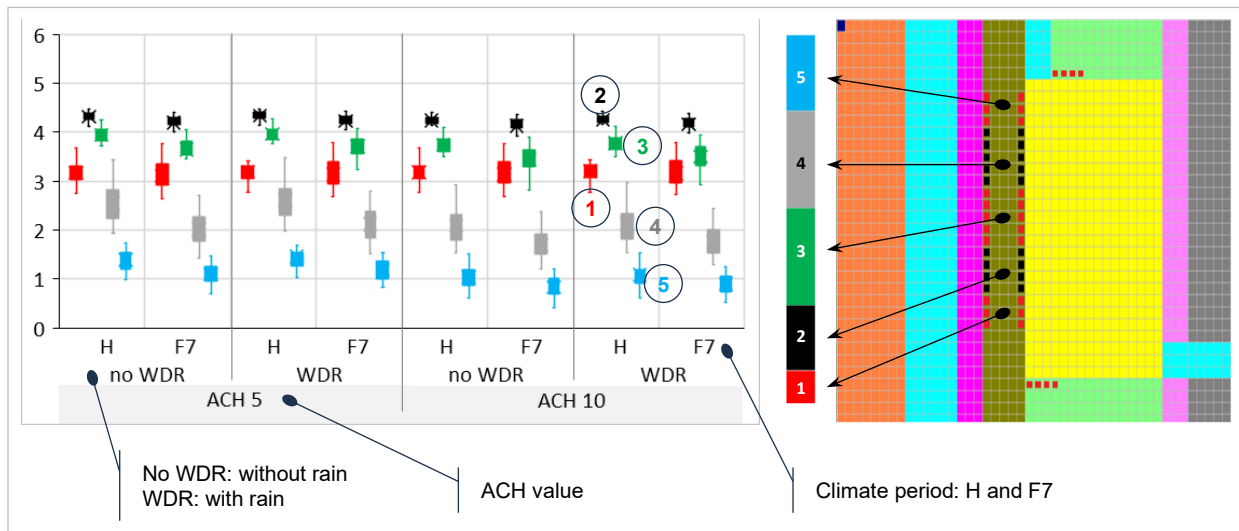
Figure 5.1. Standard representation of the results and the corresponding monitoring positions.

Mould index values explored in this study are always relative, i.e., they are used to compare one situation to another. To have more reliable absolute values for RH and T (where the mould index comes from), experimental work must be performed to benchmark the model.

5.1. Inner surface of OSB

For all positions (1 to 5) and cases (air leakage rate, ACH, WDR, and climate period), the average mould index of the third year was calculated for each of the 15 Runs (Figure 5.2 and Figure 5.3). Each boxplot shows the distribution of the 15 values together. After that, Table 5.2 shows a qualitative trend of the mould index when one variable is changing and the others are kept constant.
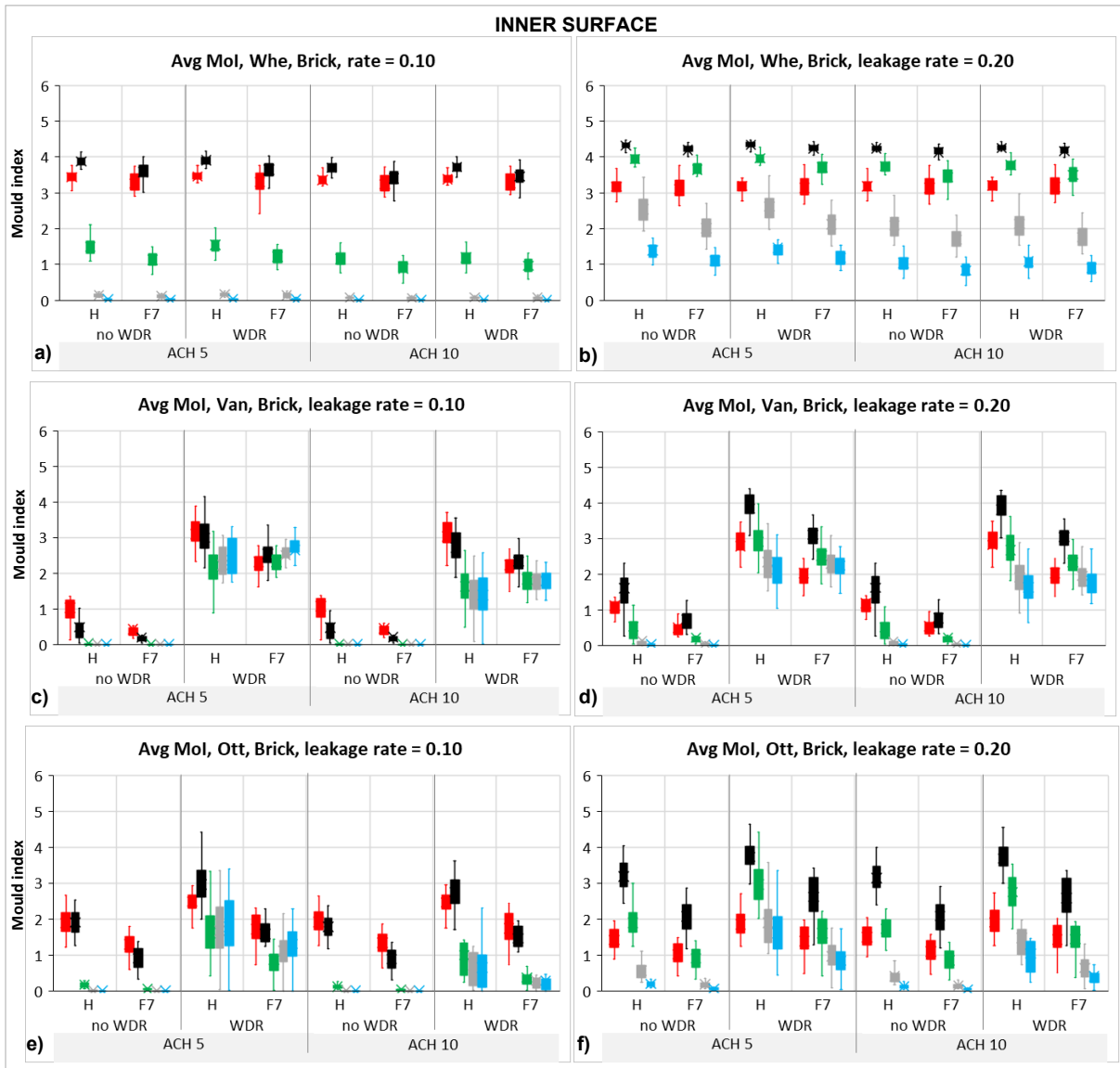
Figure 5.2. Average MoI distribution for the 3rd year at the inner surface of OSB for the three cities, 15 runs, brick cladding, historical (H) and future (F7) periods.
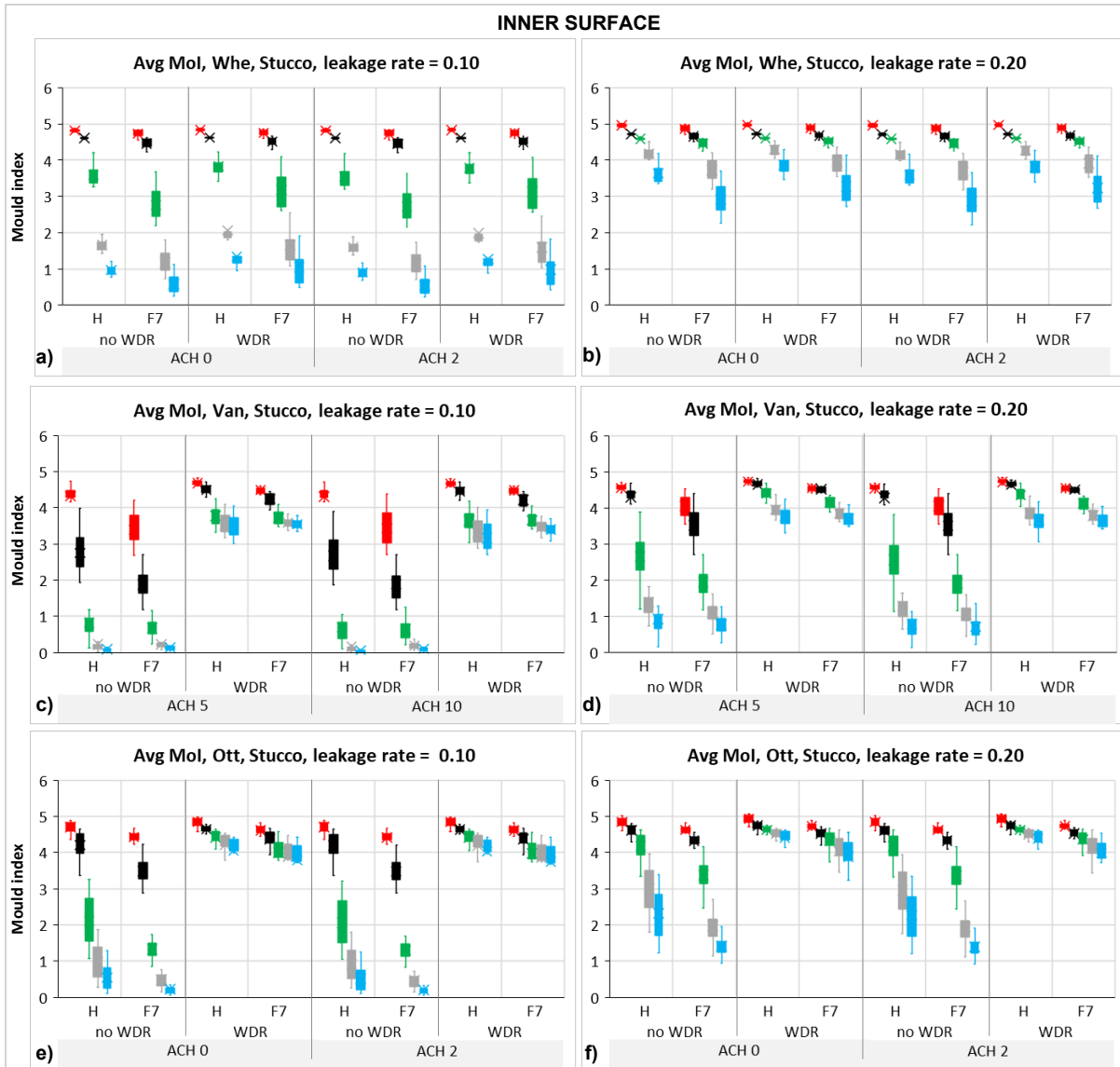
Figure 5.3. Average MoI distribution for the 3ʳᵈ year at the inner surface of OSB for the three cities, 15 runs, stucco cladding, historical (H) and future (F7) periods.

Table 5.2. General trend of the mould index at the inner surface of OSB as a function of the changing factor.

Clad	City	Changing Factor				
		0.10 → 0.20	Low ACH → high ACH	No WDR → WDR	H → F7	Brick → Stucco
Brick	Whe	↑↑↑	↓	Almost no difference	↓	↑↑↑
	Van	↑↑	↓↓	↑↑↑	↓↓	↑↑↑
	Ott	↑↑	↓↓	↑↑	↓↓	↑↑↑
Stucco	Whe	↑↑↑	↓	↑	↓↓	
	Van	↑↑	↓	↑↑↑	↓↓	-
	Ott	↑↑↑	↓	↑↑↑	↓↓	

Slight increase/decrease (↑ , ↓):   variation in the mould index up to 0.5 (greatest variation among the 5 positions)
Increase/decrease (↑↑ , ↓↓):   variation in the mould index up to 2.0 (greatest variation among the 5 positions)
Strong increase/decrease (↑↑↑ , ↓↓↓): variation in the mould index greater than 2.0 (greatest variation among the 5 positions)

5.1.1. Influence of the cladding

Figure 5.4 shows RH and T maps of the assembly for Whitehorse in December. With brick cladding, the temperature of the OSB layer remains higher than with stucco cladding, which means lower RH and lower moisture accumulation during the cold season. As this situation is similar in Vancouver and Ottawa, the charts for these two cities are not shown.
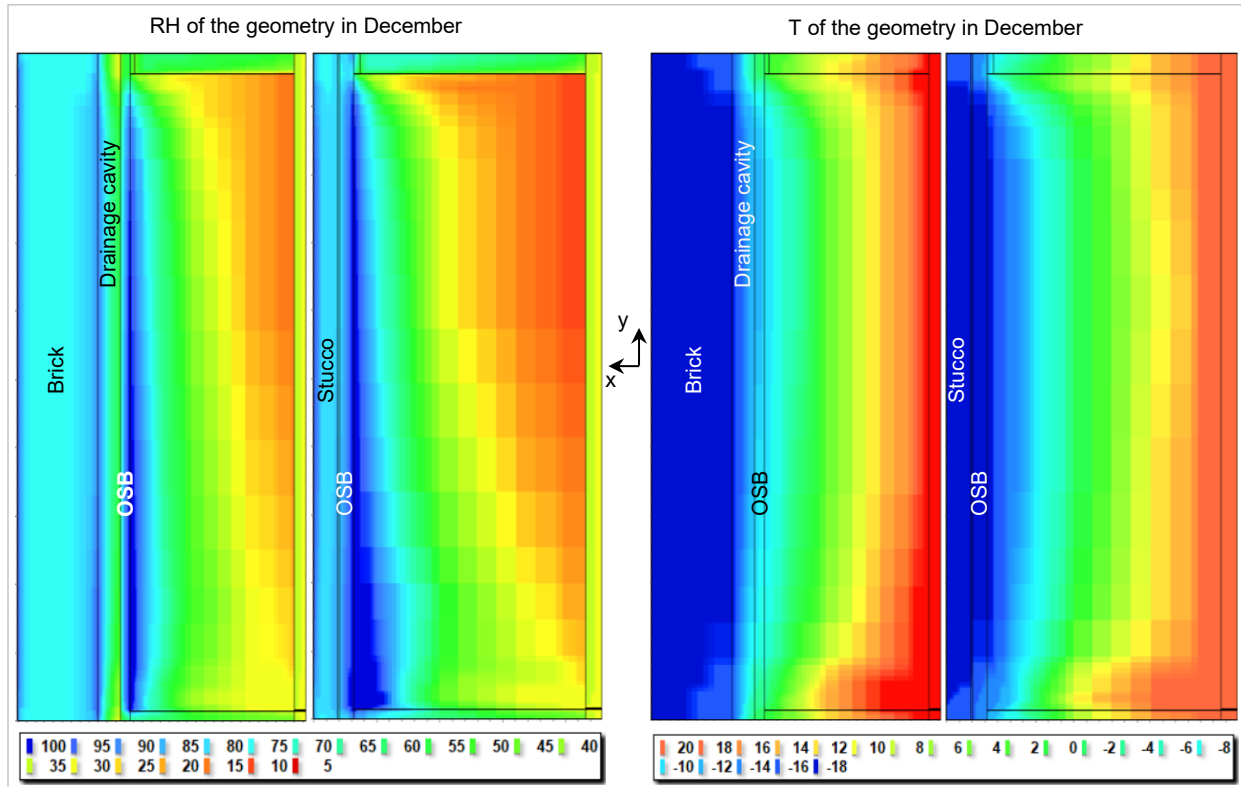
Figure 5.4. RH and T maps inside the assembly for Whitehorse in December, brick, and stucco cladding.

When the warm season comes, the higher moisture accumulation with stucco cladding provides high RH levels for longer, meaning good conditions for mould growth, but the magnitude of the differences varies according to the city. For instance, all cases in Whitehorse with brick cladding already had MoI > 3.0 at the bottom of the assembly (Figure 5.2a,b); with stucco, not only those values got worse but also the top part of the assembly became problematic (Figure 5.3b). Vancouver (Figure 5.2c,d) and Ottawa (Figure 5.2e,f) with brick cladding did not have many cases with MoI > 3, but with stucco MoI is greater than 4.0 in all cases.

5.1.2. Influence of the WDR

The cumulative values of WDR in the historical period are 10, 180 and 80 L/m^2 per year in Whitehorse, Vancouver, and Ottawa respectively (Figure 3.6). Because of its low value, the influence of WDR over the mould growth in Whitehorse is negligible (around 0.1) for both stucco and brick cladding.

With brick cladding, MoI in Vancouver jumps from below 1.0 to almost 3.0 when WDR is present and air leakage rate is 0.10 L/sm^2 (Figure 5.2c); similar behavior happens with air leakage rate of

0.20 L/sm^2 (Figure 5.2d). Ottawa is colder than Vancouver and more susceptible to moisture accumulation due to air leakage, which explains its higher MoI even when WDR is not present. With WDR, MoI increases but not as much as it does in Vancouver.

With stucco cladding, the trend is the same but more severe: in Vancouver the mould index jumps from below 1.0 to around 4.0 for both air leakage rates (Figure 5.3c,d). In Ottawa (Figure 5.3e,f) the values of MoI with WDR are similar but a little higher than in Vancouver even though Ottawa shows less than 50% of the WDR. This may be explained by the fact that Vancouver with stucco cladding has a drainage cavity of 10 mm and ACH 5 and 10, while Ottawa has a drainage cavity of only 1.5 mm and ACH 0 and 2; the ventilation effect in Vancouver is much higher than in Ottawa, which reduces the moisture accumulation due to WDR.

5.1.3. Influence of the air leakage rate

Increasing the air leakage rate from 0.10 to 0.20 L/sm^2 resulted in a higher mould index in all cases, whether with brick or stucco cladding. However, with brick cladding position "1" has lower mould index with higher leakage rate (Figure 5.2b,d,f) because this position receives the highest heat load from the indoor air among all the five, which increases its T and, therefore, decreases its RH and mould index. This behavior is not found with stucco (Figure 5.3b,d,f) and this may be explained by the fact that stucco is much colder than brick and the heat load from the air leakage is not enough to warm up position "1" and induce lower levels of RH. So, stucco cladding with higher air leakage rate resulted in higher MoI in all cases and all positions.

5.1.4. Influence of the ACH

Most of the time, higher values of ACH mean lower moisture accumulation because the excess is taken away by ventilation, whose effect is higher in a 25 mm deep cavity with ACH 10 (brick cladding) than in a 1.5 mm deep cavity with ACH 2 (stucco cladding). However, the drainage cavity is in contact with the outer surface of OSB and air leakage brings moisture to its inner surface. This means the ventilation has a limited influence over the inner part of OSB and the reduction of RH levels is low when compared to the outer surface (section 5.2).

Even being low, the effect of ventilation can be seen in all cities with brick (Figure 5.2), mostly on positions "3" to "5": as they are far from the air entry, they are less susceptible to the effect of air leakage but more susceptible to the effect of ventilation when compared to positions "1" and "2". With stucco cladding (Figure 5.3), the ventilation is lower and so is its effect. Among the three cities, Vancouver (Figure 5.3c,d) shows a greater reduction in mould index than Whitehorse (Figure 5.3a,b) and Ottawa (Figure 5.3e,f) when the ACH increases; this may be explained by the higher ventilation effect due to its 10 mm deep drainage cavity.

5.1.5. Influence of the future climate

Warmer temperatures in the future are likely to lower RH levels, leading to lower MoI. This effect can be seen in all cities and both claddings, but it is more pronounced with brick than with stucco. This is explained by the ventilated cavity behind the brick layer, which has a greater potential to take the excess moisture away than the air layer behind the stucco.

With brick cladding, Whitehorse (Figure 5.2a,b) shows a reduction in the MoI smaller than 0.5 for both air leakage rates; this may be explained by the fact that, even with the increase in the temperature, it still remains a very cold city (Figure 3.5) susceptible to moisture accumulation during many months of the year. Vancouver and Ottawa show greater variations when compared to Whitehorse and the reduction in the MoI is around 1.0. These two cities have lower MoI than Whitehorse and a further increase of the temperature in the future makes a bigger difference regarding moisture accumulation.

For stucco cladding (Figure 5.3) the explanations are similar, but the differences between historical and future periods are smaller than with brick. This may be explained by the lower ventilation rate of stucco cladding, which is not as effective on removing excess moisture as it is with brick cladding. For the three cities, the MoI reduction in the future at the bottom part of OSB is roughly 0.3.

5.2. Outer surface of OSB

For all positions (1 to 5) and cases (air leakage rate, ACH, WDR, and climate period), the average mould index of the third year was calculated for each of the 15 Runs (Figure 5.5 and Figure 5.6). Each boxplot shows the distribution of the 15 values together. After that, Table 5.3 shows a qualitative trend of the mould index when one variable is changing and the others are kept constant.
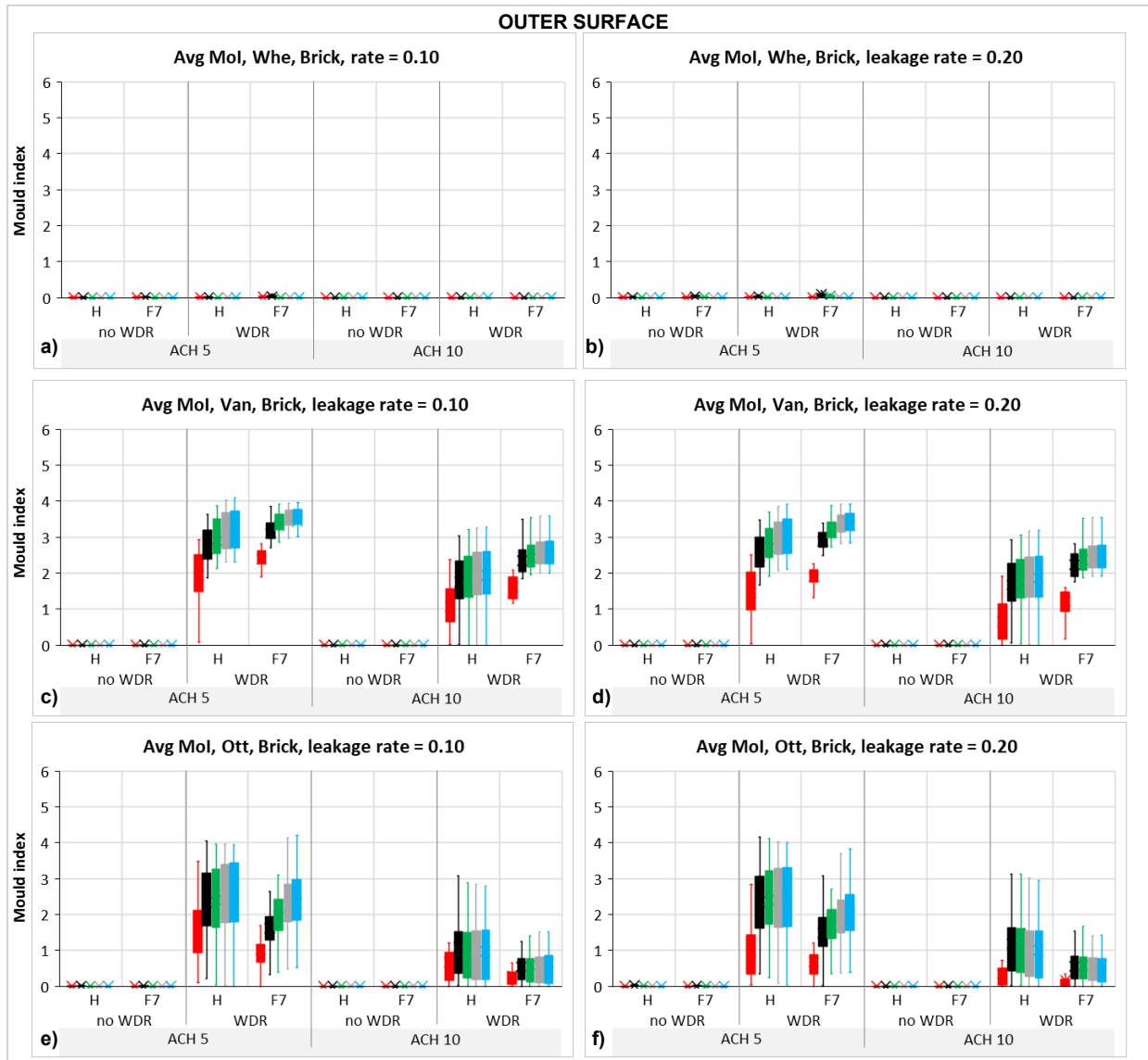
Figure 5.5. Average MoI distribution for the 3rd year at the outer surface of OSB for the three cities, 15 runs, brick cladding, historical (H) and future (F7) periods.
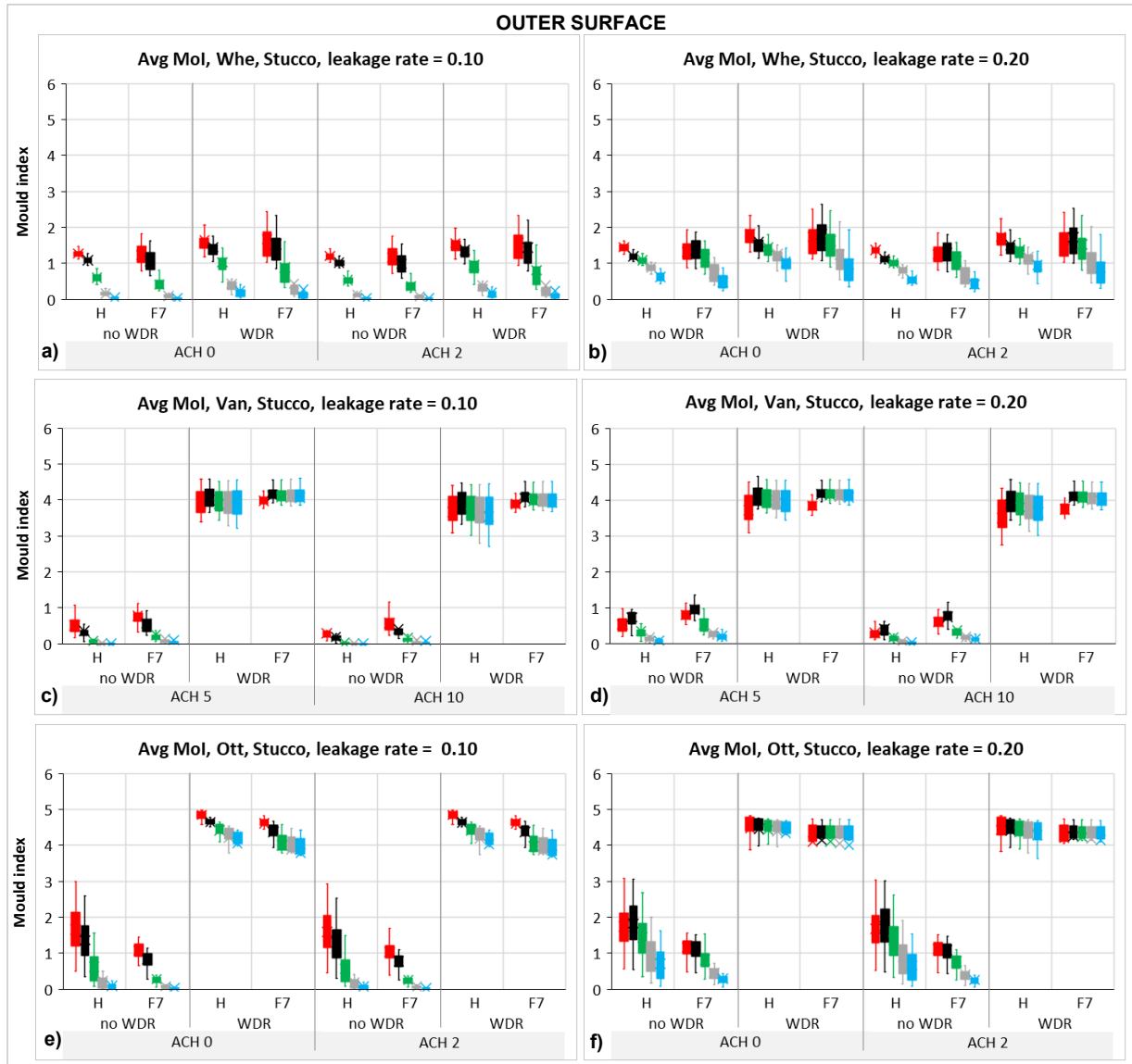
Figure 5.6. Average MoI index distribution for the 3rd year at the outer surface of OSB for the three cities, 15 runs, stucco cladding, historical (H) and future (F7) periods.

Table 5.3. General trend of the mould index at the outer surface of OSB as a function of the changing factor.

Clad	City	Changing Factor				
		0.10 → 0.20	Low ACH → high ACH	No WDR → WDR	H → F7	Brick → Stucco
Brick	Whe	Almost no change	-	Almost no change	Almost no change	↑↑
	Van		↓↓	↑↑↑	↓	↑↑↑
	Ott		↓↓	↑↑↑	↓	↑↑↑
Stucco	Whe	↑	↓	↑	↓	
	Van	↑	↓	↑↑↑	↑	-
	Ott	↑	↓	↑↑↑	↓	

Slight increase/decrease (↑ , ↓): variation in the mould index up to 0.5 (greatest variation among the 5 positions)
Increase/decrease (↑↑ , ↓↓): variation in the mould index up to 2.0 (greatest variation among the 5 positions)
Strong increase/decrease (↑↑↑ , ↓↓↓): variation in the mould index greater than 2.0 (greatest variation among the 5 positions)

The outer part of OSB is less affected by the air leakage rate and the major factor which drives the mould index is WDR. With WDR, Vancouver and Ottawa with brick cladding show mould index that increases from zero to roughly 3 because of the WDR (Figure 5.5c,d,e,f); in Whitehorse (Figure 5.5a,b), due to the low value of WDR, MoI is zero in all situations. With stucco cladding, MoI in Vancouver and Ottawa jump from roughly 1 to 4 or above (Figure 5.6c,d,e,f); Whitehorse, because of the low values of WDR, shows lower increase, about 0.5.

Without WDR, the three cities with brick cladding show no mould growth for both air leakage rates (Figure 5.5); this means the moisture load coming from the warm indoor air has negligible effect on the MoI of the outer surface of OSB. With stucco cladding (Figure 5.6), MoI with leakage rate of 0.2 L/sm^2 is only a little higher than with the lower air leakage rate; in Whitehorse (Figure 5.6a,b), for instance, MoI increases about 0.5 when moving from 0.10 to 0.20 L/sm^2.

When analyzing the Future period with brick cladding, Vancouver (Figure 5.5c,d) tends to show a slightly higher MoI than the Historical period. In Ottawa (Figure 5.5e,f), the trend is the opposite and there is a reduction in the MoI. This may be explained by the fact that Vancouver is a wet city with mild temperatures and a warmer future poses better condition for mould growth; in Ottawa, with less than half of the WDR in Vancouver, the warmer temperature in the future increases the ability of the drainage cavity to get rid of the accumulated moisture due to WDR.

With stucco cladding, Vancouver (Figure 5.6c,d) shows a slightly higher MoI in the future as it does with brick cladding, and for the same reason. In Ottawa, the MoI in the future are lower than in historical and this may be explained by the fact that higher temperatures induce less moisture accumulation in the stucco layer since the yearly WDR is similar in both periods. In Whitehorse (Figure 5.6a,b), MoI in historical and future periods are similar, with some cases showing slightly higher values for position 2. Yearly WDR in Whitehorse changes from 10 in historical to almost 20 L/m^2 in the Future period and, even though those values are low, the increase of about 100% may explain higher MoI.

When the ACH varies from 5 to 10 with brick cladding, there is a reduction in the MoI for both cities, but Vancouver (Figure 5.5c,d) is less sensitive than Ottawa (Figure 5.5e,f): while in Vancouver the reduction in the MoI is around 1.0, in Ottawa it is around 1.5. This may be explained by the fact that the accumulated WDR in Vancouver and Ottawa is 180 and 80 L/m^2 per year respectively, which means the same increase in ACH is more effective on reducing the RH levels where the accumulated moisture in the drainage cavity is lower (Ottawa). With stucco cladding (Figure 5.6), the ACH varies from zero to 2 in Whitehorse and Ottawa (direct applied) and from 5 to 10 in Vancouver (with drainage cavity), but these variations were not enough to reduce the MoI in a significant way. In Vancouver (Figure 5.6c,d) with no WDR, there is a slight reduction in the MoI of about 0.2 when ACH varies from 5 to 10. Stucco cladding has a thinner drainage cavity than brick and this leads to lower ventilation rates and, therefore, lower effectivity when removing accumulated moisture.

As a way of analyzing the influence of the ACH over the inner and outer surface of OSB, Figure 5.7 shows the mould distribution at position "1" in Vancouver with stucco cladding for four ACH values: 100, 50, 10 and 5. While ACH 5 and 10 show similar mould index, ACH 50 and 100 make evident how important the ventilation rate is to take the excess moisture away and reduce mould

growth. At the outer surface, mould index drops from 4.0 with ACH 5 to 1.5 with ACH 100 in the historical period. At the inner surface, mould index is very similar for all the ACH values because the most important source of moisture is the air leakage.

The mould index for stucco cladding with ACH 100 at position 2 is around 1.5 (Figure 5.7); however, in Figure 5.5d (brick cladding with WDR) the mould index is 2.5 for ACH 5 and 1.8 with ACH 10. This emphasizes the importance of ventilation to reduce mould index and improve hygrothermal performance: a well-ventilated stucco cladding can have a better performance than a poor ventilated brick cladding, when analyzing the outer surface.
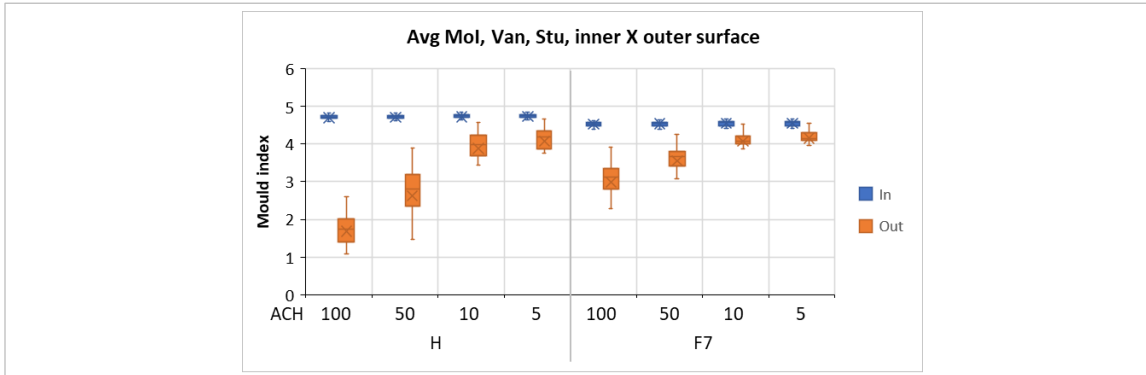
Figure 5.7. Average mould index distribution (at "2") for the third year in Vancouver with WDR, ACH 100, 50, 10 and 5, 15 runs, inner and outer surface of OSB, stucco cladding.

Chapter 6. Conclusions and future work

Air leakage is an important factor when assessing the hygrothermal performance of wall assemblies. At the same time, it is related to so many different variables and conditions that is impossible to build samples in the lab to figure out the importance of each of them. For that reason, computational models are used to perform the analysis, which introduce even more variables and simplifications. This thesis investigated the influence of different air leakage paths and air leakage rates on the hygrothermal performance of wood-frame walls. To accomplish that, the steps needed to build the smallest 2D grid were explained, convergence and accuracy of the results were evaluated, and the functional relations between air leakage rate and air permeability of the insulation were clarified. At last, the effect of two air leakage rates (0.10 and 0.20 L/sm^2) was assessed in Whitehorse, Vancouver, and Ottawa, with brick and stucco claddings, under historical and future periods.

Due to the complexity of the problem, conclusions are presented in three parts: 1) air leakage; 2) hygrothermal modelling; 3) results.

6.1. Air leakage

Both air leakage rate and path play a significant role on the hygrothermal performance and they must be analyzed at the same time, since the same air leakage rate through different paths produce different outputs. The main findings are summarized as follows:

- Even low rates of air leakage can introduce a considerably higher amount of moisture into the assembly than diffusion alone. Therefore, vapor barriers are useless if the air barrier system is compromised. On the other side, compromised vapor barriers may not introduce risk of moisture accumulation provided that the air barrier is functional and there is no forced convection.

- Since it is impossible to build flawless assemblies, their design must be robust enough to sustain air leakage rates that are likely to happen.

- Three are the main factors related to air leakage: rate, path, and properties (RH, T) of the indoor air.

- While short air leakage paths are usually related to energy loss and the risk of condensation is low, long air leakage paths tend to induce higher risks of condensation and the energy loss is less important.

- While low air leakage rates may pose a risk for concentrated paths, high rates can be tolerated if the exfiltration is diffused.

- For the same exfiltration path, the higher the RH of the indoor air, the lower is the allowable leakage rate, considering the same indoor T.

- For the same exfiltration rate, path, and RH of the indoor air, it is likely that the colder the city the higher the accumulated moisture during the cold season.

- Depending on the city and the adopted air leakage rate, its effect can be even worse than the impact of WDR because there is no ventilation inside the insulated cavity which can dissipate accumulated moisture.

6.2. Hygrothermal modelling

Since time and computational resources are limited in any project, generating a computational model which runs as fast as possible is a must and the success of this task begins when creating the mesh. So, during the discretization process, the major details to consider are:

- When discretizing the geometry to build the computational model, a thorough sensitivity analysis can help to select the best option in terms of simulation time and accuracy: reliable results can be obtained from many different options, but the best one can reduce time demand by 90% or more.

- Automatic discretization is the first try when creating the grid; however, stretch factors which work well for thick layers are not the best option when dealing with thin layers and manual intervention may be necessary.

- Different grids may output different air flows for the same pressure difference, which means the flux through the air entry must be monitored while the sensitivity analysis is performed.

- After selecting the best grid, the air permeability of the insulation may need to be adjusted so that the required air leakage rate matches with the solver output.

- The air permeability of the insulation was assumed to be the same for both x and y axis. However, due to the orientation of the fibers, it is likely that the air permeability is higher in the vertical than in the horizontal direction. This may cause a different distribution of the air flow and change the results.

- The air leakage path needs to be selected considering the likelihood of flaws of the assembly, for instance a single hole or a continuous slot. Different paths may output different results.

- After selecting the air leakage path, it is a crucial task to determine the relation between air leakage rate and flux according to the geometry of the air entry and the pressure difference.

- The same airflow through air entries of different heights may change the hygrothermal response of the assembly.

6.3. Simulation results

Mould growth is a complex mechanism related to the hourly values of temperature and relative humidity and the computational model has some simplifications and assumptions, as explained in section 3.5; also, the following comments are based on the hygrothermal results from three cities across Canada (Whitehorse, Vancouver, and Ottawa). They represent the main findings, are limited to the scope of this research, and cannot be extrapolated or generalized:

- Inner surface: in Whitehorse, which is very cold and WDR is low, air leakage is the major factor which drives moisture accumulation and WDR has a minor influence. In Ottawa, air leakage also plays an important role, but the higher value of WDR has a more pronounced effect when compared to Whitehorse. With the mild climate in Vancouver, higher values of WDR increase the moisture content of the whole OSB and have a dominant contribution to mould growth.

- Outer surface: for the three cities WDR is the major factor for mould growth, and the effect of air leakage is of minor importance.

- Higher values of ACH tend to reduce MoI at the outer surface of OSB because moisture accumulation from WDR is taken away more quickly. At the inner surface, however, the ACH value is less important when compared to the air leakage rate.

- At the inner surface, higher air leakage rates may warm up the bottom part of OSB and the critical position changes to a higher level inside the insulated cavity. This effect was observed for the three cities with brick cladding.

- At the inner surface and for the same air leakage rate, stucco cladding shows worse behaviour than brick because the temperature of the OSB layer is lower and this induces higher levels of moisture accumulation during the cold season.

- At the outer surface, stucco cladding shows worse behaviour than brick because the thinner drainage cavity with very low ACH is less effective on removing the moisture due to WDR. In Vancouver, however, with a drainage cavity of 10 mm and ACH of 100, stucco cladding shows a better performance when compared to low ACH values, which confirms the importance of cavity ventilation to reduce accumulated moisture and MoI.

- With a warmer future scenario, cold cities tend to accumulate less moisture during the cold season and MoI tends to be reduced. In already warm and wet cities, the higher temperatures in the future might increase the likelihood of mould growth.

6.4. Future work

Air leakage simulation is related to several different assumptions, either related to leakage rate, leakage path or material properties, and they always output theoretical results which can be used to analyze the relative difference among multiple scenarios. However, the practitioners need a tool that can be used to give results as close as possible to the hygrothermal behavior of an assembly incorporated to a real building, so that they can design with greater confidence when targeting long-term performance.

To accomplish that, any computational model should be benchmarked with experimental results. For instance, the way of implementing air leakage in this thesis considers air permeable insulation and pressure-driven air flow, which makes physical sense; five positions inside the assemblies were assessed and the further the position is from the air entry, the lower the risk of mould growth, which also makes physical sense. However, experimental results of RH and T can be obtained from a wood frame assembly with different claddings when subjected to controlled indoor and outdoor conditions. With those results, the computational model can be adjusted to render more accurate outputs, which can be used to predict the hygrothermal performance in a more reliable way, increasing the robustness of the design.

References

ABCB. (2019). *Condensation in Buildings handbook* (2nd ed.). Australian Building Codes Board.

Achenbach, P. R., & Trechsel, H. R. (1983). Evaluation of Current Guidelines of Good Practice for Condensation Control in Insulated Building Envelopes. *Thermal Performance of the Exterior Envelopes of Whole Buildings II International Conference*, *6*, 1090–1107.

Aggarwal, C. (2023). *Development of climate-based indices for assessing the hygrothermal performance of wood-frame walls under historical and future climates*. Concordia University.

Ananian, J. S., Fu, T. S., & Gabby, B. A. (2019). Detrimental Effects of Air Leakage on Building Enclosure Performance: Energy Consumption, Occupant Comfort, and Moisture Accumulation. In T. Weston, K. Wissink, & K. Nelson (Eds.), *ASTM STP 1615 - Whole Building Air Leakage: Testing and Building Performance Impacts* (pp. 38–60). ASTM International. https://doi.org/10.1520/stp1615-eb

Antretter, F., & Pallin, S. (2019). HAMT extension for EnergyPlus encompasses moisture sources due to air leakage. *ASHRAE Transactions*, *125*, 3–10.

Armstrong, M., Maref, W., Rousseau, M. Z., Lei, W., & Nichols, M. (2009). A field monitoring study of interstitial condensation in wood-frame walls in cold climate. *12th Canadian Conference of Building Science and Technology*, 1–12.

Armstrong, M., Rousseau, M., Lei, W., & Nicholls, M. (2010). Effect of the air and vapor permeance of exterior insulation on the flow of moisture in wood frame walls in a cold climate. *ICBEST 2010 - International Conference on Building Envelope Systems and Technologies*, 133–140. https://nrc-publications.canada.ca/eng/view/object/?id=cf6db32d-b770-4185-b352-3c4ce410fe50

ASHRAE. (2016). *ASHRAE 160 - Criteria for moisture-control design analysis in buildings*.

ASHRAE. (2017). *ASHRAE Handbook of fundamentals*. American Society of Heating, Refrigerating and Air-Conditioning Engineers, Inc.

ASTM. (2016). *ASTM C 522 - Standard Test Method for Airflow Resistance of Acoustical Materials*. American Society for testing and materials.

Babbitt, J. D. (1939). The diffusion of water vapor through various building materials. *Canadian Journal of Research*, *17*(2), 15–32.

Bauklimatik. (2022). *Validation according to EN 10211:2007*. https://bauklimatik-dresden.de/delphin/benchmarks/en-10211_2007.php#case1

Belleudy, C., Kayello, A., Woloszyn, M., & Ge, H. (2015). Experimental and numerical investigations of the effects of air leakage on temperature and moisture fields in porous insulation. *Building and Environment*, *94*, 457–466. https://doi.org/10.1016/j.buildenv.2015.10.009

Blocken, B., & Carmeliet, J. (2006). On the accuracy of wind-driven rain measurements on buildings. *Building and Environment*, *41*(12), 1798–1810. https://doi.org/10.1016/j.buildenv.2005.07.022

Boardman, C. R., & Glass, S. V. (2020). Improving the accuracy of a hygrothermal model for wood-frame walls: A cold-climate study. *Buildings*, *10*(12), 1–34. https://doi.org/10.3390/buildings10120236

Bomberg, M., & Brown, W. C. (1993). Building envelope: heat, air and moisture interactions. *Journal of Thermal Insulation and Building Envelopes*, *16*(April), 306–311. https://doi.org/https://doi.org/10.1177%2F109719639301600402

Bomberg, M., & Onysko, D. (2002). Heat, Air and Moisture Control in the Historic Basis for Current Practices. *Journal of Thermal Envelope and Building Science*, *26*(1), 3–31. https://doi.org/10.1106/109719602025857

Brown, W. C., Lawton, M., Poirier, G. ., & Di Lenardo, B. (1998). An Evaluation guide for performance assessment of air barrier systems. *Thermal Performance of the Exterior Envelopes of Whole Buildings VII International Conference*, 773–780.

BSI. (2007). *BS EN 15026 - Hygrothermal performance of building components and building elements. Assessment of moisture transfer by numerical simulation*. BSI - British Standards Insttution.

Bunkholt, N. S., Rüther, P., Gullbrekken, L., & Geving, S. (2021). Effect of forced convection on the hygrothermal performance of a wood frame wall with wood fibre insulation. *Building and Environment*, *195*(March). https://doi.org/10.1016/j.buildenv.2021.107748

Burch, D. M., Saunders, C. A., & TenWolde, A. (1995). *Manufactured Housing Walls That Provide Satisfactory Moisture Performance in all Climates - NISTIR 5558*. U.S. Department of Commerce.

Bush, E., & Lemmen, D. S. (Eds.). (2019). *Canada's Changing Climate Report*. Environment and climate Canada. http://www.changingclimate.ca/CCCR2019

Cardoso, V. E. M., Pereira, P. F., Ramos, N. M. M., & Almeida, R. M. S. F. (2020). The impacts of air leakage paths and airtightness levels on air change rates. *Buildings*, *10*(3), 1–18. https://doi.org/10.3390/buildings10030055

Chown, G. ., & Mukhopadhyaya, P. (2005). NBC 9.25.1.2: The on-going development of building code requirements to address low air and vapour permeance materials. *10th Canadian Conference on Building Science and Technology "Building Science and the Integrated Design Process,"* 45–58. https://nrc-publications.canada.ca/eng/view/object/?id=1b3c3eda-1374-42bc-b20c-d031912b7d41

CMHC. (1992). *Moisture in Canadian Wood-Frame House Construction: Problems, Research and Practice*.

CMHC. (2007). *Research report, housing technology series - Air Leakage Control Manual Existing Multi-Unit Residential Buildings*.

CMHC. (2014). *Canadian Wood-Frame House Construction* (3rd ed., Vol. 3). Canada Mortgage and Housing Corporation.

Cornick, S., Alan Dalgliesh, W., & Maref, W. (2009). Sensitivity of hygrothermal analysis to uncertainty in rain data. *Journal of ASTM International*, *6*(4), 1–17. https://doi.org/10.1520/JAI102032

Cornick, S., Djebbar, R., & Alan Dalgliesh, W. (2003). Selecting moisture reference years using a Moisture Index approach. *Building and Environment*, *38*(12), 1367–1379. https://doi.org/10.1016/S0360-1323(03)00139-2

Cornick, S., & Kumaran, M. K. (2007). *A Comparison of Measured Indoor Relative Data with Results from Predictive Models*. National Research Council Canada. https://nrc-publications.canada.ca/eng/view/object/?id=87611a33-e1d7-488f-8084-881f96e700cb

Cornick, S., & Kumaran, M. K. (2008). A comparison of empirical indoor relative humidity models with measured data. *Journal of Building Physics*, *31*(3), 243–268. https://doi.org/10.1177/1744259107081699

Cornick, S., Maref, W., & Tariku, F. (2009). *Verification and validation: establishing confidence in hygrothermal tools - Research Report IRC-RR-278* (p. 22). National Research Council Canada.

Crandell, J. H. (2021). *Assessment of Water Vapor Control Methods for Modern Insulated Light-Frame Wall Assemblies ABTG Research Report No . 1410-03*.

Crandell, J. H. (2017). Assessment of Hygrothermal Performance and Design Guidance for Modern LightFrame Wall Assemblies. In P. Mukhopadhyaya & D. Fisler (Eds.), *ASTM STP 1599 - Advances in Hygrothermal Performance of Building Envelopes: Materials, Systems and Simulations* (pp. 362–394). ASTM International. https://doi.org/10.1520/stp1599-eb

Dalgliesh, W. A., Cornick, S., Maref, W., & Mukhopadhyaya, P. (2005). Hygrothermal performance of building envelopes: uses for 2D and 1D simulation. *10th Conference on Building Science and Technology Proceedings*, *January*, 32–41.

Defo, M., & Lacasse, M. A. (2020). Resilience of Canadian homes and small buildings to the effects of climate change - Risk of deterioration due to condensation within wall assemblies. *E3S Web of*

Conferences, *172*, 1–10. https://doi.org/10.1051/e3sconf/202017202002

Defo, M., Lacasse, M. A., & Laouadi, A. (2021). A comparison of hygrothermal simulation results derived from four simulation tools. *Journal of Building Physics*, *45*(4), 432–456. https://doi.org/10.1177/1744259120988760

Defo, M., Lacasse, M. A., Laouadi, A., & Ghobadi, M. (2021). Comparative Moisture Performance of Wood/Wood-Based Claddings Predicted by Four Hygrothermal Simulation Tools. *Journal of Civil Engineering and Architecture*, *15*(2), 63–77. https://doi.org/10.17265/1934-7359/2021.02.002

Derome, D., Karagiozis, A. N., & Carmeliet, J. (2010). The nature, significance and control of solar-driven water vapor diffusion in wall systems - synthesis of Research Project RP-1235. *Ashrae Transactions*, *116*(1), 572–580.

Desmarais, G. (2000). *Impact of added insulation on the hygrothermal performance of leaky exterior wall assemblies*. Concordia University.

Desmarais, G., Derome, D., & Fazio, P. (2000). Mapping of Air Leakage in Exterior Wall Assemblies. *Journal of Building Physics*, *24*(2), 132–154. https://doi.org/10.1106/BWH8-9D3J-R939-957E

Desmarais, G., Derome, D., & Fazio, P. (2001). Moisture performance of leaky exterior walls with added insulation. *Thermal Performance of the Exterior Envelopes of Whole Buildings VIII*, 1–9.

ECCC. (2020). *Climate trends and variations bulletin*. https://doi.org/10.31390/cwbr.22.2.01

Fechner, H. (2021). *Delphin training - Further topics: air spaces*. Technische Universität Dresden.

Fechner, H. (2022). *Online personal meeting*.

Ferziger, J. H., Peric, M., & Street, R. L. (2020). *Computational methods for fluid flow.* (4th ed.). Springer. https://doi.org/10.1063/1.2815085

Fox, M. J. (2014). *Hygrothermal Performance of Highly Inuslated Wood Frame Walls With Air Leakage : Field Measumemts and Simulations. Thesis (Masters)*. Ryerson University.

Friis, N. K., Møller, E. B., & Lading, T. (2023). Hygrothermal assessment of external walls in Arctic climates: Field measurements and simulations of a test facility. *Building and Environment*, *238*(February). https://doi.org/10.1016/j.buildenv.2023.110347

Garden, G. K. (1965, December). CBD 72 - Control of air leakage is important. *Canadian Building Digest*.

Gaur, A., & Lacasse, M. (2022). Climate Data to Support the Adaptation of Buildings to Climate Change in Canada. *Data*, *7*(4). https://doi.org/10.3390/data7040042

Ge, H., & Krpan, R. (2009). Wind-driven Rain Study in the Coastal Climate of British Columbia. In *Research report submitted to Canadian Mortgage and Housing Corporation*. http://www.hpo.bc.ca/files/download/Report/WindDrivenRainStudy.pdf

Ge, H., Straube, J., Wang, L., & John, M. (2019). Field study of hygrothermal performance of highly insulated wood-frame walls under simulated air leakage. *Building and Environment*, *160*, 14.

Gellert, R. (2010). Inorganic mineral materials for insulation in buildings. In M. R. Hall (Ed.), *Materials for Energy Efficiency and Thermal Comfort in Buildings* (pp. 193–228). Woodhead Publishing Limited.

Gradeci, K., Labonnote, N., Time, B., & Köhler, J. (2017). Mould growth criteria and design avoidance approaches in wood-based materials – A systematic review [Elsevier Ltd]. In *Construction and Building Materials* (Vol. 150). https://doi.org/10.1016/j.conbuildmat.2017.05.204

Gullbrekken, L., Schjøth Bunkholt, N., Geving, S., & Rüther, P. (2020). Air leakage paths in buildings: Typical locations and implications for the air change rate. *E3S Web of Conferences*, *172*, 1–6. https://doi.org/10.1051/e3sconf/202017205010

Handegord, G. O. (1960, September). CBD 9 - Vapour barriers in home construction. *Canadian Building Digest*.

Handegord, G. O. (1982). Air Leakage, Ventilation, and Moisture Control in Buildings. In M. Lieff & H. R. Trechsel (Eds.), *Moisture Migration in Buildings, ASTM STP 779* (pp. 223–233). ASTM International.

Hansen, E. J. D. P., & Brandt, E. (2010). Timber-frame walls: Feasible with a damaged vapor barrier? *Thermal Performance of the Exterior Envelopes of Whole Buildings - 11th International Conference*.

Harreither, C., Krainz, L., Weissinger, J., & Bednar, T. (2015). Experimental determination of the influence of installing fibrous insulation materials in timber frames on the air permeability and convective air transport. *Energy Procedia*, *78*(November), 2748–2753. https://doi.org/10.1016/j.egypro.2015.11.618

Hens, H. S. L. C. (2007). Modeling the heat, air, and moisture response of building envelopes: What material properties are needed, how trustful are the predictions? *Journal of Architectural Engineering*, *4*(2), 1–11. https://doi.org/10.1520/stp45400s

Hershfield, M. (1997). *Air Barrier Systems for Walls of low-Rise Buildings: performance and assessment*.

Hirsch, C. (1988). *Numerical Computation of internal and external flows. Vol 1: Fundamentals of Numerical Discretization*. A Wiley interscience publication.

Hun, D. E., Atchley, J., & Childs, P. (2016). *Air Leakage Rates in Typical Air Barrier Assemblies* (Issue November).

Hurel, N., Pailha, M., Garnier, G., & Woloszyn, M. (2017). Impact of different construction details on air permeability of timber frame wall assemblies: Some experimental evidences from a three-scale laboratory study. *Journal of Building Physics*, *41*(2), 162–189. https://doi.org/10.1177/1744259116673983

Hutcheon, N. B. (1960, January). CBD-1 . Humidity in Canadian Buildings. *Canadian Building Digest*.

Hutcheon, N. B. (1963a, June). CBD 42 - Humidified buildings. *Canadian Building Digest*.

Hutcheon, N. B. (1963b, December). CBD 48 - Requirements for exterior walls. *Canadian Building Digest*. https://nrc-publications.canada.ca/eng/view/object/?id=6e20b761-6642-4b3d-9eb6-971b534c64e4

Hutcheon, N. B. (1989). 40 years of vapor barriers. In H. R. Trechsel & M. Bomberg (Eds.), *ASTM STP 1039 - WaterVapor Transmission Through Building Materials and Systems: Mechanisms and Measuremen* (pp. 5–7). American Society for testing and materials.

Hutcheon, N. B. (1953). Fundamental considerations in the design of exterior walls for buildings - technical report #13. *67th Anjual General and Professional Meeting of the Engineering Institute of Canada*, 1–25.

Hutcheon, N. B., & Handegord, G. O. (1980). Evolution of the insulated wood-frame wall in Canada. *8th CIB Triennial Congress*, 434–438.

ISO. (2012). *ISO 13788 - Hygrothermal performance of building components and building elements — Internal surface temperature to avoid critical surface humidity and interstitial condensation — Calculation methods* (p. 39). International Organization for Standardization.

ISO. (2017). *ISO 10211 - Thermal bridges in building construction - Heat flows and surface temperatures - Detailed calculations*. International Organization for Standardization.

Janssens, A., & Hens, H. (2003). Interstitial condensation due to air leakage: a sensitivity analysis. *Journal of Thermal Envelope and Building Science*, *27*(1), 15–29. https://doi.org/10.1177/109719603033644

Janssens, A., & Hens, H. (1998). Condensation risk assessment. *Thermal Performance of the Exterior Envelopes of Whole Buildings VII*, 199–206.

Junginger, M., Defo, M., Moore, T., Lacasse, M. A., & John, V. (2020). Assessment of Moisture Performance of National Building Code Canada Compliant Wall Assemblies under Climate Change. In C. Serrat, J. R. Casas, & V. Gibert (Eds.), *XV DBMC - Current topics and trends on durability of building materials and components*. International Center for Numerical Methods in Engineering (CIMNE). https://doi.org/10.23967/dbmc.2020.012

Kalamees, T., Alev, Ü., & Pärnalaas, M. (2017). Air leakage levels in timber frame building envelope joints. *Building and Environment*, *116*, 121–129. https://doi.org/10.1016/j.buildenv.2017.02.011

Kalamees, T., & Kurnitski, J. (2010). Moisture convection performance of external walls and roofs. *Journal of Building Physics*, *33*(3), 225–247. https://doi.org/10.1177/1744259109343502

Kan, L., & Piñon, J. P. (2007). Predicting the effect of wall-cladding ventilation on condensation due to sun-driven moisture: Comparison of hygrothermal simulation with laboratory testing. *Thermal Performance of the Exterior Envelopes of Whole Buildings X*, 10.

Karagiozis, A. N., & Kuenzel, H. M. (2009). The effect of air cavity convection on the wetting and drying behavior of wood-frame walls using a multi-physics approach. *Journal of ASTM International*, *6*(10), 1–15. https://doi.org/10.1520/JAI101455

Kayll, D., Defo, M., Moore, T. V., & Lacasse, M. A. (2020). A Methodology for Assessment of Building Assembly Air Leakage Moisture Response, Condensation Risk, and Expected Durability When Subjected to Projected Future Climate Loads. In C. Serrat, J. R. Casas, & V. Gibert (Eds.), *XV DBMC - Current topics and trends on durability of building materials and components* (pp. 51–58). International Center for Numerical Methods in Engineering (CIMNE).

Khemet, B., & Richman, R. (2021). An empirical approach to improving preconstruction airtightness estimates in light framed, detached homes in Canada. *Journal of Building Engineering*, *33*(June 2019), 101433. https://doi.org/10.1016/j.jobe.2020.101433

Kölsch, P., Zegowitz, A., Nusser, B., Zirkelbach, D., Künzel, H., & Wagner, R. (2016). Airflow through lightweight wall assemblies - influence of size and location of leakages. *Thermal Performance of the Exterior Envelopes of Whole Buildings XIII International Conference*, 459–484.

Kumaran, M. K., & Haysom, J. C. (2000). *Low-Permeance Materials in Building Envelopes* (pp. 1–6). National Research Council Canada.

Kumaran, M. K., & Haysom, J. C. (2001, January). Avoiding condensation with low-permeance materials. *Solplan Review*, 18–19.

Künzel, H., & Karagiozis, A. N. (2010). Hygrothermal behaviour and simulation in buildings. In M. R. Hall (Ed.), *Materials for Energy Efficiency and Thermal Comfort in Buildings* (pp. 54–76). Woodhead Publishing Limited. https://doi.org/10.1533/9781845699277

Künzel, H. M. (2014). Accounting for unintended moisture sources in hygrothermal building analysis. *Proc. 10th Nordic Symposium on Building Physics*, 947–952.

Künzel, H. M., Zirkelbach, D., & Schafaczek, B. (2012). Modeling the effect of air leakage in hygrothermal envelope simulation. *Building Enclosure Science & Technology (BEST3) Conference*.

Lähdesmäki, K., Salminen, K., Vinha, J., Viitanen, H., Ojanen, T., & Peuhkuri, R. (2011). Mould growth in building materials in laboratory and field experiments. *9th Nordic Symposium on Building Physics NSB 2011*, *2*, 859–866.

Latta, J. K. (1976, March). CBD 175: Vapour Barriers: What are they? Are they effective? *Canadian Building Digest*.

Latta, J. K. (1985). *The principles and dilemmas of designing durable house envelopes for the North* (p. 27). National Research Council Canada. https://nrc-publications.canada.ca/eng/view/ft/?id=b4d69c4b-8ede-41f8-ba8b-3e3aa3608031

Laukkarinen, A., Jokela, T., Moisio, T., & Vinha, J. (2021). Hygrothermal simulations of timber-framed walls with air leakages. *8th International Building Physics Conference (IBPC 2021) - Journal of Physics: Conference Series*, *2069*(1). https://doi.org/10.1088/1742-6596/2069/1/012094

Lstiburek, J. W. (1992). Historical Perspective on North American Wood Frame Construction. *Journal of Thermal Envelope and Building Science*, *15*(3), 195–200. https://doi.org/10.1177/109719639201500301

Lstiburek, J. W. (2000). *Toward an understanding and prediction of air flow in buildings*. University of Toronto.

Lstiburek, J. W., Pressnail, K., & Timusk, J. (2002). Air Pressure and Building Envelopes. *Journal of Thermal Envelope and Building Science*, *26*(1), 53–91. https://doi.org/10.1177/109719602765071658

Lux, M. E., & Brown, W. C. (1989). Air leakage control. *Building Science Insight ´86*, 13–19.

Maref, W., Armstrong, M., Rousseau, M., & Lei, W. (2010). A field monitoring investigation of the effect of adding different exterior thermal insulation materials on the hygrothermal response of wood-frame walls in a cold climate. *BEST2 Conference*, 1–15. https://nrc-publications.canada.ca/eng/view/object/?id=497102c6-d2bb-4efb-aae4-8058d45e99cf

Maref, W., Manning, M., Lacasse, M. A., Kumaran, M. K., Cornick, S. M., & Swinton, M. C. (2007). Laboratory Demonstration of Solar Driven Inward Vapour Diffusion in A Wall Assembly. *11th Canadian Conference on Building Science and Technology*, 1–8.

Merill, J. ., & Tenwolde, A. (1989). Overview of Moisture-Related Damage in One Group of Wisconsin Manufactured Homes. *ASHRAE Transactions*, *95*(1), 405–414.

Nicolai, A. (2007). *Modeling and Numerical Simulation of Salt Transport and Phase Transitions in Unsaturated Porous Building Materials* [Syracuse University]. https://doi.org/10.13140/RG.2.1.2016.2088

Nicolai, A., Scheffer, G. A., Grunewald, J., & Plagge, R. (2009). An Efficient Numerical Solution Method and Implementation for Coupled Heat, Moisture, and Salt Transport: The DELPHIN Simulation Program. In L. Franke, G. Deckelman, & R. Espinosa-Marzal (Eds.), *Simulation of time dependent degradation of porous materials - Final Report on Priority Program 1122* (pp. 85–100). Cuvillier Verlag Göttingen. https://cuvillier.de/de/shop/publications/1159

Nofal, M. (1998). *Hygrothermal damage of building materials and components: state-of-the-art report on studies of hygrothermal damage and Appproach for damage assessments* (p. 139). National Research Council Canada.

Nofal, M., & Kumaran, K. (2010). Biological damage function models for durability assessments of wood and wood-based products in building envelopes. *European Journal of Wood and Wood Products*, *69*(4), 619–631. https://doi.org/10.1007/s00107-010-0508-9

NRCC. (2017). *National Energy Code of Canada for Buildings*. National Research Council Canada. https://nrc.canada.ca/en/certifications-evaluations-standards/codes-canada/codes-canada-publications/national-energy-code-canada-buildings-2017

NRCC. (2020). *NBCC - National Building Code of Canada*. National Research Council Canada.

Ojanen, T. (1998). Improving the drying efficiency of timber frame walls in cold climates by using exterior insulation. *Thermal Performance of the Exterior Envelopes of Whole Buildings VII*, 155–164.

Ojanen, T., & Kohonen, R. (1989). Hygrothermal Influence of Air Convection in Wall Structures. *Hermal Performance of the Exterior Envelopes of Buildings IV*, 234–242.

Ojanen, T., & Kumaran, K. (1996). Effect of exfiltration on the hygrothermal behaviour of a residential wall assembly: Results from calculations and computer simulations. *Journal of Thermal Envelope and Building Science*, *19*(1), 215–227. https://doi.org/https://doi.org/10.1177/109719639601900303

Ojanen, T., & Kumaran, M. K. (1992). Air Exfiltration and Moisture Accumulation in Residential Wall Cavities. *Thermal Perfomance of the Exterior Envelopes of Buildings V*, 491–500.

Ojanen, T., Viitanen, H., Peuhkuri, R., Vinha, J., & Salminen, K. (2010). Mold Growth Modeling of Building Structures Using Sensitivity Classes of Materials. *Buildings XI - Eleventh International Conference on Thermal Performance of the Exterior Envelopes of Whole Buildings*.

Paepcke, A., & Nicolai, A. (2020). Efficient hygrothermal wall transport models inside simulations of

conditioned buildings. *E3S Web of Conferences*, *172*, 1–7. https://doi.org/10.1051/e3sconf/202017204007

Pallin, S., Boudreaux, P., Kehrer, M., Hun, D. E., Jackson, R. K., & Desjarlais, A. O. (2015). *Moisture Durability Assessment of Selected Well-insulated Wall Assemblies (ORNL/TM-2015/645)* (Issue December). Oak Ridge National Lab.

Pallin, S., Hun, D., & Boudreaux, P. (2016). Simulating air leakage in walls and roofs using indoor and outdoor boundary conditions. *Thermal Performance of the Exterior Envelopes of Whole Buildings XIII*, 485–492.

Parekh, A., Roux, L., & Gallant. (2007). Thermal and air leakage characteristics of Canadian housing. *11th Canadian Conference on Building Science and Technology*. https://www.researchgate.net/publication/269107473_What_is_governance/link/548173090cf22525d cb61443/download%0Ahttp://www.econ.upf.edu/~reynal/Civil wars_12December2010.pdf%0Ahttps://think- asia.org/handle/11540/8282%0Ahttps://www.jstor.org/stable/41857625

Quirouette, R. L. (1985). *The difference between a vapour barrier and an air barrier - Building practice note no. 54* (pp. 1–13). National Research Council Canada. https://doi.org/10.1515/9781400832361- 009

Quirouette, R. L. (1999). *On-Site Exterior Wall Monitoring Methods for Air Leakage, Condensation and Rain Penetration Control Problems*.

Quirouette, R. L. (1989). The air barrier defined. *Building Science Insight ´86*, 1–6.

Robinson, T. (1992). Moisture Challenges in Canadian Energy Efficient Housing. *Journal of Thermal Insulation and Building Envelopes*, *16*(October), 112–120.

Rousseau, M. Z. (1984). Control of surface and concealed condensation. *Building Science Insight '83 - Humidity, Condensation and Ventilation in Houses*, 29–40.

Rousseau, M. Z. (2003). Heat, air and moisture control strategies for managing condensation in walls. *IRC Building Science Insight 2003 Seminar Series*, 11. https://nrc- publications.canada.ca/eng/view/accepted/?id=73c368d6-6efe-43b0-a89f-e10c1a733095

Rousseau, M. Z., & Brown, W. C. (1995). Research update on heat, air and moisture flows in exterior walls. *Building Envelope Performance and Durability, IRC Technical Seminar*, 1–7. https://nrc- publications.canada.ca/eng/view/object/?id=3a4773ab-d418-488e-acf2-f73d2f6d2431

Rowley, F. B., Algren, A. B., & Lund, C. E. (1940). *Bulletin 17 - Methods of moisture control and their application to buidling construction: Vol. XLIII* (Issue 28). University of Minnesota: Engineering Experiment Station. https://conservancy.umn.edu/handle/11299/124212

Rowley, F. B., Algren, A. B., & Lund, C. E. (1941). *Bulletin 18 - Condensation of moisture and its relation to buidlibg construction and operation: Vol. XLIV* (Issue 18). University of Minnesota: Engineering Experiment Station. https://conservancy.umn.edu/handle/11299/124212

Rowley, F. B., Joy, M. H. L. A., & Ericson, E. T. (1947). *Bulletin 26 - Moisture and Temperoture Control in Buildings Utilizing Structural Insuloting Boord: Vol. L* (Issue 26). University of Minnesota: Engineering Experiment Station. https://conservancy.umn.edu/handle/11299/124212

Rowley, F. B., & Lund, C. E. (1944). *Bulletin 22 - Vapor Transmission Analysis of Structural Insulating Board: Vol. XLVII* (Issue 47). University of Minnesota: Engineering Experiment Station. https://conservancy.umn.edu/handle/11299/124212

Saber, H. (2014). *Report on Properties and Position of Materials in the Building Envelope for Housing and Small Buildings*. National Research Council Canada.

Salonvaara, M., Karagiozis, A., & Holm, A. (2001). Stochastic Building Envelope Modeling - the influence of material properties. *Buildings VIII: Performance of Exterior Envelopes of Whole Buildings - Integration of Building Envelopes*.

Salonvara, M., Karagiozis, A. N., Pazera, M., & Miller, W. (2007). Air Cavities Behind Claddings - What Have We Learned? *Thermal Performance of Exterior Envelopes of Whole Buildings X International Conference*.

Sander, D. M., Cornick, S. M., Swinton, M. C., & Haysom, J. C. (1995). Determination of building envelope requirements for the (Canadian) National Energy Code for Buildings. *Thermal Performance of the Exterior Envelopes of Buildings VI*, 679–685. https://nrc-publications.canada.ca/eng/view/object/?id=df0f7660-1a2e-44c1-b799-758694f258e6

Sedlbauer, K. (2001). *Prediction of mould fungus formation on the surface of and inside building components* [Sttutgart Universitat]. http://www.ibp.fraunhofer.de/content/dam/ibp/en/documents/ks_dissertation_etcm1021-30729.pdf

Simonson, C. J., Ojanen, T., & Salonvaara, M. (2005). Moisture performance of an airtight, vapor-permeable building envelope in a cold climate. *Journal of Thermal Envelope and Building Science*, *28*(3), 205–226. https://doi.org/10.1177/1097196305048628

Sontag, L., Nicolai, A., & Vogelsang, S. (2013). *Validierung der Solverimplementierung des hygrothermischen Simulationsprogramms Delphin - Technischer Bericht (Validation of the solver implementation of the hygrothermal Simulation program Delphin - technical report)* (pp. 1–80). Institut für Bauklimatik - Technische Universität Dresden. http://www.qucosa.de/fileadmin/data/qucosa/documents/12896/DelphinValidierung.pdf

Straube, J. (1998). *Moisture Control and Enclosure Wall Systems*. University of Waterloo.

Straube, J. (2007). Building science digest 014 - Air Flow Control in Buildings. *Building Science Press*, 1–18.

Straube, J. (2011). *Building Science Digest 163: Controlling cold-weather condensation using insulation*. Building Science Corporation.

Straube, J. (2001). The influence of low-permeance vapor barriers on roof and wall performance. *Thermal Performance of the Exterior Envelopes of Whole Buildings VIII*, 1–12.

TenWolde, A. (2000). Mold and Decay in TriState Homes. *2nd Annual Conference on Durability and Disaster Mitigation in Wood-Frame Housing*, 53–58.

Thue, J. V., Skogstad, H. B., & Homb, A. (1996). Wood Frame Walls in Cold Climate - Vapour Barrier Requirements. *Journal of Thermal Insulation and Building Envelopes*, *20*(july), 63–75. https://doi.org/https://doi.org/10.1177%2F109719639602000106

Torp, A., & Graee, T. (1971). *Effect of Air Currents in Moisture Migration and Condensation in Wood fram strucutres - Technical translation 1478*. https://nrc-publications.canada.ca/eng/view/ft/?id=6db6f8c7-19b7-4f24-9ff5-25783a4d3fff

Tsongas, G., Burch, D., & Cunningham, M. (1995). A parametric study of wall moisture contents using a revised variable indoor relative humidity version of the "Moist" transient heat and moisture transfer model. *Thermal Performance of the Exterior Envelopes of Whole Buildings VI*, 307–320.

Tsongas, G., & Olson, J. D. (1995). TRI STATE HOMES : A CASE STUDY OF EXTENSIVE DECAY IN THE WALLS OF OLDER MANUFACTURED HOMES WITH AN EXTERIOR VAPOR RETARDER. *Thermal Perfomance of the Exterior Envelopes of Buildings VI*, 207–218.

Tu, J., Yeoh, G.-H., & Liu, C. (2013). Computational Fluid Dynamics, Applied Computational Fluid Dynamics. In *Mechanical Engineering Series* (2nd ed.). Elsevier. http://dx.doi.org/10.1016/B978-0-12-382100-3.10010-1

USDA. (2010). *Wood handbook - Wood as an engineering material. General Technical Report FPL-GTR-190* (p. 508). Department of Agriculture, Forest Service, Forest Products Laboratory.

Van Belleghem, M., Steeman, M., Janssens, A., & De Paepe, M. (2015). Heat, air and moisture transport modelling in ventilated cavity walls. In *Journal of Building Physics* (Vol. 38, Issue 4). https://doi.org/10.1177/1744259114543984

Vereecken, E., Saelens, D., & Roels, S. (2011). A comparison of different mould prediction models. *12th Conference of International Building Performance Simulation Association*. http://www.bounceinteractive.com/bs2011/bs2011/pdf/P_1579.pdf

Viitanen, H., Krus, M., Ojanen, T., Eitner, V., & Zirkelbach, D. (2015). Mold risk classification based on comparative evaluation of two established growth models. *Energy Procedia*, *78*, 1425–1430. https://doi.org/10.1016/j.egypro.2015.11.165

Viitanen, H., Ojanen, T., Peuhkuri, R., Vinha, J., Lähdesmäki, K., & Salminen, K. (2011). Mould growth modelling to evaluate durability of materials. *XII DBMC - International Conference on Durability of Building Materials and Components*, 1–8. http://www.irbnet.de/daten/iconda/CIB22377.pdf

Walker, I. S., & Wilson, D. J. (1994). Practical Methods for Improving Estimates of Natural Ventilation Rates. *15th AIVC Conference - The Role of Ventilation*, *September*, 518–525.

Wang, L. (2018). *Stochastic Modelling of Hygrothermal Performance of Highly Insulated Wood Framed Envelopes*. Concordia University.

Wang, L., & Ge, H. (2017). Effect of air leakage on the hygrothermal performance of highly insulated wood frame walls: Comparison of air leakage modelling methods. *Building and Environment*, *123*, 363–377. https://doi.org/10.1016/j.buildenv.2017.07.012

Watt, D., Sjöberg, S., & Wahlgren, P. (2014). *Hygrothermal performance of a light weight timber wall assembly with an exterior air barrier* [Chalmers University of Technology]. https://doi.org/10.1016/j.egypro.2015.11.164

Watt, D., Sjöberg, S., & Wahlgren, P. (2015). Hygrothermal performance of a light weight timber wall assembly with an exterior air barrier. *Energy Procedia*, *78*, 1419–1424. https://doi.org/10.1016/j.egypro.2015.11.164

Wilson, A. G., & Garden, G. K. (1965). Moisture accumulation in walls due to air leakage. *RILEM/CIB Symposium - Moisture Problems in Buildings*. https://nrc-publications.canada.ca/eng/view/object/?id=aebbca87-8deb-4f03-9ca9-ba27712f9297

Wolf, D., & Tyler, F. (2013a). Characterization of air leakage in residential structures - Part 1: Joint leakage. *Thermal Performance of the Exterior Envelopes of Whole Buildings - 12th International Conference*.

Wolf, D., & Tyler, F. (2013b). Characterization of air leakage in residential structures - Part 2: Whole house leakage. *Thermal Performance of the Exterior Envelopes of Whole Buildings - 12th International Conference*.

Zarling, J. P., Rice, E., & Swanson, K. C. (1982). Moisture Problems in Buildings in the Subarctic. In M. Lieff & H. R. Trechsel (Eds.), *Moisture Migration in Buildings, ASTM STP 779* (pp. 262–274). ASTM International.
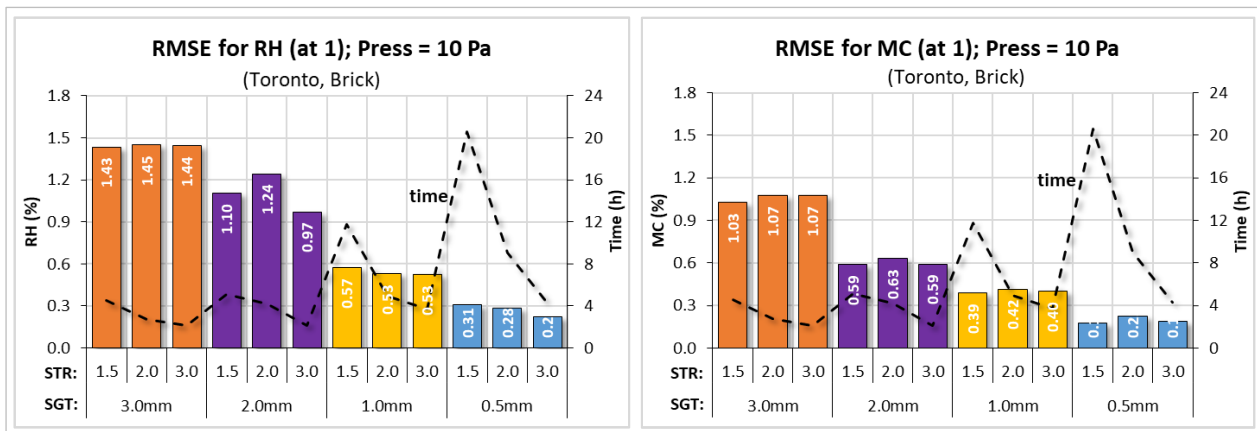
Appendix A

RMSE for RH and MC in Whitehorse with stucco cladding
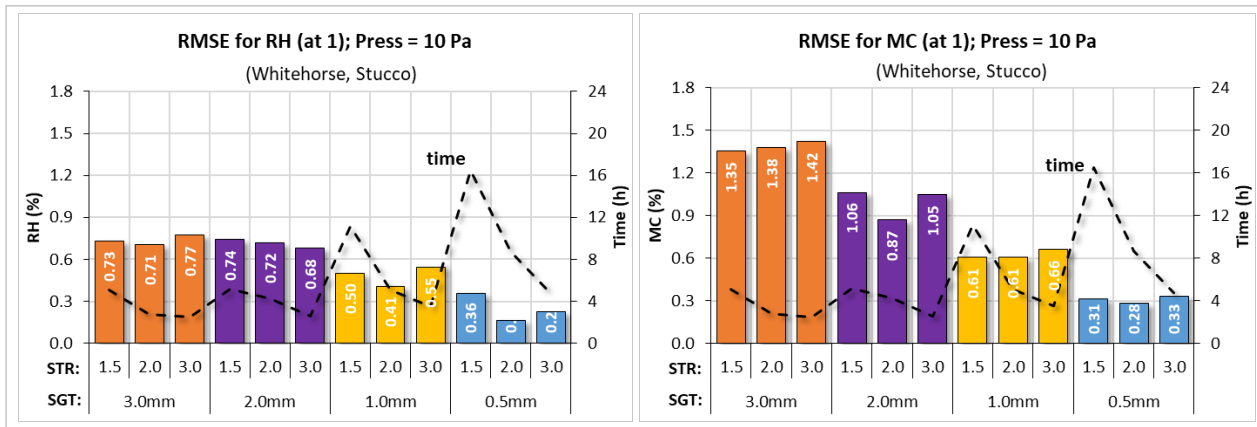
RMSE for RH and MC in Whitehorse with vinyl cladding
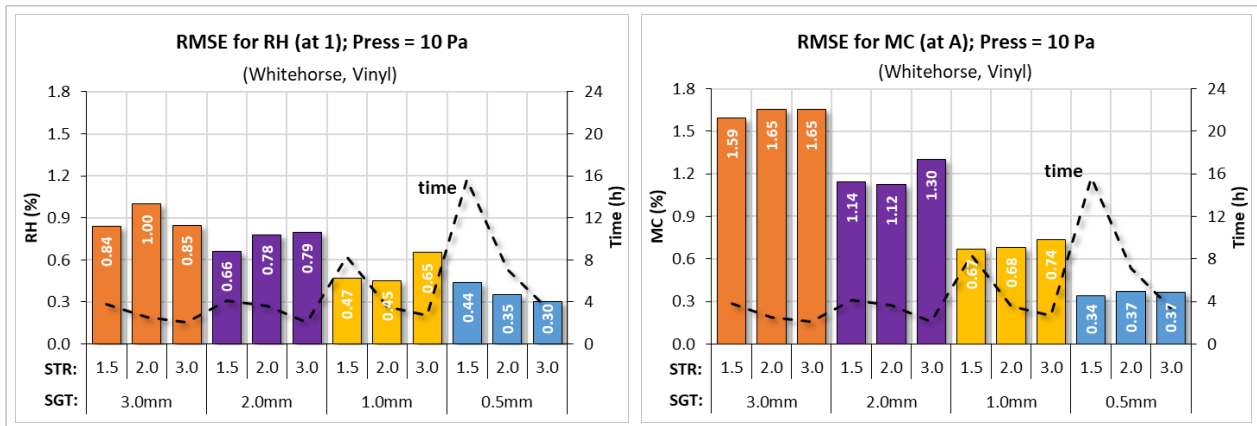
RMSE for RH and MC in Toronto with brick cladding

Mould index for different cities and claddings, North orientation

Mould index of OSB (at 1); Press = 10Pa
(Whitehorse, Stucco)

SGT; STR
0.25; 1.5 — 0.25; 2.0 — 0.25; 3.0
0.50; 1.5 — 0.50; 2.0 — 0.50; 3.0
1.00; 1.5 — 1.00; 2.0 — 1.00; 3.0
2.00; 1.5 — 2.00; 2.0 — 2.00; 3.0
3.00; 1.5 — 3.00; 2.0 — 3.00; 3.0

Mould index of OSB (at 1); Press = 10Pa
(Whitehorse, Vinyl)

SGT; STR
0.25; 2.0 — 0.25; 3.0 — 0.50; 1.5
0.50; 2.0 — 0.50; 3.0 — 1.00; 1.5
1.00; 2.0 — 1.00; 3.0 — 2.00; 1.5
2.00; 2.0 — 2.00; 3.0 — 3.00; 1.5
3.00; 2.0 — 3.00; 3.0

Mould index of OSB (at 1); Press = 10Pa
(Toronto, Brick)

SGT; STR
0.25; 1.5 — 0.25; 2.0 — 0.25; 3.0
0.50; 1.5 — 0.50; 2.0 — 0.50; 3.0
1.00; 1.5 — 1.00; 2.0 — 1.00; 3.0
2.00; 1.5 — 2.00; 2.0 — 2.00; 3.0
3.00; 1.5 — 3.00; 2.0 — 3.00; 3.0